Faculteit Ingenierswetenschappen

Academiejaar 2005–2006

Rate capability and ion feedback in GEM-detectors

Pieter Everaerts

Promotor: Prof. dr. L. Van Hoorebeke
CERN supervisors: Dr. L. Ropelewski & Prof. dr. F. Sauli

Scriptie voorgedragen tot het behalen van de graad van
burgerlijk natuurkundig ingenieur

Gent, Juni 2006

De promotor — De auteur

Prof. dr. L. Van Hoorebeke — Pieter Everaerts

Samenvatting

Gasdetectoren zijn al decennialang de 'werkpaarden' onder de hedendaagse deeltjesdetectoren. Door hun relatief lage kost, goede resolutie en het relatief grote volume dat ze kunnen bestrijken, speelden ze een belangrijke rol in de hoge-energie experimenten zoals die aan de LEP-versneller op CERN, Geneve. Bij de opbouw van de nieuwe generatie versnellers, protonenbotsers zoals de LHC op CERN, bleken de beperkingen van de huidige gasdetectoren stilaan bereikt. Gasdetectoren zijn niet volledig uit de LHC-experimenten gebannen -vooral niet in de muonkamers- maar hun aandeel is veel beperkter dan tevoren. Silicium heeft stilaan hun plaats ingenomen. Maar sinds de invoering van de micro-strip gas chambers (MSGC) in 1988, lijkt die evolutie afgeremd te worden. De MSGC's zelf zijn wel nog beperkt in hun bruikbaarheid omwille van een grote kans op aanzienlijke schade bij 'discharges', een soort destructieve spanningssprongen die optreden en dan de strips kunnen doorbranden. De detector kan daardoor permanent beschadigd worden. In de tweede helft van de jaren '90 werden deze problemen opgelost door de micropattern gas detectors die veel robuuster zijn en dus minder fragiel.

De Gas Electron Multiplier (GEM), geïntroduceerd door Fabio Sauli in 1997, is een van de voorbeelden van de nieuwe generatie gasdetectoren. GEMs bestaan uit een dunne (50 μm) isolatorlaag. Met een speciale chemische etstechniek worden biconische gaten -door het dubbele masker en het etsen van twee zijden - gemaakt in deze Kapton-laag. In deze gaten zal de eigenlijke elektronvermenigvuldiging plaatsvinden. Deze gaten hebben gewoonlijk een diameter van 70 μm en hun middelpunten zijn 140 μm van elkaar verwijderd (de zogenaamde 'pitch'). Deze configuratie kan gevarieerd worden, zo zullen we in dit werk ook kort GEMs met grotere gaten (100μm) behandelen en conische equivalenten. Deze kunnen allemaal op hun gebied nuttig blijken. Via lithografische processen worden op de isolator aan weerskanten een 5 μm koperlaag aangebracht. Deze zullen als elektrodes dienen.

Wanneer over de GEM een spanning wordt gezet van om en bij de 500 V, dan zullen die een sterk dipool-veld ($\propto 10^5$ V/cm) in de gaten veroorzaken. Elektronen die dan door de aangepaste driftvelden (van de driftelektrode naar de GEM) in de gaten worden geleid, zullen vermenigvuldigd worden. De gecreëerde elektronen worden dan door een inductieveld (van GEM naar read-out) naar de read-out geleid en zullen daar gecollecteerd worden. Door de

grote spanningen op de GEM en de grote oppervlakte die altijd ongebruikt blijft, kunnen elektronen en ionen ook naar het oppervlak van de GEM worden geleid. Daardoor wordt de GEM-werking een uniek samenspel van de verschillende velden om te proberen een zo sterk mogelijk signaal te krijg zonder andere nuttige eigenschappen niet uit het oog te verliezen. Zo is het bijvoorbeeld vaak wenselijk om de terugstoot van ionen naar het driftgebied te verminderen. GEMs doen dit al automatisch tot op zekere hoogte maar een aangepaste veldenconfiguratie kan deze 'ion feedback' nog verder verlagen. GEMs hebben ook enkele speciale eigenschappen omwille van hun opbouw. Zo bestaat er een fenomeen dat 'charging-up' werd gedoopt en het gevolg is van ladingsopstapeling op de biconische Kapton-oppervlakken in de gaten. De vermenigvuldingsfactor zal hierdoor in de eerste 5 minuten 20% toenemen. Eens opgeladen, blijkt dit fenomeen een geheugen te hebben van meer dan 1 dag. Karakteristiek, zoals bij alle gasdetectoren, is ook het probleem van plotse spanningsvallen, 'discharges', die kunnen optreden.

GEMs hebben verscheidene extra voordelen tegenover de oude en gevestigde generatie gasdetectoren zoals de multi-wire proportional chambers (MWPC). De resolutie is beter, er wordt geen ionenstaart meer waargenomen in het signaal aangezien de elektronen rechtstreeks gedetecteerd worden en 'discharges' stellen minder problemen dan in oudere detectoren. Dit omwille van twee redenen. Ten eerste kan men de grootte van de mogelijke spanningsval over de GEMs al behoorlijk verlagen door GEMs in een soort cascade op te stellen. Elke GEM moet dan maar een fractie van de vooropgestelde vermenigvuldigingsfactor voor zijn rekening nemen en de gehanteerde spanningen zijn dus veel lager. Bovendien heeft proefondervindelijk onderzoek nog een aanzienlijke verlaging van de kans op 'discharges' opgeleverd: een lichtelijk asymmetrische (10%) spanningsdeling blijkt voordelen te bieden. Naast de verlaagde kans op 'discharges', is ook de mogelijke impact van zulke schadelijke ontladingen gereduceerd bij GEMs. In GEMs is het mutliplicatieproces namelijk onafhankelijk van het uitlezen van de data. Dit zorgt dat de elektronica niet meteen vernietigd wordt bij zo een 'discharge' als voorheen het geval was. De vermenigvuldiging gebeurt ook niet aan de elektrodes, zodat ook deze niet aangetast worden. Veroudering van de detector blijkt daardoor vrijwel niet op te treden. Al deze voordelen hebben van GEMs een van de vaandeldragers van de nieuwe generatie gasdetectoren gemaakt. Samen met de Micromegas lijken ze de beste toekomstperspectieven te bieden, bijvoorbeeld voor de volgende generatie lineaire versnellers, zoals de International Linear Collider. (ILC)

Een van de grote voordelen van de GEM is ook zijn sterke bestandheid tegen sterke deeltjesimpacten. Tot nu toe bleek hij alle grote 'rates' (hoeveelheid deeltjes per oppervlakte- en tijdseenheid) aan te kunnen. De gemeten limiet was 10^5 Hz mm^{-2}. In dit werk hebben we getracht deze limiet meer dan een grootte-orde naar omhoog te trekken. Dit bracht twee nieuwe effecten aan het licht. Het eerste vond plaats tussen 10^5 Hz mm^{-2} en 10^6 Hz mm^{-2} en werd totaal niet verwacht en was zelfs anti-intuïtief. In dit gebied bleek de 'gain' (ver-

menigvuldigingsfactor) te stijgen tussen 10 en 50 % afhankelijk van de precieze omstandigheden. Aangezien dit fenomeen onverwacht was en er op het eerste gezicht geen duidelijke uitleg voor handen was, besloten wij het dieper te onderzoeken. Spanningen werden gevarieerd, zowel symmetrisch als asymmetrisch, in de hoop de invloeden van de 'gain' en de precieze spanningsverdeling te scheiden. Uit het onderzoek naar 'discharges' was immers al gebleken dat niet alleen de totale spanning een invloed had maar ook de manier waarop die spanning tussen de verschillende GEMs gedeeld werd. Het verschil met dubbele en enkelvoudige GEM-detectoren werd nagegaan, net als de invloed van andere GEM-geometrieën. Velden en afstanden werden gevarieerd. Daarnaast werden ook de invloed van het gas onderzocht in de hoop daar ideeën in te vinden. Natuurlijk probeerden we ook alle mogelijke fouten in onze metingen uit te sluiten. Finaal lijken de resultaten in de richting van een ladingsophoping in de detector te wijzen, een ladingsophoping die dan de vermenigvulding zou versterken. Het precieze proces dat hierin een rol speelt, is nog steeds niet duidelijk, maar het fenomeen lijkt vast te staan. Misschien kunnen simulatie, snellere electronica of snellere gassen nog extra uitsluitsel brengen. Bij de uitermate snelle gassen in de LHC-b detector blijkt het fenomeen immers niet op te treden, wat een ladingsophoping nog plausibeler maakt. Een tweede observatie lijkt de echte limitatie van GEMs in te houden: 'rates' over 10^6 Hz mm^{-2} leiden tot een afname van de 'gain'. Zulke afnames werden bij MWPCs bijvoorbeeld ook al waargenomen en bepaalden ook daar de bruikbaarheidsgrens van de detector. Alleen ligt deze demarcatiewaarde bij GEMs twee grootteorden verder.

Zoals hierboven vermeld, hebben de GEMs het intrinsieke voordeel dat het aantal teruggestuurde ionen naar de driftruimte klein is. Dit samen met ander voordelen als het afwezig zijn van $\vec{E} \times \vec{B}$-verstoringen van de elektrontrajecten (door de precieze opbouw van een GEM detector), lijken GEMs handig te maken voor het gebruik in Time Projection Chambers (TPC). Dit zijn gasdetectoren met een enorm volume waarin een uniform elektrisch veld heerst. Dit elektrisch veld leidt de elektronen die in het ionisatiepad van het passerende deeltje worden gevormd, naar een van de sluitingsstukken ('endcaps'). Deze 'endcaps' zijn normaal gezien opgebouwd uit gasdetectoren die dan de X- en Y-coördinaat van het deeltje kunnen bepalen. Via de opgemeten drifttijd kan dan met de kennis van het uniforme elektrisch veld ook de Z-positie van het ionisatiepad worden bepaald. Zo bekomt men een 3-dimensionaal beeld van de gebeurtenissen. Een extra magnetisch veld helpt in de momentum-bepaling. GEMs bieden nu vele voordelen om in zulke 'endcaps' te worden gebruikt. De betere resolutie is er al een van. Maar de onderdrukking van de 'ion feedback' is een andere en misschien nog belangrijkere. De ionen die gecreëerd worden in het vermenigvuldingsproces en zich terug naar het driftvolume bewegen kunnen daar immers het elektrisch veld behoorlijk verstoren. Ophopingen van de positieve ionen in dat driftvolume veranderen de configuratie van de veldlijnen een beetje en dan geldt de eenvoudige positiebepaling niet meer maar moeten allerlei extra factoren in rekening worden gebracht. Dit leidt tot onoverkomelijke problemen en daarom probeert men

te vermijden dat ionen in het driftgebied terechtkomen.

Jammer genoeg blijken GEMs het terugzenden van de ionen nog niet voldoende te onderdrukken. Een optimalisatieproces met de verschillende spanningen en gasmengsels, leidt tot een minimale feedback verhouding (teruggestuurde ionen/gecollecteerde elektronen) van 5 promille. Om echt verlost te zijn van de vervelende bijwerkingen van de teruggestuurde ionen zou de verhouding rond 10^{-4} moeten liggen. Aangezien we een 'gain' bij normaal gebruik van 10^4 hanteren, zou dit dan 1 teruggestuurd ion per primair ion opleveren en dit is min of meer de aanvaardbaarheidsgrens. Verder reduceren kan op twee manieren gebeuren. Ten eerste zou men met een metalen rooster ('mesh') kunnen werken waarop men spanningen aanlegt om eerst de elektronen door te laten in een richting en dan de ionen daarna te blokkeren in de andere richting. Dit is mogelijk aangezien men toch met pakketjes deeltjes werkt die een zeker tijdsinterval van elkaar gescheiden zijn. Maar zo een rooster zou opnieuw storende effecten introduceren zoals de $\vec{E} \times \vec{B}$-storingen tengevolge van de geïntroduceerde extra velden. Bovendien blijkt de transparantie voor elektronen uit onze metingen lager te zijn dan voordien werd aangenomen en bij het precieze geval van GEMs treden extra storingen op, omwille van de velddistorties. Een mogelijke oplossing zou zijn om te 'gaten' (dus doorlaten van elektronen, tegenhouden van ionen daarna) met een extra GEM. Uit ons onderzoek blijkt bovendien dat een maximum aan transparantie bestaat bij slechts 10 V. Dit zou de benodigde spanningen sterk verlagen en dus gemakkelijker te realiseren zijn dan de 'mesh'-opbouw. De transparantie blijkt nog beter te zijn bij GEMs met grotere gaten - zoals te verwachten viel. Het enige probleem is dat er een lichte verslechtering van de energieresolutie optreed, wat dus bij de TPCs die een goede dE/dx nodig hebben voor deeltjesidentificatie storend kan zijn. Maar de deterioratie zou nog voldoende klein moeten zijn opdat de methode bruikbaar zou zijn in TPCs.

Een andere oplossing voor de terugstromende ionen hebben we gevonden in een DC ion filter. Voor TPCs is dit resultaat wellicht minder bruikbaar, maar voor de GEM-photomultipliers (PMT) kan het wel een mogelijke oplossing bieden. Bij dit onderzoek maakten we gebruik van speciale, zogenaamde dikke GEMs. Deze GEMs zijn opgebouwd uit een dikkere laag isolator en hebben ook grotere gaten die mechanisch geboord worden in het oppervlak en een cilindrisch uiterlijk hebben. We maakten gebruik van deze speciale GEMs omdat die gemakkelijker macroscopisch ten opzichte van elkaar te bewegen zijn en we dus een bewegende set-up konden maken waarin we twee GEMs -we maakten dus gebruik van een dubbele GEM detector- in 1 richting over elkaar lieten bewegen. Op elk punt maten we de elektronenstroom en de ionenstroom en bepaalden zo de 'ion feedback'. De resultaten tonen dat er een aanzienlijke reductie van het aantal terugstromende ionen optreedt wanneer de opstelling zo opaak mogelijk is. Wanneer de gaten dan precies boven elkaar worden gepositioneerd, treedt het maximum in 'ion feedback' op. De drift- en transfervelden (tussen de GEMs) blijken een rol te spelen in het precieze patroon en vooral hoe 'diep' en 'breed' de put naar het mini-

mum is. Een vermindering met maar liefst 40% blijkt mogelijk door op deze manier drift- en diffusie-eigenschappen te exploiteren. Mogelijke verdere reductie zou nog kunnen optreden door met de diameter van de gaten te spelen, in 2 dimensies de GEMs te verschuiven of de afstand tussen de GEMs te variëren. Voor het gebruik van standaard GEMs ligt de moeilijkheid in de precieze plaatsing van de GEMs. De afstanden zijn veel kleiner dan in dit geval en de benodigde precieze in hun positie is dan ook veel moeilijker te halen.

Acknowledgements

Without Fabio Sauli, I would never have been able to perform this research. He accepted me in his Gas Detector Development Group and offered me this interesting topic to work on. I would like to thank him a lot for this. The various discussions with him helped me to understand more about the finesse of gaseous detectors and the many processes –like diffusion– that influence their operation. For almost every strange result we measured, he could think of a possible reason and although some of these ideas had to be adjusted after new measurements, it learned me a lot about reasoning in the gaseous detector field.

Of course I am also endebted to Leszek Ropelewski who was my daily supervisor. Every day I discussed the new results with him and he also taught me the practical side of the work. I certainly learned most from him. With his patient and gentle nature he managed to point out all my mistakes, while in the meanwhileteaching he taught me physics and electronics.

Solving my mistakes, was also what Miranda Van Stenis sometimes had to do. As our technician, she was responsible for the hardware of our detector: the screws, the gas-tight chamber, the framing of the meshes and the GEMs,... Even despite my clumsiness (e.g. with soldering irons), she managed to solve all my small problems with a smile. Many thanks for that.

My many friends at CERN made my stay there unforgettable and I will always remember that.

At my home university I would like to thank prof. Luc Van Hoorebeke who was prepared to take the responsibility for my thesis and who helped me a lot with the writing process.

Finally I would also like to thank my family and especially my parents, for always supporting me, listening to me on the telephone and visiting me in Geneva, actually just for being there...

Contents

Chapter 1

Introduction

As an introduction the Gas Electron Multiplier will be situated in the bigger network of gaseous detectors whose trail of triumph began with the multi-wire proportional chambers. Their grandchildren, micro-pattern gaseous detectors like micromegas or Gas Electron Multipliers, stay competitive in today's tough detector world. To prove this, we will also focus on applications of gas detectors in the current era.

1.1 History of gaseous detectors

1.1.1 Multi-wire proportional chambers (MWPC)

One of the biggest revolutions in the world of high-energy detectors took place in 1968. At that time Charpak *et al.* (1968) built the first multi-wire proportional chambers. Because of their high-rate capability and millimeter-precision they blew away the competition of bubble and spark chambers.(Sauli, 2004) A MWPC is a chamber with many parallel wires, arranged as a grid and put at a high voltage, with the metal casing being on ground potential. As in the Geiger counter, a particle, traversing the detector volume, leaves a trace of ions and electrons, which drift toward the case or the nearest wire, respectively. The ions drift to the cathode-plates, while the electrons are collected by the anode-wires. The strong electric field close to the thin anode-wires causes avalanche multiplication. While one needs many independent detectors for spatial resolution with single-wire counters, it is now possible to determine the position of the incoming particle with only one detector. A lot of variations on this design have been developed during the years, for example to solve the problem of the 3rd dimension: time projection (chapter 6.1), ring imaging chambers ... Today multi-wire chambers are still important components of many particle-physics detectors. Nevertheless, with the higher demands of the experimental physicists, the limitations of the detector also became obvious. It turned out to be difficult for example, to place and hold the thin anode wires closer than a few mm. Also a critical wire length was discovered, above which instabilities occurred due to electrostatic repulsion. This limit was around 10 cm for a 1 mm spacing of the wires. Another

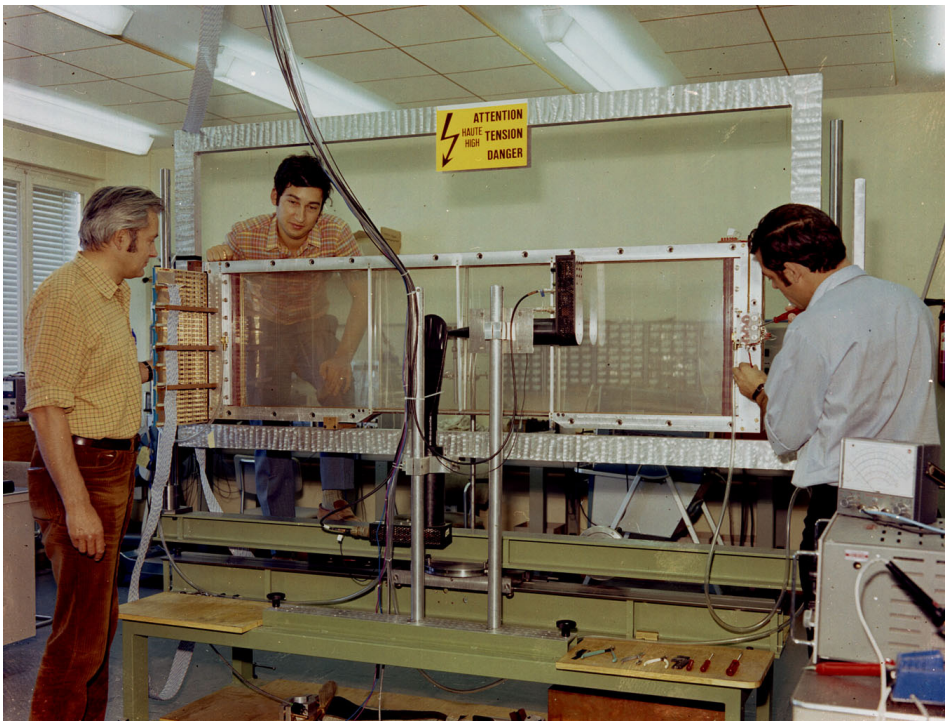

Figure 1.1: G.Charpak, F. Sauli and J.-C. Santiard working on a multi wire chamber in 1970

problem was the abundant production of positive ions in the avalanches. These positive ions alter the electric fields and give rise to a dramatic drop of the proportional gain at a flux above $\propto 10^4$ mm^{-2}s^{-1}. The attempts to overcome these problems, almost all failed and so a new type of gas detector became necessary.

1.1.2 Micro-strip gas chambers (MSGC)

At the 'Institut Laue-Langevin' in Grenoble, Oed (1988) presented such a new kind of detector in 1988. This detector contains no wires at all but uses instead very narrowly spaced conductor strips . The field strength necessary to produce gas amplification is generated between neighboring strips and not by the voltage difference between the strips and the detector cathode which can be at a large distance. Because of this, a much higher position resolution can be obtained. The electrode spacing can be scaled down an order of magnitude in comparison with a MWPC, largely improving the multi-hit capacity. The ions are also neutralized much quicker by the nearby cathodes, reducing the accumulation of space-charge. Because of this, also the high-rate capability increases. A schematic view of a MSGC can be found in figure 1.2.

The main problems with MSGCs arise with long-term operation. Imperfections of the detector or unusually large energy losses can cause discharges. These discharges can damage one of

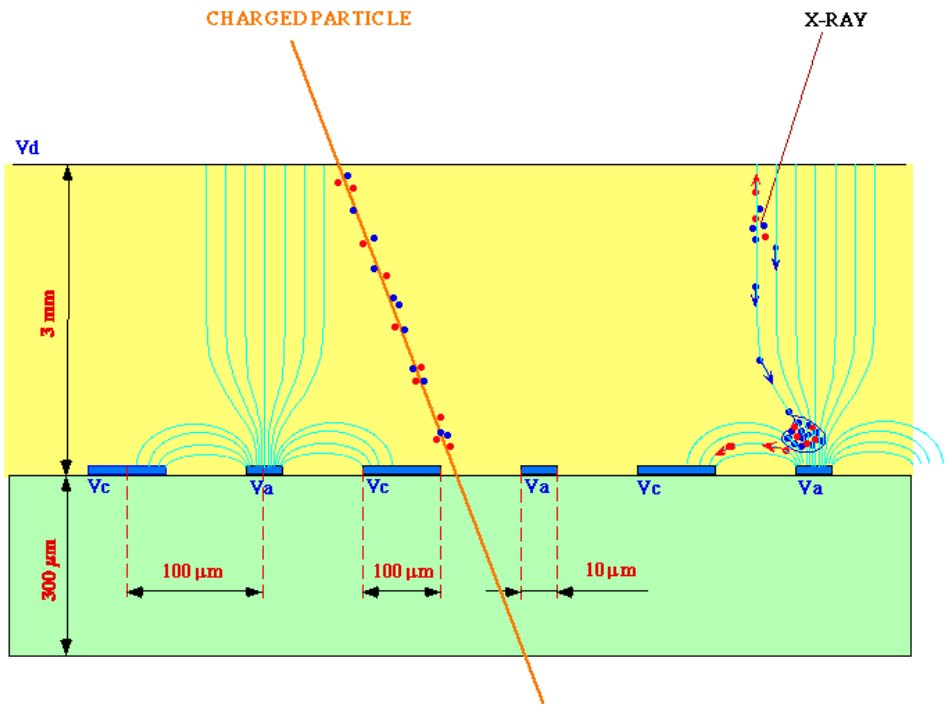

Figure 1.2: Schematic view of micro-strip gas chamber. Vc and Va are respectively the cathode and anode voltages.

the strips (fig. 1.3) or –in the worst case– even produce a short circuit in the detector. A very high increase of the discharge probability is noticed at gains above a few thousand. So the only solution seemed to be: splitting up the multiplication process. The second main

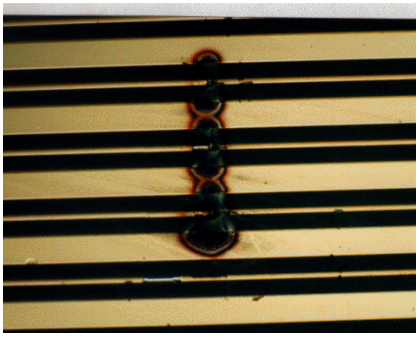

Figure 1.3: Damage caused by a discharge in a MSGC.

problem was the slow degradation of performance during sustained irradiation, called aging. The permanent damage was attributed to polymers created in the avalanches and sticking to the electrodes or insulator, causing discharges or disturbing the counting process. A careful choice of gases and materials used in the MSGC could lower the effects. But the world of

detectors was eager to take once again a new step.

1.1.3 Micro pattern detectors

During the last decennium many variations on this theme were invented. Created by photolithographic processes, having small dimensions...in this way the family of micropattern detectors was born. A wide variety of them can be found.(Hoch, 2004; Bressan *et al.*, 1998; Sauli & Sharma, 1999) Micro-dot chambers, for example are proportional counters made up of anode dots surrounded by annular cathodes. The "'compteur á trous"' or CAT has holes drilled through a metal-insulator sandwich that concentrate the field lines from a drift to a high-field region. Another very popular design is the micromegas, which consists of a very thin metal mesh stretched at a very small distance, 50 to 100 μm, above a readout electrode. The very high field (30 kV/cm) over the gap collects and multiplies the electrons. Lots of other structures exist, such as micro-gap chambers and thin-gap parallel plate structures, but their exact operation principles are less relevant here. the Gas Electron Multiplier, the detector type we used for our research, is also one of these advanced micro pattern detectors.

1.1.4 Gas Electron Multiplier (GEM)

Introduced by Sauli in 1997, the gas electron multiplier (fig. 1.4) consists of a two-side copper-clad Kapton foil, perforated with a high density of holes (typically around 100 per square mm).(Sauli, 1997) Etched by a photolithographic process, these holes have a pitch of usually 140 μm and diameters of about 70 μm ('standard geometry'). Application of a potential difference between upper and lower electrodes creates a high electric field inside the holes. Almost all the field lines in the drift region are squeezed into the the holes in the GEM plates. In the holes the electrons following these field lines are multiplied because of the very high field. (fig. 1.5)

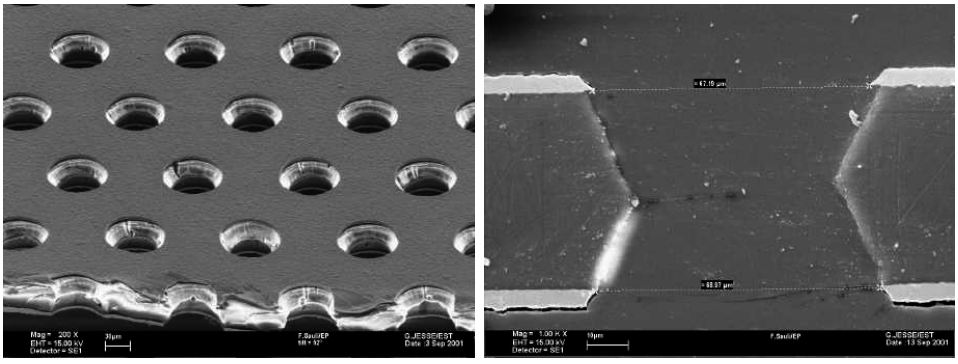

Figure 1.4: Structure of a GEM plate (left) and of a GEM hole (right)

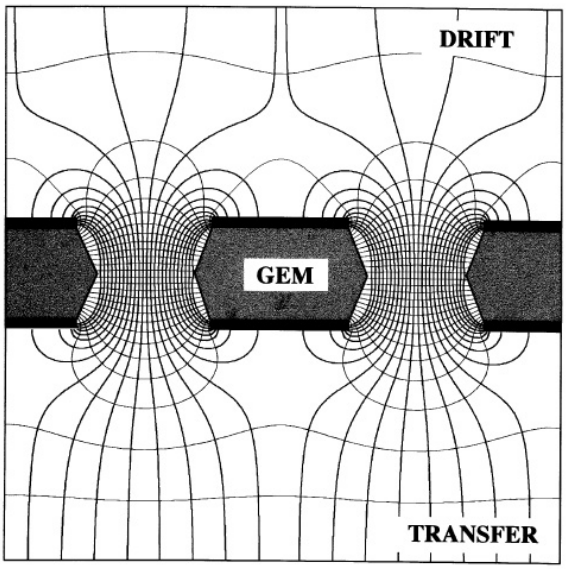

Figure 1.5: The electric field lines are squeezed into the GEM hole.

Originally GEMs were used as a preamplification stage for MSGCs, but nowadays GEMs are used as detectors themselves, read out by strips, pads or a metal plane. GEMs still suffer from discharges, but this can be considerably improved by cascading the GEMs and permitting all of them to work at a lower gain. (3 GEMS with gain 20 yield a total gain of 8000) A big advantage of GEMs is that they conserve the original ionisation pattern. Because of this, the readout system can be designed independently from the GEM structure and in such a way that it suits best the use of the detector. Hexaboard read-outs, cartesian and non-cartesian strip structures have been used for this purpose and even a combination of both will be implemented in the new TOTEM detectors. The decoupling of the amplifying structure and the read-out board is also one of the big GEM advantages. This construction protects the electronics from discharge damage. GEMs also have the natural tendency of suppressing ion feedback, making them very interesting for Time Projection Chamber uses (chapter 6.1).

1.2 The need for and use of gaseous detectors

1.2.1 LHC

Despite the good results obtained with the multi-wire proportional chambers in high-energy experiments, their limits were, like mentioned before, more or less reached in the 80's. At that moment the new generation of gaseous detectors was not yet developed and thus the future detectors were unlikely to be found in the gas detector family. Even the micro-strip gas chamber would probably not have saved the day, since it is quite vulnerable to discharges.

Therefore at that moment, new detectors with improved resolution and radiation hardness were developed: the silicon micro-strips. Space coordinates with microns accuracy suddenly became available. An additional advantage of silicon detectors was the concurrent development of low cost, highly integrated electronics. nMOS and CMOS-technology were used to design low-noise and low-power signal processors for the new generation of experiments. The design studies for the Large Hadron Collider (LHC) at CERN also started in the eighties and therefore it seems logical that the LHC experiments mainly use solid-state detectors.

Gaseous detectors have nevertheless still their use in today's experiments. The excellent performance of silicon detectors also carries an impressive price tag along. Due to their spatial resolution of a few micrometers and their high rate capability, they are very well suited for the area close to the interaction point. However, at large radius where also large areas have to be covered, like in the muon chambers, gaseous detectors are still the best option. At intermediate distance, silicon detectors and the micro-pattern gas detectors seem to be almost interchangeable, since they fulfill both the requirements for precision, rate capability and radiation hardness.

Therefore the LHC experiments did not cast out gaseous detectors completely. Atlas, CMS, LHC-b and Alice all use gaseous detectors for their muon chambers, since these have to cover a large surface. Also for particle tracking the gaseous detectors still play an important role. Some examples of gaseous detectors used in the LHC experiments are the ATLAS Transition Radiation Tracker (TRT), the ALICE Time Projection Chamber and the Muon Cathode drift Chambers. GEM detectors in particular are used in two of the new CERN experiments. TOTEM, which will measure the total proton-proton cross section, will use GEMs for tracking. LHC-b uses triple-GEM detectors in the innermost region of the muon detectors because of the higher beam intensity there. In the rest of the muon chambers MWPCs are still used.

1.2.2 Other high-energy experiments

GEMs were first used in a fixed target experiment, COMPASS, at CERN. COMPASS uses a triple-GEM detector in the small-area-tracker. After 4 years of operation, the detectors still seem to work perfectly. An other high-energy experiments using GEMs is the PHENIX upgrade at Brookhaven National Laboratory. The main future use of GEMs seems to lay in Time Projection Chambers (TPCs). The reduced ion back flow in GEM detectors, together with increased robustness, fast signals and better two-track resolution, seems to favor this kind of detectors for these applications. Some experiments (like LEGS and BoNuS) already adapt or plan to adapt GEM-TPCs and the concept is also heavily under study for the the next generation of linear colliders, like the International Linear Collider (ILC). In this work we will also try to reduce the ion back flow even further, improving the advantageous properties for GEMs in a TPC even further.

1.2.3 Other fields

GEMs are also studied for use in different other fields. (Sauli, 2003a) In medical imaging their use can for example reduce the amount of necessary radiation, since GEM detectors have proven to be sensitive to single photons. To stay in the medical field, the use of GEMs in an on-line control and verification device for radiation treatment for cancer patients, is under study at KTH, Stockholm. In plasma diagnostics GEMs seem to be useful because of their high rate capability and also GEM photomultipliers are under investigation. A photoelectric X-ray polarimeter for the study of neutron stars and black holes has also been developed and also in neutron detection GEMs seem to have a future. More information about these applications and new uses of the GEM concept can be found at the website of CERN's Gas Detector Development group: `http://gdd.web.cern.ch/GDD/`.

1.3 Structure of this thesis.

Chapter 2 will now continue with the basics about gaseous detectors, introducing the necessary concepts. Then we will move on in chapter 3 to our experimental set-up and look at how it is built up. Chapter 4 should provide the reader with an idea about the main characteristics of GEMs. It introduces with charging-up a specific GEM concept and looks at important features of gaseous detecors, like aging, long term stability and discharges. In Chapter 5 we will then explore the high-rate operation of GEMs. We will investigate the behaviour of a triple-detector in the region between 10^5 and $2\,10^6$ Hz mm^{-2}. Finally, in chapter 6 our results concerning reduced ion feedback are presented.

Chapter 2

Gas detectors

Spotting the particles created in collisions or ejected by other particles, is done by particle detectors. Such detectors exploit the different interactions to notice the presence of those particles. Gaseous detectors mainly use the electromagnetic interaction. Therefore it is useful to look at the interaction of charged particles and photons with matter before going into the details of gas detectors.

2.1 Interaction charged particles with matter

A charged particle, traversing a gaseous or condensed medium, can be detected in many ways. Of all possible interactions, however, the electromagnetic one is -by several orders of magnitude- the most likely to occur. The weak or strong interaction therefore only only tend to play a significant role in the case of neutral particles. Neutrino's are for example detected by their weak interaction with nuclei and leptons. Coulomb interactions between the passing charged particle and the medium lead to excitation and ionization of the atoms of the medium itself. The particles passing by can immediately create an ionization path and thus release electrons from the gas molecules. But it could also be that first an intermediate excited species is created. If the excitation energy of this species A is higher than the ionization energy of another species B present in the gas, then A can de-excite by liberating electrons from the B-molecules in the gas. All these created electrons are called primary electrons. These electrons can still loose their excessive energy by further ionizing the gas, creating secondary electrons. Other electromagnetic interactions like Bremsstrahlung, Čerenkov and transition radiation provide negligible contributions.

2.1.1 Bethe-Bloch formula

The electromagnetic energy loss of a heavy ($m > m_e$) charged particle traversing a medium (even with thin materials) is a statistical process, a result of many discrete interactions. On penetrating the material the particle scatters inelastically upon molecules, electrons and

nuclei. If the energy deposit is larger than the binding energy of the atom, ionization takes place. Otherwise the collision leads to an excitation of the atoms in the material. Bethe and Bloch derived in the framework of relativistic quantum mechanics, an expression for the average differential energy loss due to electromagnetic interaction (Eidelman *et al.*, 2004):

$$-\frac{dE}{dx} = 4\pi r_e^2 m_e c^2 Z_x n_x (\frac{Z_a}{\beta})^2 (ln\frac{2m_e v^2}{< I >} - ln(1-\frac{v^2}{c^2}) - \frac{v^2}{c^2}) \quad . \tag{2.1}$$

In this formula m_e and r_e are the electron mass and radius, $\beta = \frac{v}{c}$, with v the velocity of the particle passing through the medium. Z_a and Z_x are the charge numbers for the incident particle and the gas molecules, respectively, n_x is the gas density. Finally $< I >$ is the average energy lost in ionization, the so-called ionization constant. It can be approximated by $I \approx 0.16 {Z_x}^{0.9}$. This expression is valid for different kinds of heavy particles, if the velocity stays large compared to that of the orbital electrons.

The minimum of $\frac{dE}{dx}$ can be found at $\beta \approx 0.95$, almost independently of the medium. In practical cases, most relativistic particles have energy-losses close to this minimum. They are called minimum ionizing particles or MIPs. For higher energies the energy-loss rises slightly, due to large energy transfers to a few electrons. At lower energies we enter a range of very high energy-loss. Photoelectrons with energies of a few keV (e.g. from X-rays) or α-particles of a few MeV (e.g. from ^{90}Rn) are examples of these heavily ionizing particles. In a mixture the energy losses in the two gas types can be added taking into account the appropriate weight factors of the two components.(Sauli, 1977)

2.1.2 Primary and total ionization

On the passage of a charged particle, a number of primary ionizing collisions takes place, producing electron-ion pairs in the medium like described earlier. The ejected electrons can sometimes have enough energy (larger than ionisation potential of the absorber) to further ionize the gas. The newly created electrons are secondary electrons. Primary and secondary ionization can now be combined to give the total ionization. For the calculation also the effective average energy to produce one electron-ion pair W_i is needed. This value is also gas-dependent. Table 2.1 gives these values for different commonly-used gases.

The total number of ions pairs formed is now given by (Sauli, 1977):

$$n_{tot} = \frac{\Delta E}{W_i} \quad . \tag{2.2}$$

For a mixture, we can use a simple composition law introducing weigh factors.

Gas	Z	A	δ (g/cm³)	E_{ex}	E_i (eV)	I_0 (eV)	W_i	dE/dx (MeV/g cm⁻²)	dE/dx (keV/cm)	n_p (i.p./cm) a)	n_T (i.p./cm) a)
H_2	2	2	8.38×10^{-5}	10.8	15.9	15.4	37	4.03	0.34	5.2	9.2
He	2	4	1.66×10^{-4}	19.8	24.5	24.6	41	1.94	0.32	5.9	7.8
N_2	14	28	1.17×10^{-3}	8.1	16.7	15.5	35	1.68	1.96	(10)	56
O_2	16	32	1.33×10^{-3}	7.9	12.8	12.2	31	1.69	2.26	22	73
Ne	10	20.2	8.39×10^{-4}	16.6	21.5	21.6	36	1.68	1.41	12	39
Ar	18	39.9	1.66×10^{-3}	11.6	15.7	15.8	26	1.47	2.44	29.4	94
Kr	36	83.8	3.49×10^{-3}	10.0	13.9	14.0	24	1.32	4.60	(22)	192
Xe	54	131.3	5.49×10^{-3}	8.4	12.1	12.1	22	1.23	6.76	44	307
CO_2	22	44	1.86×10^{-3}	5.2	13.7	13.7	33	1.62	3.01	(34)	91
CH_4	10	16	6.70×10^{-4}		15.2	13.1	28	2.21	1.48	16	53
C_4H_{10}	34	58	2.42×10^{-3}		10.6	10.8	23	1.86	4.50	(46)	195

a) i.p. = ion pairs

Figure 2.1: Properties of most important gases in a proportional counter.(Sauli, 1977)

2.2 Interaction between photons and matter

For our experiments the interactions between photons and matter will be the most important interactions, since all our measurements are performed using X-rays. The attenuation of a photon beam traversing a medium of thickness X and with N molecules per unit volume is given by:

$$I = I_0 e^{-\sigma N X} = I_0 e^{-\mu \rho X} \quad . \tag{2.3}$$

Here μ is the mass attenuation coefficient thickness and ρ the density. σ is the total cross section for photon-matter interaction and determines the probability of absorption. This total cross section is the sum of the cross section for all the individual processes that might occur: photoelectric absorption (for us the most important phenomenon), Compton (incoherent) scattering and pair production. All the processes dominate in a certain energy range, which depends strongly on the atomic number, as can be seen in fig. 2.2. In the low energy range consider in this work, till several keV, photo-electric absorption is the most important process. The mass attenuation coefficient is related with the absorption coefficient:

$$\mu = \frac{N_A}{A}\sigma_{tot} = \frac{N_A}{A}(\sigma_{PA} + \sigma_{CS} + \sigma_{pp}) \quad , \tag{2.4}$$

with N_A Avogadro's number and A the mass number of the absorber material. Now we will go on to focus more closely on the physics of the different processes.(Sauli, 1977)

2.2.1 Photoelectric absorption.

For energies below 500 keV, this is the dominant process in argon. The exact range also depends strongly on the atomic number. Photoelectric absorption is a quantum process

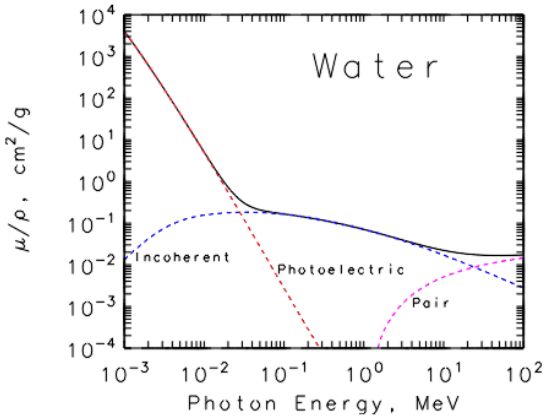

Figure 2.2: Total photon cross-section in water as a function of energy. (Coursey, 2001)

that involves one or more transitions in the electron shell of an atom. If the energy of the incident photon E_γ exceeds the binding energy E_i of the electrons in the shell i, the photon is completely absorbed. Energy and momentum are transferred to the interaction partner (a bound electron) and ionization and excitation of the atom take place. The cross section of this process has a maximum at the absorption edges and then decreases rapidly.

Absorption of a photon with energy E_γ in a shell of energy E_i results in the emission of a photoelectron of energy E_e=E_γ-E_i. In a gas detector such an electron is emitted in a preferential direction, depending on the photon energy. Up to about 20 keV the direction is nearly orthogonal to the direction of the incident photon, which limits the spatial resolution for photons in such a detector. The excited atom can return to its ground state through 2 competing mechanisms:

- fluorescence: transition of an electron from a shell with energy $E_j < E_i$ to the i-shell, with emission of a photon with energy E_i-E_j.
- radiationless transition or Auger effect, which is an internal rearrangement involving electrons from several lower-energy shells, resulting in the emission of an electron with an energy close to E_i.

The fraction of de-excitations producing the emission of a photon is called the fluorescence yield. For the K-shell the fluorescence increases with the atomic number. In argon, for example, 15% of the photoelectric absorptions are followed by an emission of a photon of an energy just under that of the K-shell. The secondary photon with an energy just below the K-edge has a very long absorption length and can therefore escape the volume of detection. This creates the characteristic escape peak of argon, at an energy E_γ-E_K. In 85 % of the cases, two electrons are emitted, one of them being an Auger electron.

2.2.2 Compton scattering

When the photon energy rises above the energy of the highest atomic energy level (around 1 MeV for argon) Compton scattering becomes dominant. The incident photon is scattered by a quasi free electron (because its binding energy is negligible compared to the energy of the incident photon), transferring only a part of its energy and momentum to the electron. The incident photon with energy $h\nu$ is scattered by the electron at an angle θ and its new energy becomes $h\nu'$, defined as follows:

$$\frac{1}{h\nu'} = \frac{1}{h\nu} - \frac{1}{m_e c^2}(1 - cos(\theta)) \quad . \tag{2.5}$$

The principle of conservation of energy then yields us the energy of the scattered electron. For low energies (<10 keV) the angular distribution of the Compton photon is symmetric around 90°. At higher energies the forward scattering prevails. The position of the Compton edge depends on the atomic number and can vary from tens of eV (in H) to several MeV in heavy elements.

2.2.3 Pair production

The pair production process is energetically possible, when the photon energy exceeds twice the rest mass energy of an electron plus the recoil energy, which is transferred to the nucleus. Due to $m_{nucleus} \gg m_e$ this threshold energy is about 2 $m_e c^2$. The process thus starts at energies above 1.022 MeV. The cross section for this process increases rapidly with the photon energy and for energies above 10 MeV it becomes the dominant effect.

2.3 Drift and diffusion

The secondary electrons created in an ionization event rapidly loose their energy in multiple collisions with the gas molecules. They finally obtain the same thermal energy distribution as the gas which is giving by the Boltzmann-Maxwell distribution:

$$P(\epsilon) = C\sqrt{(}\epsilon) e^{-(\epsilon/kT)} \quad . \tag{2.6}$$

This function gives the probability of finding an electron with energy ϵ at a temperature T.

2.3.1 Diffusion

Electrons and ions in a gas subject only to an electric field move on average along the electric field lines. This phenomenon is called drift. Individual electrons on the contrary deviate from the average due to scattering on the atoms of the gas. Scattering leads to variations in velocity, called longitudinal diffusion, and to lateral displacements, called transverse diffusion. The scattering process in each direction can to a good approximation be considered Gaussian on a microscopic scale.

In the absence of other effects, the Gaussian law for diffusion of a localized charge distribution is the following (1-dim.):

$$\frac{dN}{N} = \frac{1}{\sqrt{4\pi Dt}} e^{-\frac{(x-x_0)^2}{4Dt}} dx \quad . \tag{2.7}$$

dN/N is the fraction of charges found in the element dx at a point x after a time t. D in this equation is nothing else than the diffusion coefficient, which depends on the gas and the temperature. The standard deviation of this distribution is given by:

$$\sigma_x = \sqrt{2Dt} \quad . \tag{2.8}$$

This means that the diffusion increases with the time which makes sense. In the presence of both an electric and a magnetic field, the average motion becomes three-dimensional with components parallel to $\vec{E}$, $\vec{B}_T$, the component of $\vec{B}$ which is transverse to $\vec{E}$, and $\vec{E} \times \vec{B}$. This has as a result that the diffusion coefficient and thus the standard deviation have different components too: these values will differ whether we consider the diffusion parallel or perpendicular to the electric field. The standard deviation can also be used to present the relative difference in diffusion between different gases. In graph 2.3 the transverse diffusion (dashed line) is shown in different Ar-CO_2 mixtures, since this will still turn out to be useful for physical interpretations of our results later.

2.3.2 Drift

In the presence of an electric field, a net movement of the ions along the field lines is observed. The electrons also move, instead of randomly in the case of diffusion, in an orderly fashion along these field lines, but in the opposite direction. Because of the higher mass of the ions, their drift speed is about three orders of magnitude smaller than that of the electrons. The easiest way to represent the drift velocity is by the mobility. In absence of other forces, we then simply get the relation:

$$\vec{u} = \mu \vec{E} \quad . \tag{2.9}$$

The speed is thus parallel to the electric field. The presence of static magnetic fields can change the drift speed. In the time between two collisions the Lorentz force then superposes a circular motion to the linear drift motion. Also electron capture in electronegative gases can occur, which then causes the total number of electrons to decline. The dependency of the drift velocity on different gases is also given in fig. 2.3 (full line). The effect of the gas mixture is more difficult to interpret than that of the transverse diffusion, since it now depends strongly on the fields too.

2.4 Charge amplification

In the previous section we looked at electric field strengths up to a few keV, which allow transportation and collection of the liberated electrons. This mechanism is used in ionization

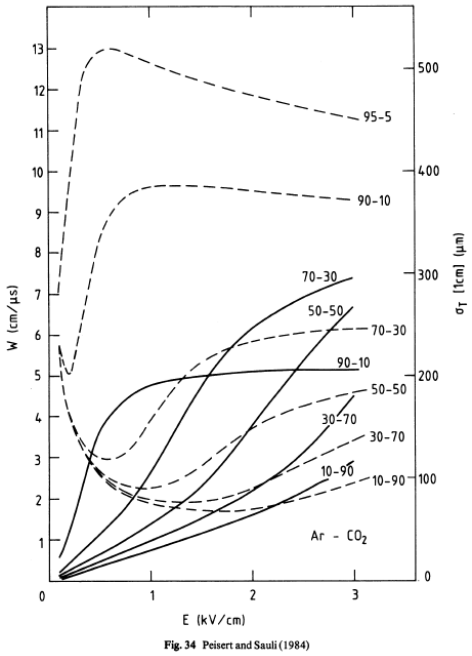

Figure 2.3: Drift (full line) and diffusion (dashed line) properties for Ar-CO_2 gas-mixtures.(Sauli & Peisert, 1984)

chambers for the detection of ionizing particles.
In higher electric fields (above a few keV), electrons receive enough energy in between two collisions to excite and ionise gas molecules. This leads to a multiplication of the primary and secondary charges in an avalanche (fig. 2.5). The avalanche has a drop-like shape, the result of the big difference between electron and ion drift velocity. ($u_e/u_i \approx 1000$) When the energy of an electron increases over the first ionizing potential of a gas, the result of a collision can be an electron-ion pair while the first electron still moves on. The probability for ionization increases rapidly over this threshold and reaches a maximum. For most gases this maximum can be found around 100 eV. This probability is also strongly dependent on the type of gas. (Sauli, 1977)

The basic field regions in which a gas detector works can be easily clarified making use of graph 2.4, which shows the gain-voltage characteristic for a gaseous detector. At very low voltages, charges begin to be collected, but recombination is still the dominant process. Then full

domination (region II) starts: the ion saturation mode is reached. For even higher voltages, multiplication starts setting in and the gain of the detector will start to increase.

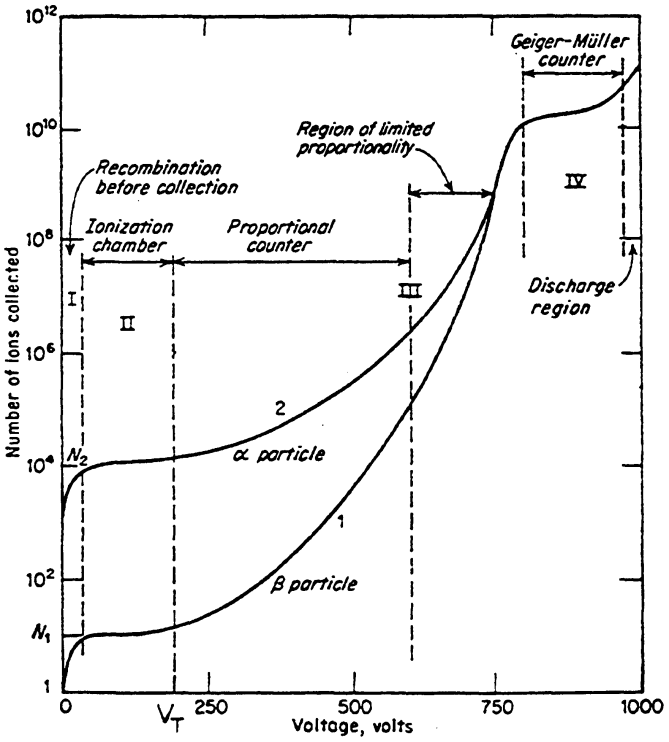

Figure 2.4: The different regions in detector behavior in a gain-rate diagram.(Sauli, 1977)

Three important regions can be found in the multiplication area: the proportional region, the Geiger-Muller region and the discharge region.

2.4.1 Proportional region

The energy of the electrons produced in an ionization process is subject to statistical fluctuations because of the collisions and the energy distribution function. But every now and then an electron will have an energy slightly above the ionization potential and then an ionization event might occur. The statistics are now combined in the average distance an electron has to travel for such a collision to occur: the mean free path. The first Townsend coefficient α is defined as the inverse of the mean free path.

An electron, free to move in a region where a uniform electric field is present, will produce

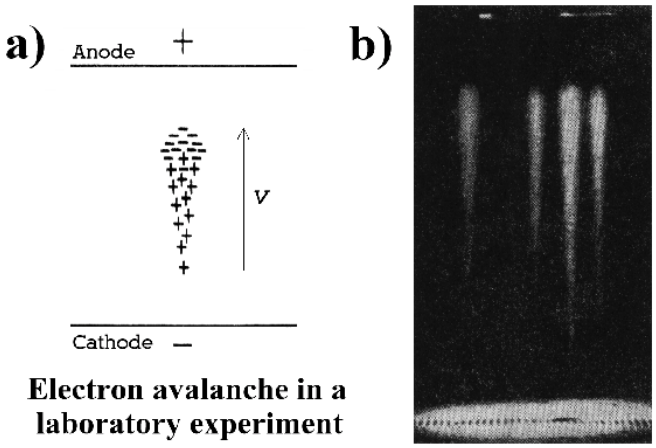

Figure 2.5: The drop-size form of an avalanche.(Stanley, 2000)

one electron pair after a mean free path α^{-1}. Thus two electrons will start drifting and these will create two electron-ion pairs and like this a chain of multiplication occurs. If n is the number of electrons at a certain position, then the increase in this quantity will be after a distance dx:

$$dn = n\alpha dx \quad . \tag{2.10}$$

The first Townsend coefficient is a strongly-depending function of the reduced electric field E/p with p the pressure. Therefore it will depend severely on the position in a non-uniform electric field. The multiplication factor M can then be derived:

$$M = \frac{n}{n_0} exp(\int_{x_1}^{x_2} \alpha(x)dx) \tag{2.11}$$

M can also be called the gain. Usually this integral is not calculated exactly but only an approximative method is used. Most important is that the strength of the signal remains proportional to the energy of the incoming photon. It will, for example, still be possible to notice whether Cu or Fe X-rays are detected.

2.4.2 Geiger-Müller area

At higher fields, the proportionality is gradually lost, because of electric field distortions due to the large space-charge. The positively charged ions move slowly and cause a long dead time because of this. At even higher fields, the proportionality is completely lost and the charge collected per ionizing event is essentially independent of the number of primary ion pairs. At this moment the gas breakdown really needs to be stopped before a new event can

be measured. Therefore the electronics need to be adapted or a quencher needs to be added. (see section 2.6)

2.4.3 Discharge area

At really high fields, secondary processes, like photon emission and the space-charge deformation of the electric field (strong at the front of the avalanche) will lead to streamer formation and a spark breakdown. The Raether condition is a phenomenological limit for the multiplication before breakdown:

$$\alpha x \approx 20 \quad , \tag{2.12}$$

or $M \approx 10^8$. The statistical distribution of the electron energy usually does not even allow to work at gains higher than 10^6 if one wants to avoid breakdown. Also the gap thickness -between electrodes- has a clear influence. The Raether limit will be met at decreasing values of α as the thickness increases.

2.5 GEM-detectors

GEM detectors belong to the proportional area of the previous scheme. On the application of a potential difference (typically 350-500 V) between the two copper electrodes of a GEM, an electric dipole field is created in the holes. The external electric fields are focused in the holes. An example can be found in fig. 1.5. When inserted in the drift field of a gas detector, electrons from the drift volume above are guided into the holes of a GEM-foil, where they are multiplied in a gas avalanche amplification process. Each GEM-hole works as an individual proportional counter. A simulation of a multiplication process inside a GEM can be found in fig. 2.6 During drift and gas amplification, the electrons are subject to diffusion, which causes a fractional amount to be lost to the GEM-electrodes or the Kapton walls. A field dependent fraction of the electron charge is thus collected by the bottom of the GEM electrode, whereas the ions are collected on the top of the electrode.

The ratio between the number of electrons leaving and entering an amplification stage is called the real gain G. Because of the losses occurring at the GEM surfaces, this real gain is not equal to the effective gain which is determined by the magnitude of the anode current. To increase the global gain (a single GEM can yield a gain of 10^3) further, GEMs can be stacked because of their special geometry. At that moment the different transfer fields and induction fields play a more important role. The losses will be larger and thus also the difference between real and effective gain. Fig. 2.7 shows the basic set-up and fields of the different GEMs. The GEMs are numbered starting from the drift electrode and besides drift field, which is the field closest to the cathode, also the terms induction field (from last GEM to read-out) and transfer fields (between GEMs) are used.

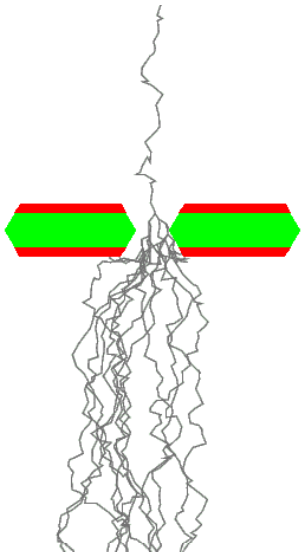

Figure 2.6: Avalanche propagation through a GEM foil.

The ratio of the charge reaching the amplification region to the total charge arriving at the GEM is defined as electrical transparency. As indicated in fig. 2.7 the drift field is applied between the cathode and the top of the first GEM. Depending on the strength of the drift field the field lines go through the holes or terminate on the copper layer. For a fixed GEM voltage and a suitable induction field, the electrical transparency increases, when the drift field is enhanced. At a certain value a plateau is reached. At too high drift fields a certain fraction of field lines end on the copper surface, this means electrons following these lines are lost. The electrical transparency can in certain cases reach almost unity. In a gaseous environment the transparency will be smaller than the one obtained in such an easy field-line calculation. Due to the diffusion losses inside the holes and the statistical process of the gas amplification, a deflection of the electron trajectory occurs. They will not follow their ideal way through the holes like in vacuum anymore, but more of them will end up at the surfaces.

The GEM voltage also plays a role in the transparency. Until now it was always thought that the transparency just increased slowly with the voltage and that at a certain voltage additional multiplication set in. In chapter 6.1 we will show new measurements that indicate that the actual behavior is less simple and that a first maximum in transparency is already reached at very low GEM voltages.

Increasing the induction field increases the collection efficiency. Less electrons will end up at the bottom GEM surface and more will reach the anode. Therefore the induction field is usually set to a rather large value, 3 to 5 kV/cm. At even higher electrical fields, there may be distortions of the GEM geometry (e.g. bending of the GEM foil) which will end up in non-uniformities in the gain profile. The effect of transfer fields is a little less easy

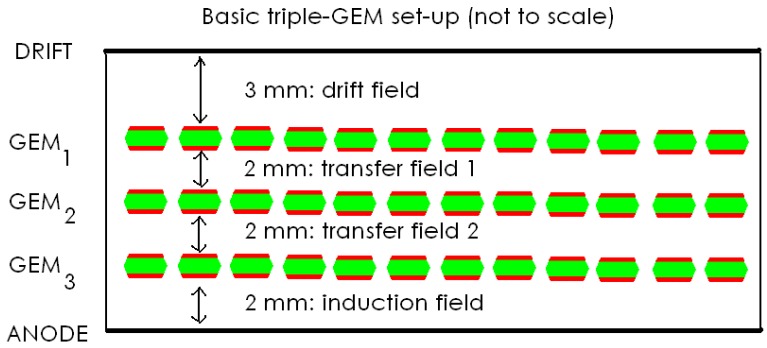

Figure 2.7: A schematic triple-GEM set-up to clarify the used names for voltages and fields.

to understand, since for one GEM it acts like a drift field, while the other one sees it as an induction field. Usually the value is also set rather large (3 kV/cm) and for the magnitude of the signal this turns out -logically- to be the best option. For specific circumstances, however, an optimalisation is required. To give an example: for reduced ion feedback it can be shown that the first transfer field is better set to a rather small value while the other one is kept on his high value. This asymmetric set-up prevents the ions further of drifting back. The value of the drift field depends on the specific use of the detector. For particle tracking a drift field of 1 kV/cm is commonly used while in Time Projection Chambers 150 V/cm is usual.

The biggest advantage of the GEM-detector is probably the separation of gas amplification and read-out stage. This limits the chance of discharges damaging the electronics and offers great flexibility in geometry read-out structures (hexaboard, strips, non-cartesian strips,...) (fig. 2.8). The read-out structure can thus be separately optimized. The distance between amplification and read-out also helps protecting the electronics slightly from discharges.

2.6 Counting gases/quenchers (gas mixture)

The chemical structure of the gas mixture is crucial for the performance of a gas detector. Usually the mixture is made up out of 2 gases with different properties to permit the best detector operation. In noble gases (argon, krypton, helium, ...) avalanche multiplication happens at much lower fields than in more complex molecules. Therefore noble gases are used for the main component that takes care of the electron multiplication in the detector. They are called counting gases. But pure noble gases would make the detector too vulnerable for discharges -they can only return to the ground state through radiative emission- and because of this reason quencher gases are added. These quenchers are usually polyatomic gases, like CO_2 which can dissipate a considerable amount of energy, because they can have

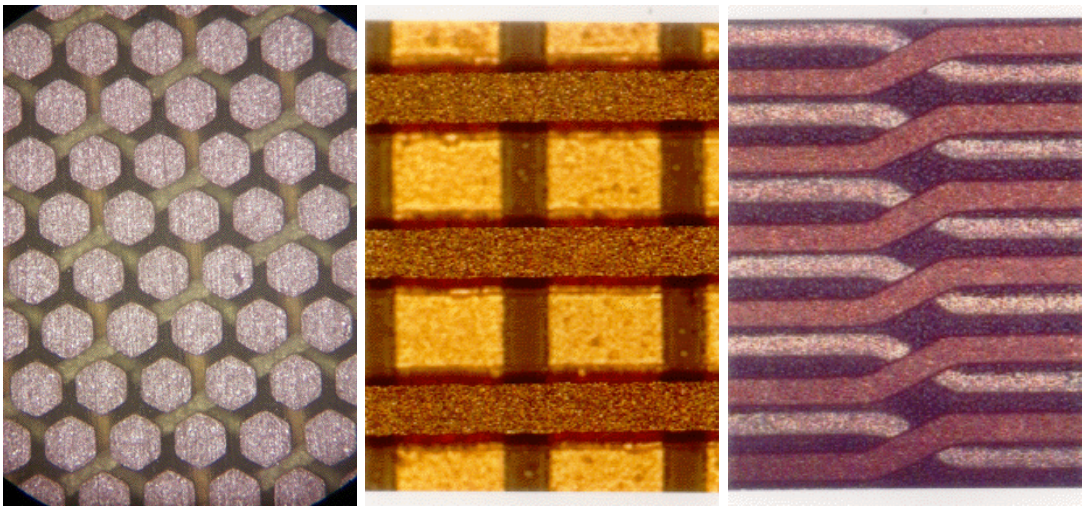

(a) (b) (c)

Figure 2.8: Hexaboard (a), cartesian(b) and non-cartesian (c) strips as read-out system.

radiationless transitions into their excited vibrational and rotational modes. Combined in suitable proportions these two types of gases permit an effective, stable operation of the detector. Their specific qualities can also be exploited. If for example one wants to find out whether the discharges are occurring because of the external electrical circuit, one can fill the detector with pure CO_2. If the discharges continue, the electronics are to blame, since discharges in the gas volume can not occur in pure CO_2. Otherwise, the internal part of the detector, for example the GEMs themselves, cause the problems. Changing the gas mixture can also be used to look at the influence of increased drift and diffusion on the phenomenon. Transverse diffusion, which plays an important role in some GEM phenomena, increases with the ratio of Ar in the mixture, as shown in graph 2.3. This characteristic will be exploited throughout our research.

Chapter 3

Building a GEM detector

3.1 Production of GEMs

Gas Electron Multipliers consist of very thin copper-clad polymer foils perforated with small holes. The production process was created and optimised by the CERN surface Treatment Service (R. De Oliveira. A. Gandi and L. Mastrostefano). A 50 μm insulating Kapton foil with two 3-5μm layers of copper is the starting point of the process.(Hoch, 1998; Bressan *et al.*, 1999)

1. Before the production really starts the surface of the raw foil has to be cleaned.
2. Two identical masks with the desired pattern are realised on a film.
3. The masks are optically aligned with an accuracy of 5 microns.
4. The film has to be coated with a photosensitive layer. Then the foil is inserted between the two masks.
5. The structure is then exposed to UV-light, so that the copper hole pattern is engraved in the photoresist on both sides of the sheet.
6. A conventional sequence of solvent and acid baths is used to etch the metal.
7. Then the Kapton layer gets etched using chemical etching. The pattern in the metal layer serves as a mask and the holes are dug from both sides, producing the characteristic double-conical shape. The technique used for this etching is the ChemicalVia technique. This chemical technique of making microvias was also developed at CERN and consists of 3 different chemical baths ((Na_2CO_3-, $FeCl_3$- and ethylene-diamine bath). With chemical etching it is possible to make lots of small diameter holes in a cheap and fast way. The process always takes 10-15 min, independently of the number of holes desired since all the holes can be formed in the same chemical bath. Using a laser technique it would take around 11 hours, since every hole should be made independently.

8. After masking the hole area, the superfluous copper is etched away, leaving a narrow frame with just Kapton around the structure.

9. To clean the foil from all aggressive liquids it is washed in 4 different bathes: floating water, deionized water, demineralised water and alcohol. Afterwards the foil is dried in air at 80 degrees Celsius.

10. In a first test with an ohmmeter in air, the resistivity between the two GEM foils has to exceed 3 GΩ.

11. The GEMs are packed individually into dust free cotton sheets and a protecting mylar envelope.

In scheme 3.1 one can see the most important steps in the production process shown in a schematic way.

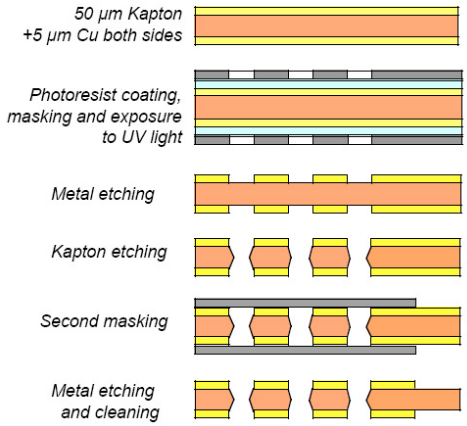

Figure 3.1: Scheme of GEM production process

The final result is a GEM foil consisting of double-conical holes with standard measures of 70 μm diameter and 140 μm pitch.

3.2 Handling GEMs

The electronic circuits workshop delivers flexible GEM foils. These GEM foils then need to be connected to the support in order to get a working set-up. For this reason, the GEMs need to be framed –by Miranda Van Stenis–in frames of 10 ×10 cm. A raw GEM foil, $15 \times 15\,cm^2$ area and a $10 \times 10\,cm^2$ active region is therefore softly stretched by two Plexiglass frames. This stack is then placed into an oven and gently heated to 40 degrees Celsius. Thermal expansion then uniformly extends the foil. Epoxy is then spread over two fiberglass frames

placed on top and bottom of the GEM foil. The stack ends up in the oven again for the time necessary for the epoxy to harden. After moving the support and cutting away the excess Kapton, the framed GEM can be used in a detector.

Already before framing them and also once again after framing, GEMs are checked for discharges and too high leakage currents. The foils are always flushed first first with (non-reactive) nitrogen gas to get rid of the majority of dust particles. Then a 500 V difference is applied between the two copper layers of the GEM. If this already provokes a discharge or the leakage current exceeds 2 nA, then the chances on discharges increase a lot and for this reason such GEMs are not used. If the GEM does not behave properly, then the next scheme is followed in order to save the GEM.

1. The GEM foil is flushed again for a longer period with the nitrogen gas. This step can be repeated several times before seeking his fortune in more drastic methods, especially if the behavior shows improvement after the routine.

2. It can also be that a big short-circuit is found, in such a way that there are no discharges but that the GEM shows a very high leakage current which can even, working hand in hand with the current limit of the HV-source, prevent the foil from rising to the 500 V level. Then connecting the detector to a low-voltage power supply with a high current setting (several hundred microamps) can sometimes burn the shortage and render the foil normal again.

3. If the GEM is still not working, one can still try to return the GEM foil to the electronics workshop where it will be cleaned again in chemical baths.

4. If none of the above methods work, the GEM foil can not be used anymore and has to be replaced.

After checking the GEM performance, the foil can be installed in the mechanical support and after connecting the external resistors with the GEM foils, a final check can be made in a similar way. Grounding one of the GEM ends and connecting the other one to the power supply yields the final check.

3.3 Our experimental set-up

3.3.1 Detector

For all our measurements s high level of flexibility was desired. Therefore we made use of a special designed research detector. A schematic drawing of such a detector is shown in fig. 3.2. This basic set-up structure allows flexible changes in the number and type of GEMs, the distances between the plates and the read-out and the powering scheme.

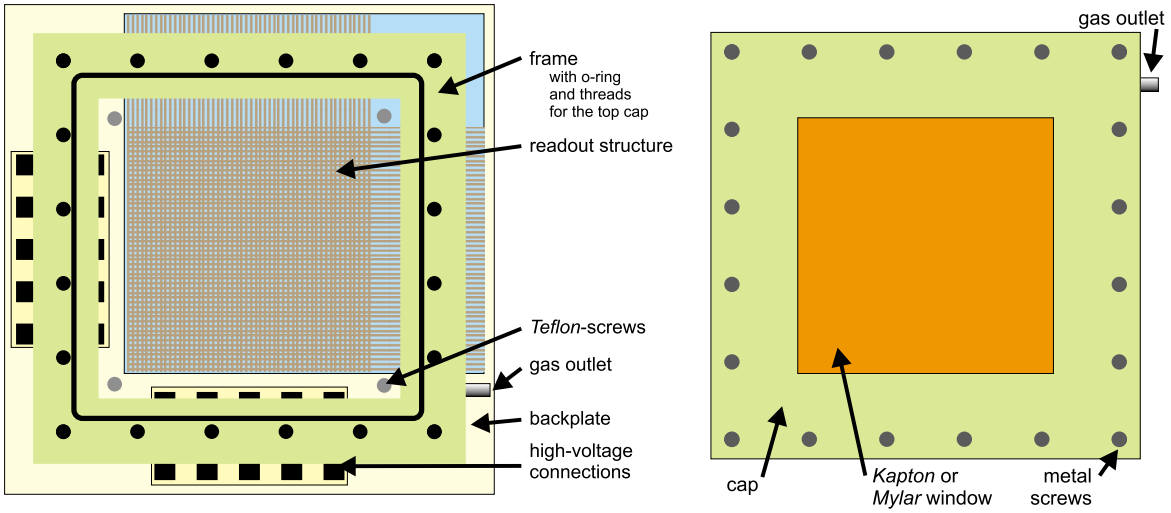

Figure 3.2: Schematic drawing of our experimental detector.Kappler (2000)

The read-out structure (pads or strips) is placed on a fiberglass backplane. Then a fiberglass frame is glued to the structure around the read-out structure, permitting external read-out. Also the high-voltage connections and a first gas outlet can be found in this frame. A second frame part, also made out of fiberglass, also host a gas outlet, so that the detector can be constantly flushed with the detector gas. This frame also has a Kapton or Mylar window through which the X-rays can enter the detector. The two frames are kept together by metal screws while rubber joints provide gas tightness.

This detector supports GEMs and read-out structures of $10 \times 10\,cm^2$. GEM foils and drift cathodes (either a full metal-Kapton plate or a metal mesh) are mounted on thin square frames (see 3.2) with 4 holes in the corner, as can be seen in fig. 3.3. These can be mounted on Teflon screws. Insulating spacers together with the frame (thickness usually 1 mm, 0.5 mm on each side of the GEM) define the distance between the two GEMs and also between GEM and read-out. For the read-out, usually strips or pads are used. A full metal plate can also be used as a read-out, ensuring an easier read-out but also provoking more electronic noise.

3.3.2 X-ray sources

Most of the time we use a collimated beam of soft X-rays, coming from a X-ray generator. These X-rays are created on a Cu-target and thus the X-rays have an energy of 8.9 keV. This beam has a Gaussian profile and we have different size collimators for the beam. The X-ray generator is also mounted on an optical set-up, permitting us to move it flexibly in different

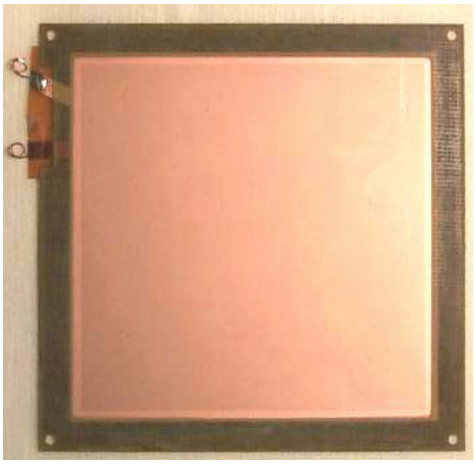

Figure 3.3: A framed GEM foil.

directions. The intensity of the generator can be changed by changing the filament current. This current can be changed from 0.04 to 4 mA and so we can change the intensity of the beam –without use of absorbers– over two orders of magnitude. Sometimes we also use an ^{55}Fe source that yields us 5.9 keV X-rays, but we do not obtain a nicely collimated beam then. Just for checking whether the detector works, sometimes a more powerful beta-emitter, ^{90}Sr, is used. This leads directly to electrons which can be measured.

3.3.3 Voltage set-up

To set the correct voltages, a voltage divider is strongly recommended. A discharge and thus sudden decrease of one of the voltages then leads to a global decrease of the voltage. As such, extremely high fields in the structure are avoided. With separate power supplies, the local decrease could provoke a big difference for example in the transfer field leading to destruction of the detector. In order to reduce the chance of discharges, the first GEM foil (closest to the drift electrode) has the highest voltage difference, while this value decreases with more or less 10% over each foil, as described in section 4.4. The transfer and drift fields are also pre-set by the resistor values. Usually the global voltage is set to reach a gain of more or less 8000, the standard working condition. In our experimental set-up we work with separate high-voltage sources in order to keep more freedom of operation. This leads to more broken GEMs but because of the easy accessibility of the detector and its components. This does not cause major problems, since the GEM foils can very easily be replaced if a problem occurs. The high level of flexibility that comes with these seperate power supplies is just indispensable for our research.

3.3.4 Gas system

As gas mixture, we have to use a combination of a noble gas and a quencher. In our system we usually use the combination of argon and carbon-dioxide. The advantages of this combination are that it is a relatively cheap mixture, non-toxic and non-flammable. Therefore we can use it in an open gas system, which is easier to operate. Quite often we just use a premix of Ar-CO_2 70-30 in our set-up, since this has similar diffusion properties as the gases used in the real detectors. This also improves the reproducibility of our results. The gas flow can be adjusted by a flow meter. If we want to vary the gas mixtures, then we connect Ar and CO_2 to separate flow meters. By setting the values for these meters, the fraction of Ar and CO_2 and the total flow of the gas mixture can then be chosen.

Chapter 4

Characteristics of GEM detectors

In this chapter we would like to go deeper into the physics and technology behind GEMs, discussing the operation mode as well as the most striking physical phenomena.

4.1 Spectrum

Ionisation of the counter gas –Ar in our case–by X-rays is the key process. As X-rays enter the detector, they interact with gas molecules through photoelectric absorption. In the majority of the cases a photoelectron and an Auger electron (resulting from the rearranging the excited gas molecule) are emitted and the full energy is deposited in the sensitive volume of the detector and thus detected. The peak position in an energy spectrum is now proportional to the energy of the X-rays and therefore we can detect the difference between Cu 8.9 keV and ^{55}Fe 5.9 keV X-rays.(Sauli, 1977)

If the energy of the X-rays is greater than the threshold energy for an argon K-shell ionization (3.203 keV), then the X-ray may create an extra Ar-Kα or (less likely) Ar-Kβ X-ray. Only Kα X-rays from elements with Z $\geq$ 19 have sufficient energy to excite Ar-Kα X-rays. If such an event now occurs and if the Ar-Kα X-ray escapes from the detector, an amount of energy is lost from the detector equal to the energy of the escaped Ar-Kα X-ray (i.e., 2.958 keV). The initial X-ray would still create Ar^+/e^--pairs, but the number of such pairs will be less than should have been produced. In this case, a pulse is still collected, but its corresponding energy is less than that of the incident photon by an amount equal to the energy of the Ar-Kα photon. The total number of weaker pulses make up what is called the **argon escape peak**.

Because of this phenomenon, the spectrum now shows two peaks. The first one will be visible in the energy spectrum at an energy of 8.9 keV, which is simply the peak coming directly from the energy of the Cu X-rays. One will also see an argon escape peak at around 6 keV. This one will contain less counts. An example of a spectrum recorded with a GEM-detector can be found in fig. 4.1. One can easily observe the two contributions. The energy resolution of

a spectrum recorded by a GEM-detector can also be derived from this curve. The full width at half maximum is more or less 18% at 5.9 keV. For Fe X-rays we will get the main peak at 5.9 keV and the escape peak at 3 keV. A rule of thumb can be used to differentiate between the spectra. The spectrum from the X-ray generated beam with a Cu cathode has a ratio 2:3 between the energy of the peaks, while the escape peak of Fe is located in the spectrum at half the energy of the main peak.

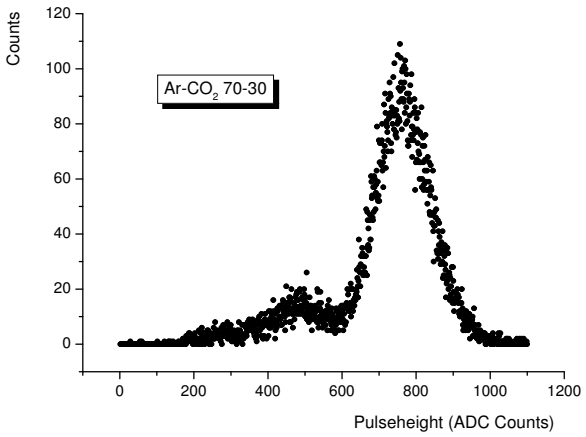

Figure 4.1: Typical pulse height spectrum recorded by a GEM detector for 8.9 keV X-rays.

4.2 Charging-up

One of the most characteristic features of GEM physics is charging-up. Charging-up takes place when one starts irradiating the detector. Because of the biconical geometry of the holes and more precisely of the kapton layer, some of the field lines at first hit the kapton surface. Because of this, more and more electrons are collected on one side of the hole, while the other side is filled with ions. These space charges in the kapton layer slightly increase the electric fields in the GEM holes and thus the gain increases as well. The field lines are bent a bit more to the middle of the holes and less field lines reach the kapton surface. This rise continues until an equilibrium is reached in which no field lines end up at the Kapton anymore. Measurements with standard GEMs indicate a gain increase of more or less 20%. This rise already takes place in a matter of minutes and the memory of this event turns out to be around a day. So even after stopping the irradiation, the gain will stay a bit elevated during several hours. This charging-up is a local effect since it is caused by space-charge accumulation which can only take place under irradiation.

Measurements with cylindrical GEM holes gave more support to the theory behind the

charging-up mechanism, since they hardly showed any increase in gain. This is to be expected since the field lines are not likely to end up at the kapton surface. To put it more precisely, the field charges seem to accumulate in order to get the field lines to become parallel to the kapton surface. With cylindrical GEMs this comes down to no difference for the field orientation, while a standard GEM squeezes the field lines together in the middle. A conical GEM, on the other hand, shows very strong charging-up if the GEM is used in one direction and very little if it is used in the other direction. The strong charging-up takes place when the electrons enter at the wide side of the GEM and therefore have a big chance of hitting the kapton surface before being extracted at the narrow side. (Bachmann *et al.*, 1999b)

Charging-up, once understood, does not give rise to major problems with GEM operation. A short period of strong irradiation already leads to the maximum charging-up of $\propto$20% after which the gain stays constant if one does not take pressure and temperature changes into account. But most of the GEMs fabricated by industry show enhanced charging-up and other strange phenomena which can turn out to be problematic for the GEM operation. In graph 4.2 an example of bad behavior is shown. This graph shows the results we measured using a GEM of an American company, Tech-Etch. In section 4.6 we will discuss these GEMs and their necessity. A factor 4 of charging-up even without irradiation can be derived from the curves. Irradiation provokes a decrease in the gain. This decrease depends on the precise level of irradiation. More irradiation yields a bigger decrease. Actually a double effect takes place here. A global increase, probably caused by the polarisation of the material, gets superposed with a local decrease caused by the irradiation. Reducing the irradiation leads again to an increase of the gain. Every level of irradiation has its equilibrium which can be reached in any way. Coming from a stronger irradiation, it will be reached after a period of increasing gain while increasing the intensity of the X-ray generated beam leads to a decrease. In region one the detector was only irradiated for half a minute every five minutes (to perform a pulse height measurement). After not irradiating the detector for an hour over lunch, the gain had increased even more, but starting again irradiation at the old regime the same equilibrium value was reached. Increasing the radiation, first by irradiating constantly at low intensity (region 2), then by increasing the beam intensity in 2 steps (regions 3 and 4) lead to further decreases. The behavior is clearly different from that of a normal GEM, which just shows a 20 % increase after a few minutes.

This phenomenon causes problems using GEM detectors and can not be tolerated. As shown in section 4.6 the problems with the Tech-Etch GEMs have been solved.

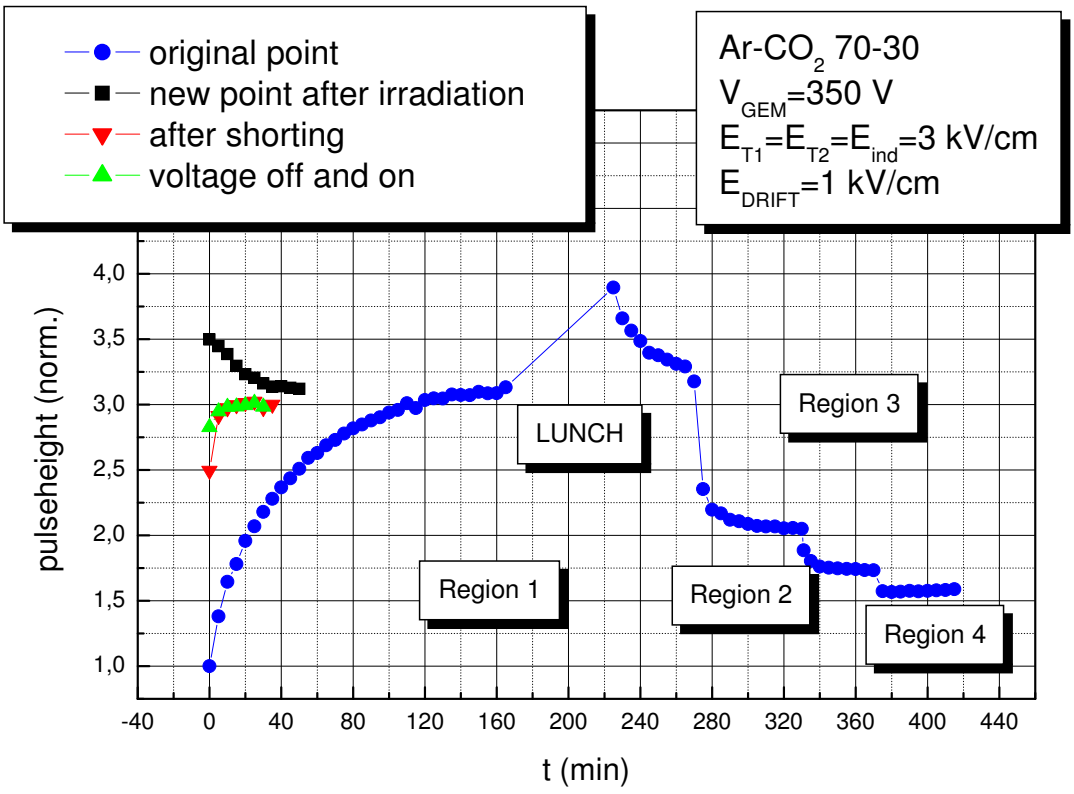

Figure 4.2: Strange charging-up behavior of a Tech-Etch GEM. Explanation in text.

4.3 Long-term stability and aging

GEM gains turn out to be dependent on temperature and environmental pressure like in almost every gas detector. This causes the gain to shift slightly during long term measurements and this could influence the measurements slightly. These fluctuations can be as large as 20 %. (Altunbas *et al.*, 2002) Because of this researchers tend to correct for these effects. This can be done in two ways. First the temperature and pressure can be monitored at the same moment so that their influence can be taken into account later. But this also presumes that these dependencies are almost perfectly known, though the precise shifts are usually difficult to predict. That is why a different easier and more straightforward method is preferred: to put a single-wire counter, irradiated constantly by a radioactive source, in series with the GEM detector. This single-wire counter will undergo the same pressure and temperature changes and even small shifts in the gas mixture will turn out to be similar. In this way one can subtract these influences in order to get the pressure- and temperature-independent signal. Of course this method is not completely exact, since the response to the fluctuations will be a bit different for the two detector types, but a good estimate can be made in this

way.

In most of the micropattern detectors one of the most occurring problems is aging.(Altunbas *et al.*, 2003) Aging effects lead to surface degradation of the electrodes and the read-out. In general, active species produced in the avalanche plasma, attack the electrode surfaces or a kind of organic deposit can be produced. This deposit can then collect electrons (a kind of charging-up) and in that way deform the electric fields. (Sauli, 2003b) Aging effect will only show in long-time irradiation, since the results accumulate. This can worsen the detector operation. According to experiment, GEM detectors suffer very little from such aging effects. Even with the rather large COMPASS detectors no aging effects would be visible after normal operation during 7 years. (Altunbas *et al.*, 2002) Possible reasons for this excellent behavior, might be the large area available for polymer deposits and/or the independence of the gain from the presence of a thin insulating layer. Also the fact that the amplification takes place in the holes, far away from the read-out and electrodes can explain this good performance. (Altunbas *et al.*, 2002)

4.4 Discharges

One of the major problems micro-pattern detectors have to deal with are the discharges. The high electric fields used for the amplification can, certainly at certain sharp edges, provoke discharges. These voltage drops can be devastating for the detector and ruin the strips, the read-out or the electronics. So these discharges need to be avoided as much as possible and the detector has to be able to resist them, since they (being a statistical phenomenon) can never be entirely excluded. The first method in trying to avoid them is using GEMs that do not show any indications of deterioration. For this reason the GEMs are tested repeatedly before installing them into the detector.

GEMs are able to stand discharges quite good since the hole geometry is not affected by them. The read-out is also separated from the detector protecting the electronics some more. But in real operating circumstances some discharges will normally extend to the read-out plane and thus hit the electronics. That is why usually special protective chips are made to disconnect these high voltage differences from the real read-out system. These circuits are tested by provoking discharges, for example by guiding strongly-ionizing particles, like alpha's into the detector. If the electronics survive this raid of discharges, then the protective chips work as they should.

Another interesting feature of GEMs with regard to discharges is the possibility of stacking them. One GEM-plate with a voltage of over 500 V necessary to reach a standard gain of 8000, will discharge quite easily because of the necessary high voltages. If on the other hand, one manufactures a triple-GEM, then every plate only has to yield a gain of 20, more than two

orders of magnitude lower. The required voltages and thus the discharge probability decrease. This is one of the main reasons why stacked GEMs are used and it also points down one of the main advantages of this type of detector. Asymmetry in the voltages over the different GEMs can even lead to a further probability decrease. Bachmann *et al.* (2002) showed that a 10% higher voltage on the first GEM than on the second foil and then again a 10% lower voltage over the third one, gave the smallest discharge probability.

The discharge probability can be measured by inserting highly ionizing particles in the detector. Usually alpha-particles are chosen for this research. An ^{241}Am-source can be used for the introduction of the alpha's or a mesh of Thorium, decaying to gaseous ^{220}Rn, can be inserted in the gas flow. (Bachmann *et al.*, 2002) In our research we used the second method. First the number of alpha-particles entering the detector should be calibrated. This is done by counting the pulses at low amplification. Fig. 4.3 shows a measured spectrum of the alpha particles. This spectrum has a peak value and then an exponentially decreasing tail. The amount of energy lost is dependent on the distance the alpha crossed and thus from the direction in which it was emitted. On the oscilloscope one can also see the alpha-particles crossing the different GEM foils. When the alpha passes by all the plates, three pulses are recorded almost simultaneously in the detector because of the voltage drops over the three plates. The alpha particles are emitted in all directions in the detector by the radon damped off from the Th-mesh. That is why there is such a strong distance dependency of the energy spectrum. After determining the alpha rate, we can determine the discharge probability by counting the number of discharges occurring in the detector. We performed such discharge studies for GEM foils with larger holes (100 μm instead of 100 μm for standard GEMs), since these GEMs had better behavior concerning charging-up and rate capability (chapter 5). The results presented in graph 4.4 show that the discharge probability is a lot higher than in a standard triple-GEM detector. Already for gains around 8000 the discharge probability is not negligible anymore. Asymmetry in the applied voltages leads to an improvement but not sufficient enough to make this type of detector suitable for use in today's detectors.

4.5 Gain: definition, rate and voltage dependency

The experimentally measured values of effective gain show an increase of the gain with reducing hole diameter, keeping the pitch constant. This rise stops around 70 μm, the value used for standard-GEMs. Measuring all the currents in the structure, it was deduced that the real gain was actually still increasing and thus did not show saturation.(Bachmann *et al.*, 1999b) It turns out that more and more electrons end up at the bottom of the GEM if the ratio between hole diameter and GEM thickness descends to 1 keeping the effective gain constant .

For us the effective gain is the most important, since this is actually what we measure. The

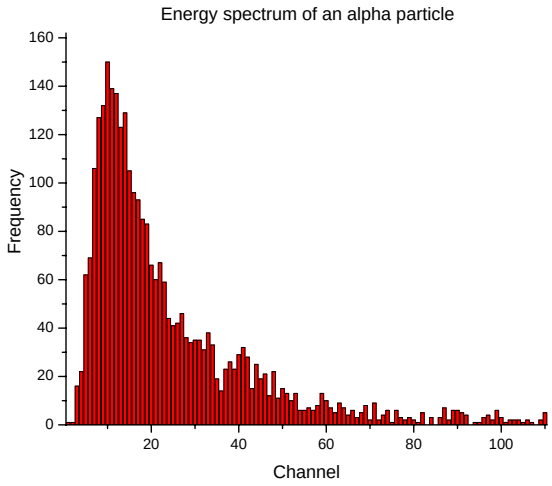

Figure 4.3: Energy loss spectrum of an internal ^{220}Rn α source.

effective gain can now be calculated as:

$$G_{eff} = \frac{I}{n_{tot} Re} \tag{4.1}$$

with I the current in Ampere, R the rate and e the electron charge (1.602 10^{-19} C). n_{tot} is the number of primary and secondary electrons.

Rate dependency of the gain was investigated up till rates of around $10^5 Hzmm^{-2}$. No gain decrease of other effect was observed, which indicates very good high-rate behavior of GEMs. This could be useful, since particle physics experiments require detectors that can stand more and more severe conditions. Also for plasma diagnostics GEMs are an option because of this good rate capability. We investigated this independence at even higher rates (exceeding $10^6 Hzmm^{-2}$), which gave surprising results. (chapter 5)

Of course the effective gain depends also strongly on the voltage. Amplification sets in with a standard-GEM around 250-300 V and then the increase is exponential. The voltage dependency of the detector gain is quite important, since sufficient gain is necessary for good operation. After assembling a new detector (at least if it is not a standard one, of which the properties are well-known), the first thing we do is measuring a gain-voltage curve. This helps us in further research determining the voltages necessary for operation. Fig. 4.5 shows such a graph measured for the triple-GEM detector with big holes (100 μm) and standard pitch(140 μm). In order to compare this behavior with the basic one, we also remeasured the curve for the standard (70 μm) triple-GEM chamber.

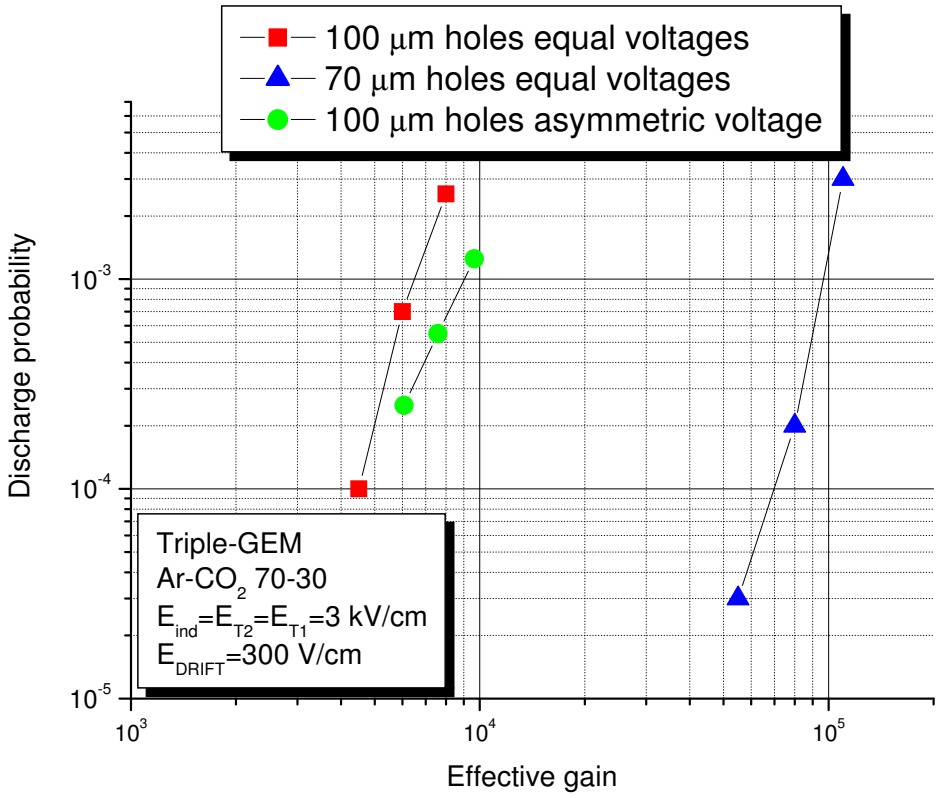

Figure 4.4: Discharge probability in triple-GEMs with bigger holes compared with standard GEMs.

4.6 Other GEMs

For different reasons other types of GEMs seem to be useful. Therefore we investigated their properties. In the following section reasons for the use of three types of special GEMs and the obtained results are presented.

4.6.1 Tech-Etch GEM

The majority of GEMs are still fabricated at CERN. This poses a problem for the industrial uses of the detectors. The CERN production capacity is not large enough to provide industry with GEMs and priority is given to high-energy experiments. Therefore the GEM-future outside of the laboratory could be limited. The last few years more and more companies have tried to produce GEMs but had some problems because the manufacturing process is not described in detail. The used chemical baths for cleaning have not been revealed completely. One of those companies, Tech-Etch, contacted us to test their GEMs. A first test revealed big flaws in their method. The GEM, as described in section 4.2, showed a peculiar type of charging-up. The material seemed to get polarized and therefore gained a factor 4 in

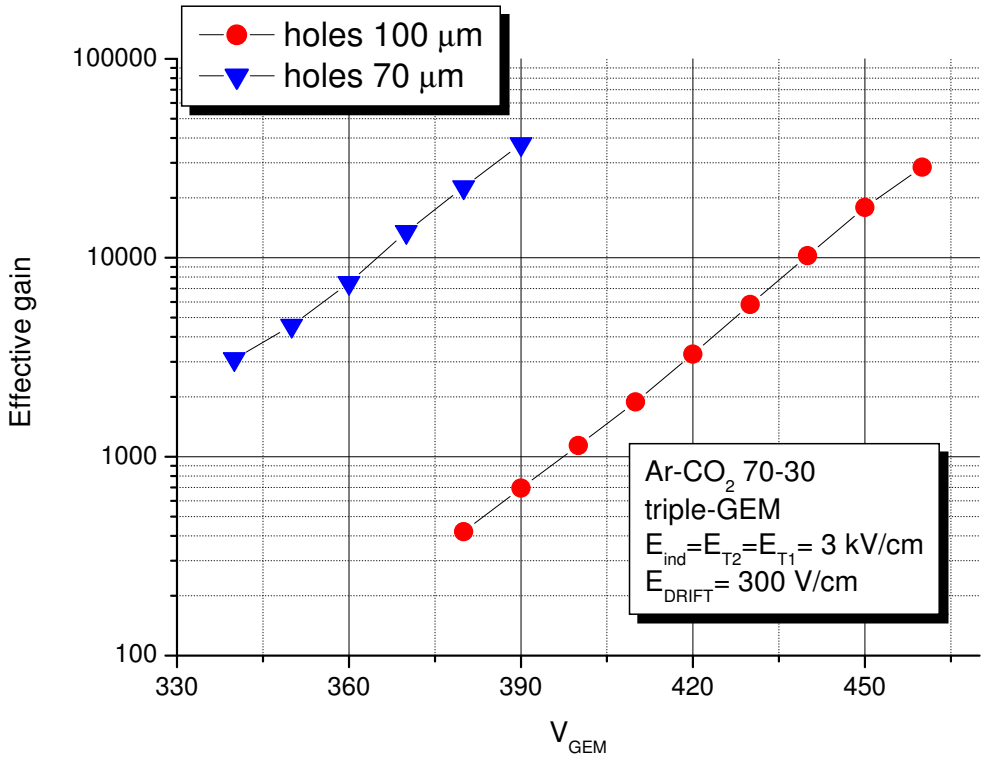

Figure 4.5: Voltage-dependency of the gain for a triple-GEM with large (100 μm) and one with standard (70 μm) holes.

effective gain. Radiation seemed to enhance a local lowering of the gain which was completely contradictory to standard GEM behavior.

We therefore performed a material test in which we used their basis material but the GEM was manufactured at CERN following basic CERN routines. This GEM gave normal results, excluding the different isolator from the list of possible causes. Tech-Etch changed their method of manufacturing a little and a second test was performed on these new GEMs. A general behavior which was very similar to standard GEMs was observed. Two kind of GEMs were distinguished in the group. One was biconical like standard CERN GEMs and they showed the usual gain increase of 15-20%. A second group had more cylindrical holes and also here the effect coincided with the CERN cylindrical GEMs: a small decrease, a charging-down, was observed. The outcome of this research was that clearly the detergents and cleaning methods used during production play an important role. It would also be useful if Tech-Etch would come to a standard procedure for creating the GEMs so that all GEMs would automatically have the same geometry and therefore this should not be checked in advance anymore. Then all the Tech-Etch GEMs would also show the same charging-up

behavior.

4.6.2 GEMs with large holes

GEMs with larger holes than and the same pitch as the standard GEMs have many advantages. The electron transparency increases and the charging-up decreases because the holes are more cylindrical. On the other hand, the energy resolution deteriorates a little. But because of their strong behavior on electron transparency, their possible use in GEM detectors was checked. First, the charging-up was checked and as expected, was lower than that of standard GEMs. The charging-up turned out to be just below 10%, this better behaviour is due to the fact that the large holes, created in the chemical baths, are less biconical than the standard GEM holes and therefore have less excessive Kapton. Also the high-rate phenomenon -rise between 10^5 Hz mm^{-2} and 2/,10^6 Hz mm^{-2}, which we will discuss in section 5.3 was less pronounced and therefore the gain stayed more or less stable at higher gains.

A possible problem was an increased discharge probability. It had been noticed in the past that cylindrical GEMs, because of the less shielding by Kapton between the two sides, showed increased discharge probability. Moreover, larger GEMs require higher voltages to create the same fields at the center of the holes and to obtain the same amplification. To reach the same gains, 80-90 volts higher voltage than in standard GEM operation was required. The discharge probability seemed to worsen with more than an order of magnitude, as shown in graph 4.4. At gains of around 4000, discharges were not negligible anymore, which makes the detector impossible to use (standard working gain 8000). Even exploiting the asymmetry of voltages, which reduces the discharge probability according to Bachmann *et al.* (2002) did not help enough to make the discharge probability acceptable for use in a GEM detector. So the use of GEMs with larger holes seems to be limited.

4.6.3 Conical GEMs

Another problem GEMs are encountering at this moment, is the eternal quest for larger detector areas. Until now that was solved by combining small GEMs. But future experiments really ask for large GEMs. One of the main limitations for making large GEMs is the production process with the precision of two masks at both sides of the GEM. With even larger areas to cover, this alignment will become even harder. Conical GEMs could give a solution since they can be manufactured by using only one single mask. (Benlloch *et al.*, 1998a) The alignment is then not necessary anymore. This idea of a conical GEM was abondonned in the early days of GEM-technology. (Bressan *et al.*, 1998) For single-GEMs the discharge probability turned out be too elevated. But perhaps the use of triple-GEMs and the extra knowledge that was acquired through the years could provide an outcome for the problems. Conical GEMs could then become a good option after all.

The first results seem to be encouraging. The charging-up behavior of single conical GEMs could be extrapolated to the triple structures. Placing the GEMs in such a way that the electrons enter the GEM at the narrow side, results in almost no charging-up. Placing the GEM the other way around has devastating results with a rise in gain of over 50% occurring, so this mode of operation is no option. The narrow-to-wide positioning on the other hand has another problem: a slightly elevated discharge probability. Moreover the voltages are around 60 volts higher for the same gains. The discharge probability seems to be too high when working with equal GEM voltages. But inserting asymmetry in the voltage, causes the discharge probability to shift. Now a gain of 20.000 can be reached before a noticeable discharge probability occurrs. This points out that the detector can have practical use after all. The ion feedback seems to be similar to the standard case. The energy resolution is worsened at low drift fields, but seems to be sufficient for fields over 400 V/cm. One of the major problems that still has to be overcome, is the lack of uniformity. Because of the chemical etching method used, the holes have a lot of small flaws and differences. Especially the narrow side is quite non-uniform. This leads to differences in the observed gain. In the triple-GEM detectors, fluctuations of not less than 50% were observed, while this is limited in a standard set-up to less than 20%. Perhaps improving the etching technique could yield a solution here.

4.7 Summary

Quickly resuming the main characteristics and performances of GEM-detectors:

- Operation in most gas fillings, including pure noble gases
- Proportional gains above 10^5
- Energy resolution 18%FWHM at 5.9 keV
- Space localization accuracy 60μm rms or better
- Rate capability above 10^5 counts/mm^{2}sec
- Active areas up to 1000 cm^2
- Flexible detector shape and readout patterns
- Robust, Low cost

Chapter 5

Rate capability

One of the main limitations of multiwire proportional chambers is their rate capability. Especially in today's high-luminosity events that gives rise to problems. Crossing the limit of $10^4\,Hzmm^{-2}$ yields considerable space-charge effects, leading to a decrease of the gain with the rate. The micro-pattern gas detectors like GEMs (Altunbas *et al.*, 2002; Bressan *et al.*, 1999), have been proven to keep a constant gain for rates up to $10^5\,Hzmm^{-2}$. A decrease of the gain was so far never observed and as such GEMs were thought to have a stable gain for even higher rates. The main limitation to GEMs would then be the discharge probability. In this chapter we will try to cross the $10^5\,Hzmm^{-2}$ and look at even higher rates, even more challenging future experiments in mind. Benlloch *et al.* (1998a) attempted these measurements as well but working with a single-GEM the gains that were accessible for them ($\propto 100$) were too low, therefore limiting the practical use of their result.

5.1 Set-up

Our usual small prototype chamber (fig. 5.1) was used for these tests. It was filled with a full metal plane as read-out board, three standard GEMs at 2 mm distance of each other and 2 mm distance from the read-out. Pushing the X-ray generator to maximum intensity, gave insufficient rates with the standard drift set-up (full plane and 3 mm drift space). Therefore the full Kapton\ copper plane was changed into a metal mesh and the drift space was increased to 13 mm. The measurements were always done with pulse-height spectra as long as the rate permitted it, for the higher rates we changed to current measurements and rates estimated by putting an absorber in front of the beam. In standard conditions we used the gas mixture $Ar - CO_2$ 70-30. The fields were adapted on the situation. A high induction field seemed for example useful to avoid discharges and reach slightly higher rates at high gains.

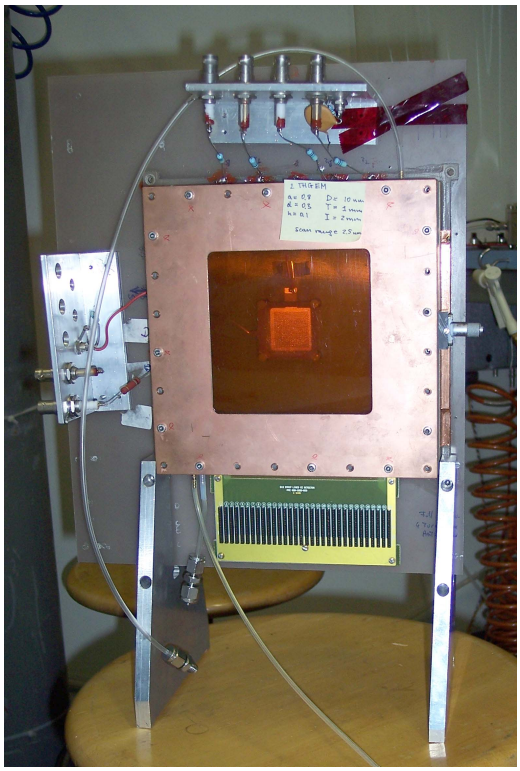

Figure 5.1: Our standard detector chamber.

5.2 Method

To measure the effective gain, we used a combination of two commonly used methods. At low rates we measured the pulse height spectrum of the signal with a peak-sensitive analog-to-digital converter (ADC). The basic read-out program, written in Quick basic, just records the spectrum and writes it to a file. To measure this pulse height spectrum, we needed to turn down the intensity of the beam in order not to get too high event rates for our electronics (limit $\propto$ 20 kHz). Since our X-ray generator only allowed changing the beam over 2 orders of magnitude, the minimum rate was still too elevated for pulse-height and rate measurements. Therefore we introduced copper absorbers to lower the rate even further. First we calibrated them, as shown in graph 5.2. (Since they are not pure copper, the slope of the curve is a little bit different than expected.) Then we worked with these absorbers to measure the pulse height at low rates. With the absorbers we were also able to calibrate the intensity of the X-ray generated beam. We measured the rate with absorbers at different current settings for our X-ray generator. Our calibration then permitted us to extrapolate these numbers to the ones we would get without absorbers. A basic pulse height spectrum can be seen in fig. 4.1.

The second part of the measurements were done in the current mode. We measured the

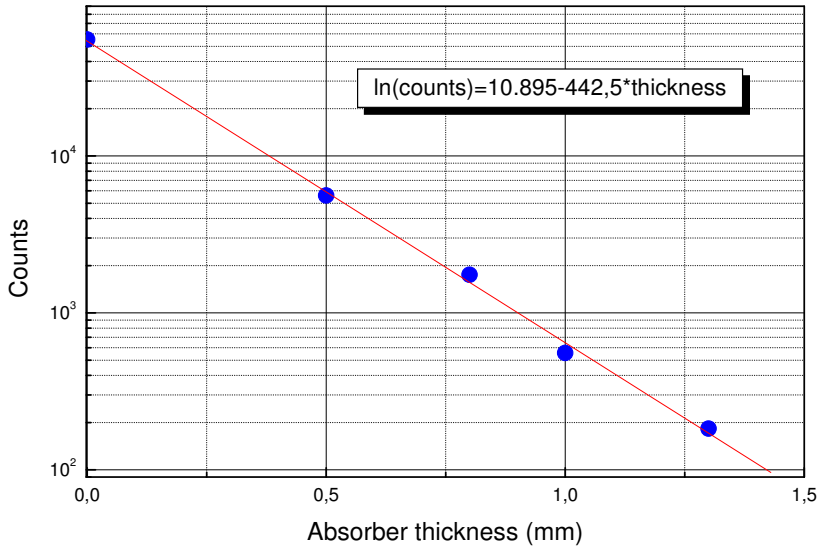

Figure 5.2: Calibration curve for our absorbers.

current on the anode plane and together with the estimated rates –which we get from the combination of data in the pulse height mode and absorber calibration–this gives us the effective gain according to formula 4.1. We also needed to measure the current in the last point of pulse height operation, since pulse heights only give a relative idea of the gain and do not give an absolute value. The pulse heights depend on the amplification settings of our electronics and changing the electronic amplification does not make a difference in gain but would make a difference in our measured pulse height. Therefore an independent current measurement which determines the absolute value of the gain at one point of the pulse height measurements is necessary. The other absolute values can then be deduced using the relative differences measured in the pulse height and this one current-measured value. At the low rates where pulse height measurements were performed, current measurements would not have been possible because of the very small currents. The results would then lose relevance because of the limited accuracy of our current measurements. We were able to determine currents only with an accuracy of about 0.4 nA.

5.3 First results

For the voltages the start conditions were 350 V over each GEM and the transfer fields were set at 3.25kV/cm. The induction field was with 5.5kV/cm slightly higher and the drift field (350 V/cm) considerably lower. The shown effect (fig. 5.3) came as a big surprise. GEMs did

not seem to be stable at very high irradiation rates, but while most detectors start loosing gain at very high rates, there was a clear increase of the gain in this detector. The second part of the curve did however show the expected decline. In this first measurement the decline was less obvious than in later experiments, but it can still be noticed. The rise immediately indicated to us possible difficulties occurring in the measurements. A kind of charging-up (4.2) could be involved or perhaps the GEM-currents were responsible for the effect. A systematic research seemed crucial for pointing down the main characteristics of this phenomenon.

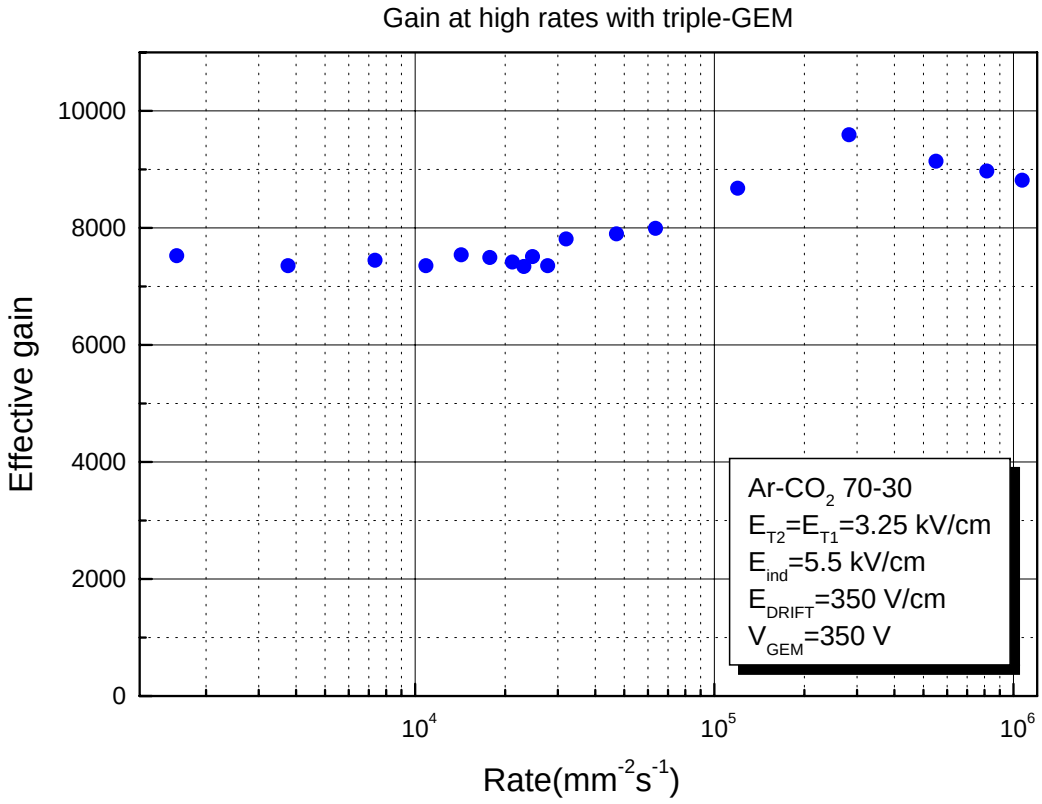

Figure 5.3: Evolution of gain at high rates.

5.4 Possible errors

Before writing the measured phenomenon down as a real effect, we needed to exclude any possible errors made and typical GEM phenomena.

5.4.1 Counting methods and measured currents

The first effect to exclude, was that of our **absorbers**. At the high rates we were measuring we could not directly measure the rates but we used calibrated absorbers. We tried to improve this method first by checking the pulse height spectrum with and without absorbers and then we verified the exponential dependence of the thickness by only using absorbers of different thickness made out of the same material (copper). Both measurements pointed out that the problems were not due to this method. To exclude all doubts, we then decided to direct the beam to our single-wire counter and to check whether the relative relationship between these rate measurements and pre-set beam intensity were still the same. This measurement confirmed that our method for determg the rate was valid.

At first we also thought the **GEM-currents** might influence the measurement. So different initiatives were taken to check this effect as well. First, the resistors were changed from 10 to 1 MΩ. Now the effect of the currents had to be considerably smaller, but the gain-rise nor disappeared nor decreased. We also changed the size of our collimator. Now we ended up with the same order of magnitude of the currents at a much lower rates/mm^2. The total number of events stayed the same, so the total currents were similar. The bigger collimator irradiated with lower beam intensity per surface area did not provoke the rise and therefore the effect was clearly not GEM-current-induced. Actually this was also observed with the measurements with only slightly different (factor 2) collimators which showed exactly the same rise at the same rates despite their different size.

5.4.2 Time dependency: charging-up?

One of the first possible explanations we also thought about was charging-up, since this was the only phenomenon known so far that leads to a gain increase. As explained in paragraph 4.2 the gain increases in this case as a function of irradiation time. Some of the field lines end at the beginning on the insulating Kapton layer. The electrons and ions which are conducted there get caught by the Kapton, because of its insulating character. This leads to an increase of the electric field in the GEM and thus to a higher gain. The charging-up takes place in a couple of minutes, but since an insulator does not quickly release charges, the memory of the phenomenon is several hours, sometimes even longer than a day. Because of this time dependency it could easily be checked whether this phenomenon was due to charging-up. It would then be an advanced kind of charging-up since the normal phenomenon is well-known and -researched.

Therefore we checked the time-dependency in 2 different ways. First, we tried to change the place of the beam during the measurement, making sure that it was no local effect (like normal charging-up) and was really an intrinsic property of the whole GEM. Therefore we moved the beam around to change the irradiation point. We also measured the graph twice,

once in the normal direction, going from low to high rate, once immediately after the first measurement in opposite direction, going from high to low rates. If charging-up was occurring we would expect the second curve to end up with higher gains at low rates because of the phenomenon's memory. Since in both cases the opposite effect was observed, this initial idea of super-charging-up had to be abandoned.

5.5 The influence of various parameters

In order to understand the phenomenon better, we decided to look deeper into the effects it undergoes when parameters are changed. Voltages, fields, GEM geometries, etc. were changed in the hope that this would increase our insights.

5.5.1 GEM-voltages

We started by keeping the GEM-**voltages** of the three foils at an equal value while changing this value. In this way we changed the gain of the detector without focusing on the different importance of the separate GEMs. The used field settings were always the same: transfer fields at 3.25 kV/cm, induction field 5.5 kV/cm and drift field 350 V/cm. From the results represented in graph 5.4 two effects can be recognized:

- The absolute magnitude of the effect increases with higher gains.
- The effect starts for a higher gain at a lower rate. This shows that the effect is probably due to a high concentration of charges, which would occur quicker at higher gain.

These two influences are even likely to be correlated.

Of course also the differences between GEMs could play a role. The bottom GEM for example gets hit – as the last step of the multiplication process–by the highest number of electrons. Therefore we decided to change the relative voltages of the different GEMs, keeping the total gain at high rate ($2\,10^6\,Hz\,mm^{-2}$) constant. This lead to the graph shown in figure 5.5. The drift field was kept at 300 V/cm, while the 3 other fields were 3 kV/cm. From this graph two influences can be deduced:

- The higher the voltage on the first GEM, the stronger the anomalous effect. This seems to have the strongest influence.
- Decreasing the voltage on the last GEM seems to have a similar but smaller effect.

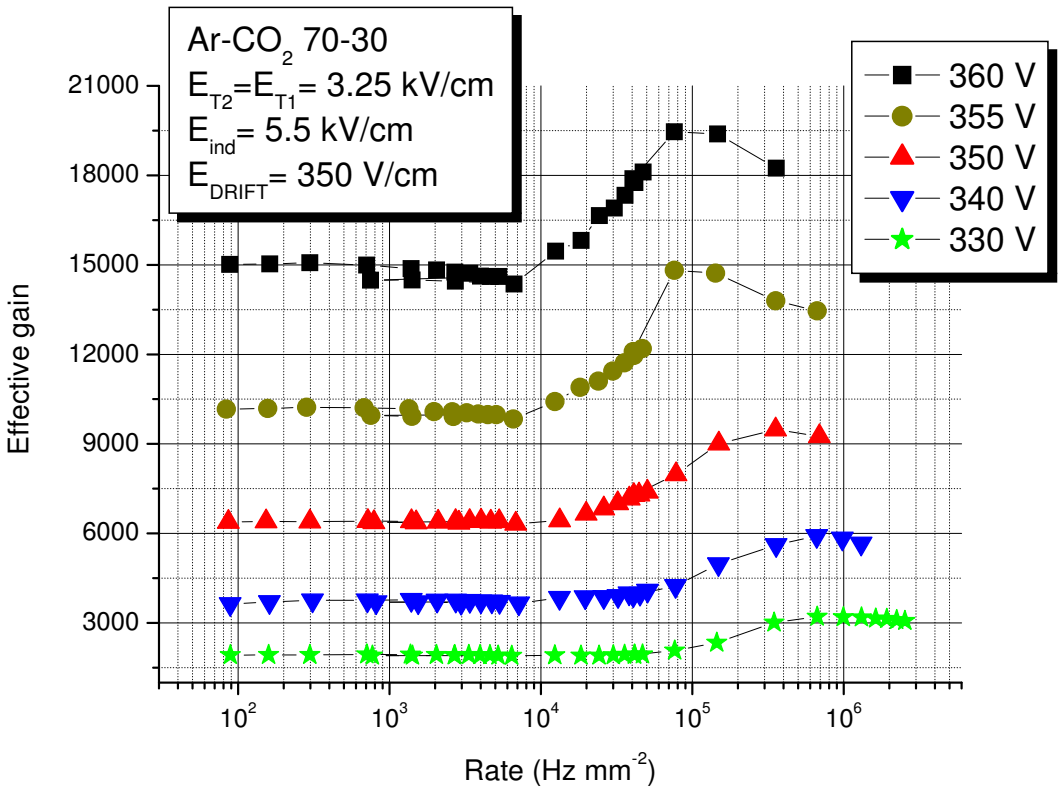

Figure 5.4: High rate for different, but equal GEM voltages

5.6 Gain-current

One of the recurring explanation possibilities was a space-charge phenomenon. In that case the total charge would determine the effect. This could explain why at lower gains higher rates were needed before the increase was observed. To check this idea, we did not need extra measurements, but we plotted the old ones in a effective-gain\current plot (fig. 5.6). From this graph it can be easily derived that the rise starts at more or less the same anode current. This points even more in the direction of a space-charge effect. The currents are the same, so also the number of electrons will be more or less the same and apparently there is a minimum number of electrons that need to be attained before the gain starts to rise.

What can also be deduced from the graph, is the influence of the voltages. In this graph we did not plot the effective gain, but we plotted the effective gain normalised to the first point of the current measurements ($\approx 5000\, Hzmm^{-2}$). Apparently the proportional rise is smaller if the voltage is higher. If this would be correct, then we would expect that a double-GEM employed at more or less the same gains, shows an even lower rise. Reaching the same gains in a double cascade understandably asks for higher voltages over the GEMs. Graph 5.7 proves

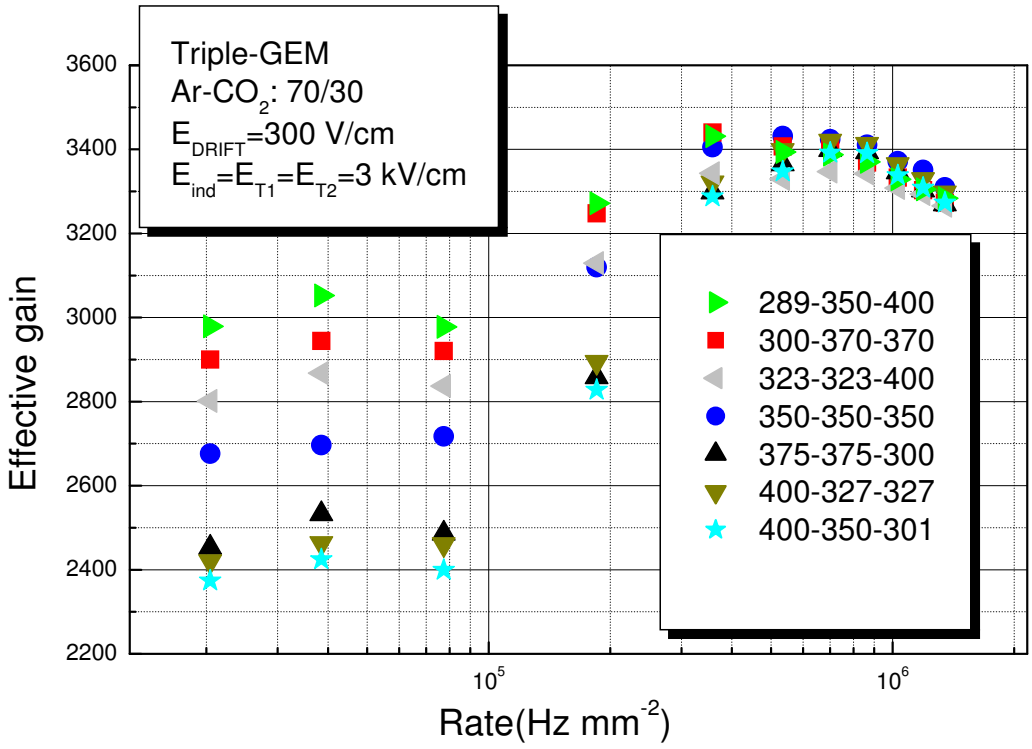

Figure 5.5: High rate measurements with changing voltage ratio.

this idea.

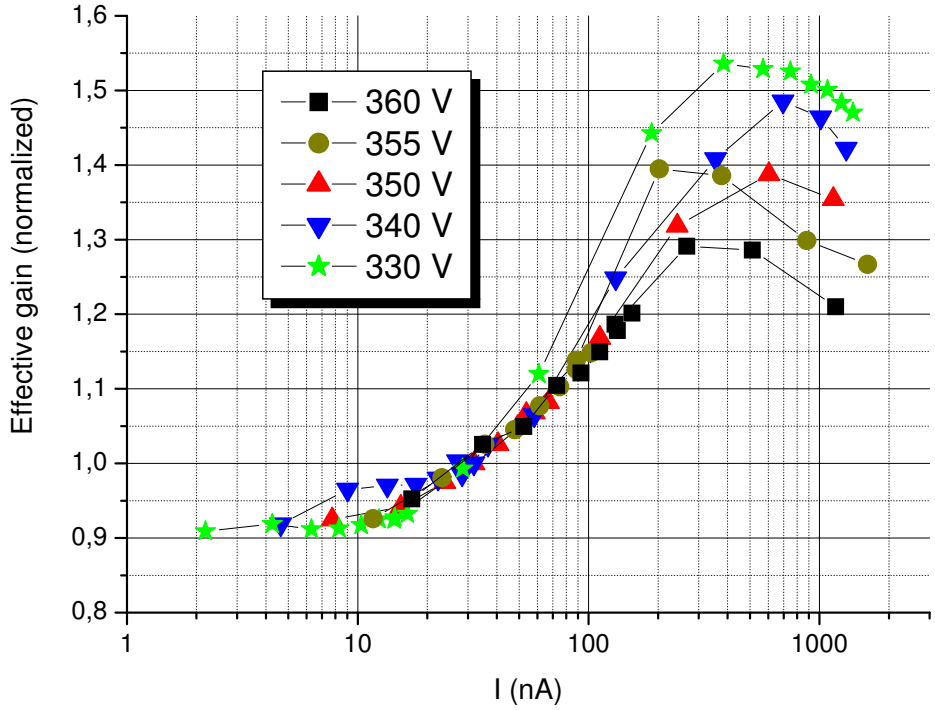

Figure 5.6: Effective gain as a function of the measured anode current for equal GEM voltages, indicating a space-charge effect (see text)

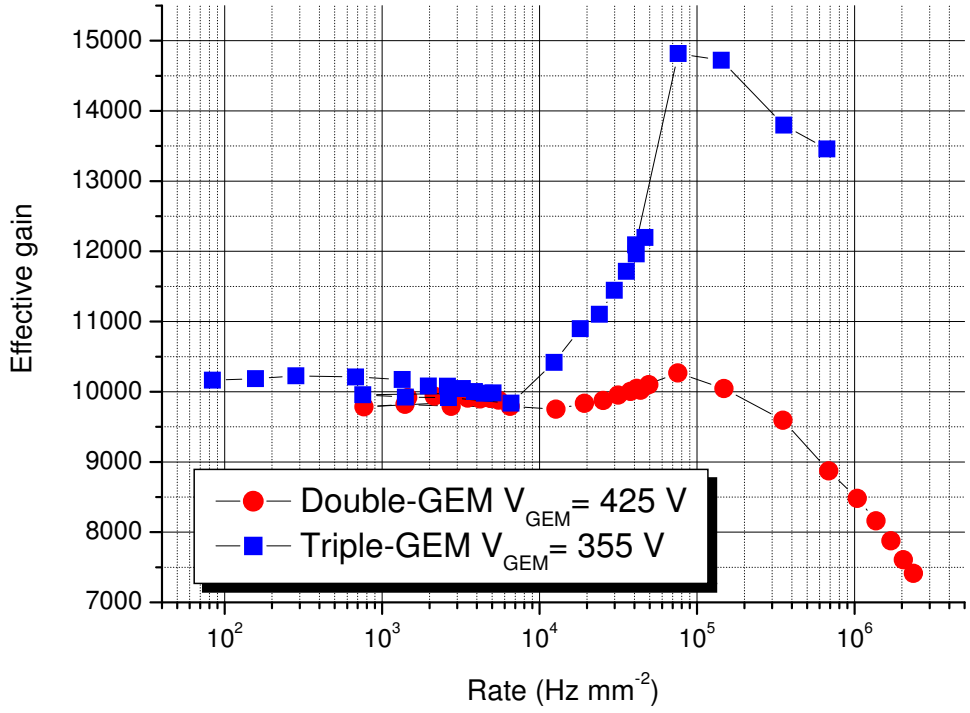

Figure 5.7: Comparison of the high-rate effect in a double- (425 V) and triple- (355 V) GEM

5.6.1 Gas mixture and flow

Changing the **gas mixture** had an obvious influence. $Ar - CO_2$-mixtures were always used but the fraction of the two components were changed to change the drift and diffusion properties. The GEM voltages were also adapted so the measurements could be done at the same starting gain of around 4000. The field settings were once again 3 kV/cm for transfer and induction fields and 10 times smaller for the drift field. The effect shown in graph 5.8 is that a bigger content of argon in the gas mixture, increases the effect. The transverse diffusion increases with the Ar-fraction (fig. 2.3) and so perhaps this could lead to the electrons being more strongly attracted into the holes. The drift velocities of course also play a role and their effect is less clear since their behavior in such a gas mixture depends on the exact values of the different fields. Above 3 kV/cm, the drift velocity of electrons in a 50-50 mixture for example surpasses that of the 90-10 variant. (Binnie, 1985).

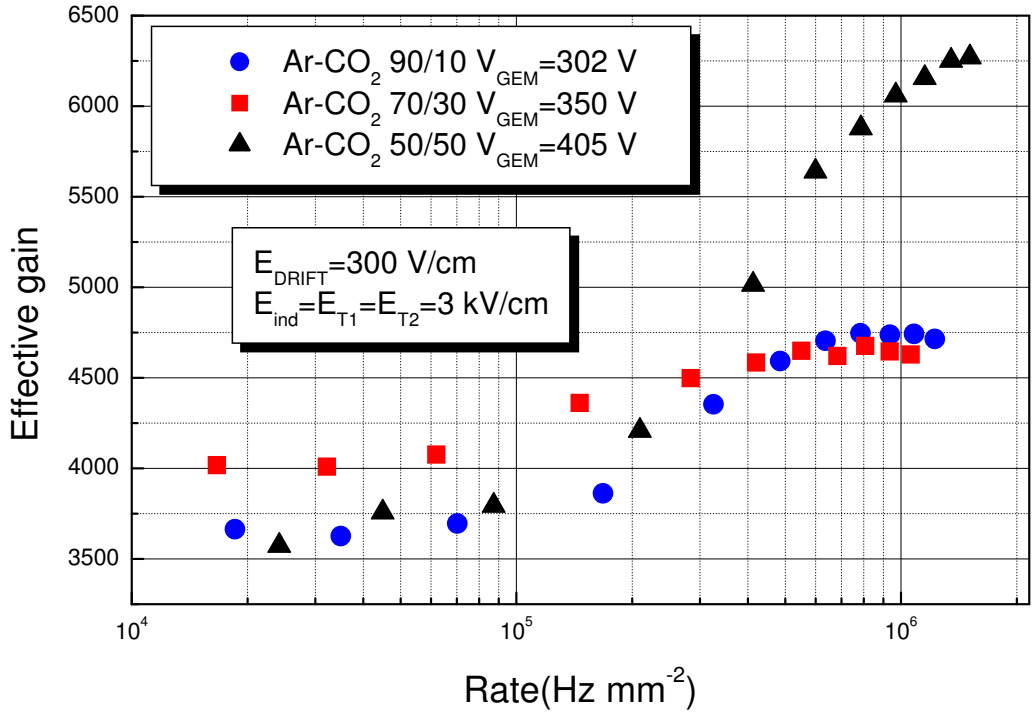

Figure 5.8: Influence of the $Ar - CO_2$ gas mixture.

Changing the **gas flow** did not have any clear influence.

5.6.2 Different fields

Studying the influences of the different **field** settings pointed out that the drift field had hardly any influence on the high-rate effect. The induction field showed the same lack of influence. Decreasing the transfer fields on the other hand had a clear result on the gain at high rates. The high-rate increase followed its tendency: a decrease of the transfer field also decreased the intensity of the phenomenon. In fig. 5.9 the graphs obtained by changing the first transfer field are shown. Those for the second transfer field look similar. In this graph there are two curves shown for lower transfer fields. Since the gain also decreases we wanted to check whether the reduction of the effect was only due to these lower gains and thus the smaller absolute values or whether the lower transfer fields also led to a smaller relative effect. Therefore the gain of the first GEM was slightly increased so that the starting point would overlap with the curve for the higher transfer field. The curves show very clearly that a real relative reduction occurs when the transfer fields are lowered.

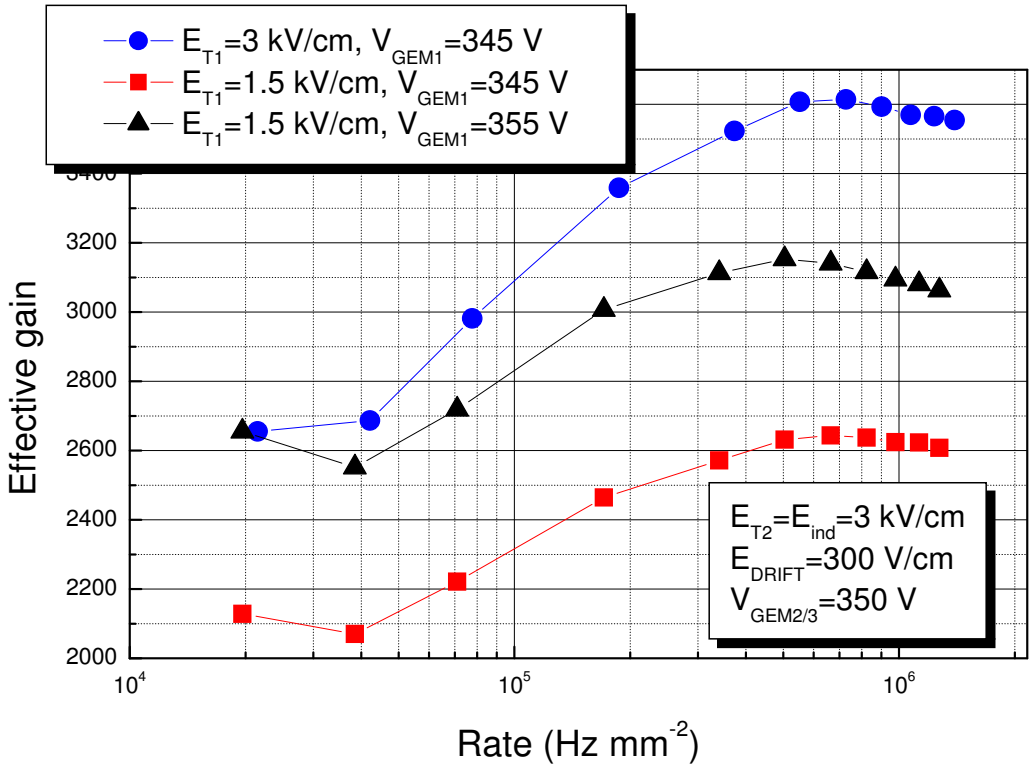

Figure 5.9: Influence of first transfer field on high-rate phenomenon.

5.6.3 Different configurations: GEMs+set-up

Changing the configuration was first done by introducing special GEMs in the structure. (fig. 5.10). A GEM with bigger holes, but the same pitch as the standard GEM did only show an effect when it was introduced at the bottom of the detector as GEM closest to the read-out. At that moment a clear decline occurred. As first GEM (close to the drift) no effect could be recognized. The voltages over the GEMs were adapted in such a way that the gains at low rates were similar. This observation implies that the charges would gather at the bottom GEM to form a space-charge.

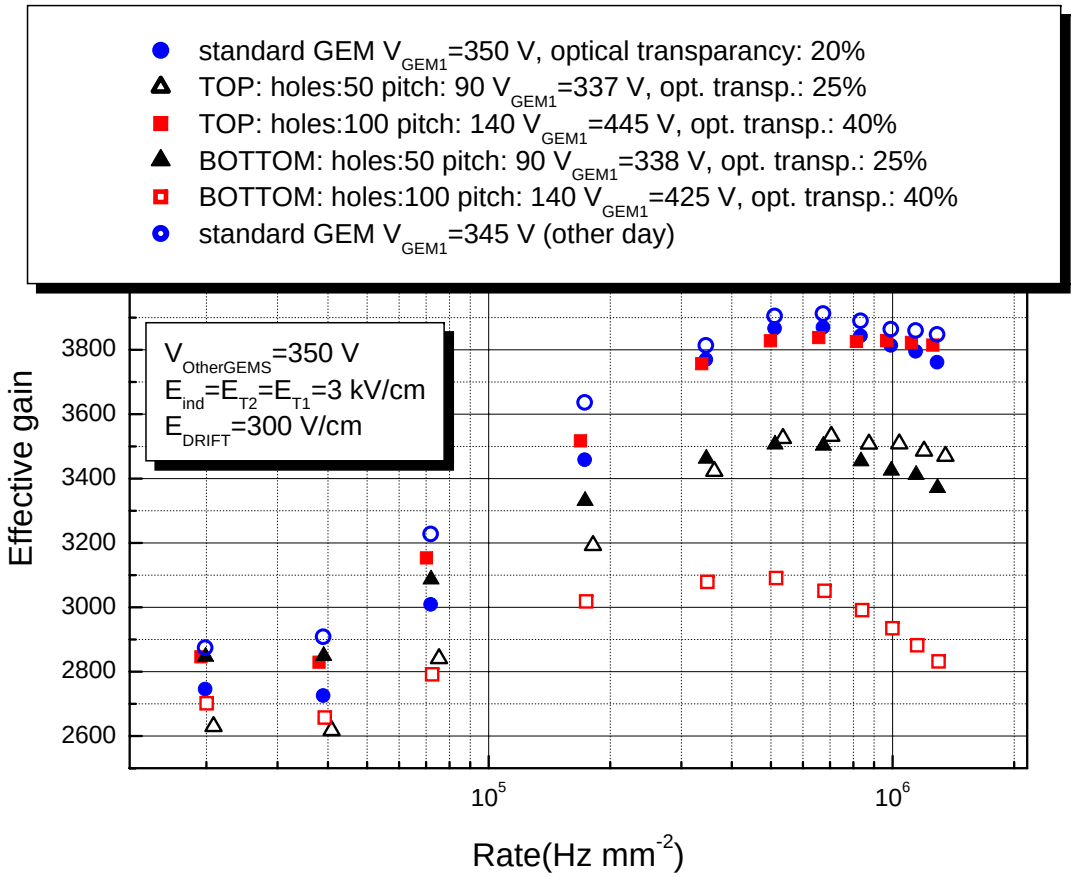

Figure 5.10: Using special GEMs with different hole diameter and pitch in high-rate measurements.

Introducing the GEM with smaller holes and smaller pitch, gave the same effect regardless of its exact position: a small decline of the effect. Checking the hole to surface ratio –the so-called optical transparency– of the GEM pointed out that this one was in between the standard GEM and the one with the big holes, thereby confirming the previous effect. Why the weakening occurred when placing this GEM closest to the drift, was not clear.

The observation with the GEM with standard pitch but bigger holes and also the gain-current measurements points to a space-charge accumulation which causes the phenomenon. Checking this was done with a complete triple-GEM detector made out of 3 GEMs with such big holes. These measurements (fig. 5.11) confirmed our suspicion and showed a considerable lower rise. This made this type of GEMs look more favorable to use –they also show less charging-up– but a discharge study (section 4.4) showed that the detector already had problems with discharges in the normal working area.

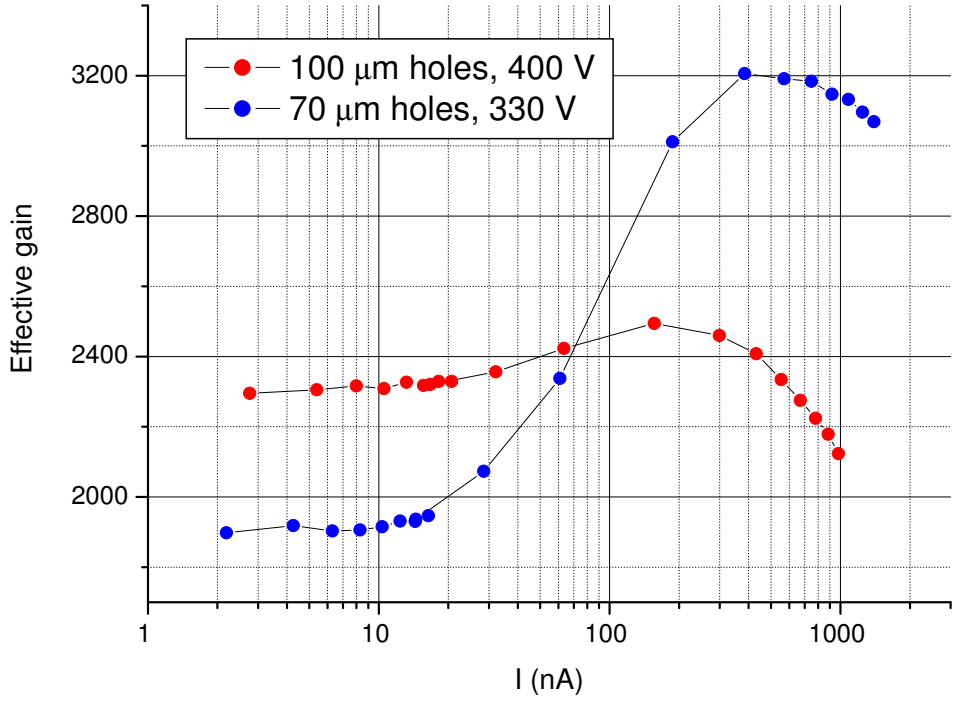

Figure 5.11: High rate dependency of a triple-GEM assembled from 3 foils with big (100 μ m) and standard (100 μ m) holes.

Changing the drift and induction **spaces** did not result in any changes. Comparisons between **single- double and triple-GEMs** showed that the effect was not noticeable with a single-GEM, probably due to the lower number of electrons and lower currents in this case.

5.7 High-rate limit of GEMs

Another result that can be deduced from all the previous measurements, is that there is a high rate limit for GEMs. The short rise only causes minor problems because it only asks

for corrections in the read-out if we are able to document the phenomenon extensively and to understand it completely. The gain gets even higher and so minimum ionizing particles can still be easily detected. What could pose a bigger problem, is that after the short rise, the effective gain starts to decrease, this can be seen in many of the graphs, for example fig. 5.4. This limits the use of the GEM detectors because lower gains could hinder the detection of particles. This limit for high-rate operations of GEMs seems to lay around $10^6\,Hzmm^{-2}$. This is still considerably higher than what has been reached with all other kinds of detectors, but does limit its use in more exotic fields like plasma diagnostics.

5.8 Conclusion

This systematic research indicated that a rise in the effective gain is occurring for rates between 10^5 and $10^6 Hzmm^{-2}$. This rise seems to be caused by a space-charge effect. The detector also seems to start loosing gain for rates over $10^6 Hzmm^{-2}$. The difference between our results and those of Benlloch *et al.* (1998a) can probably be explained by the lower gain and therefore the lower level of accumulated charge for the latter. In our case the space-charge will be around 100 times higher.

Chapter 6

Ion feedback

6.1 Time Projection Chambers (TPC)

A time projection chamber (TPC), introduced by Nygren (1975), consists of a gas-filled cylindrical chamber with gas detectors (nowadays often MWPC's) as endplates. Along its length, the chamber is divided into two halves by means of a central high voltage electrode disc, which establishes an electric field between the center and the endplates. Furthermore, a magnetic field is applied along the length of the cylinder, parallel to the electric field, in order to minimize the diffusion of the electrons coming from the ionization of the gas and to help determining the momentum of the detected particle. On passing through the detector gas a charged particle will produce primary ionization along its track. The z-coordinate, the coordinate along the cylinder axis, is determined by measuring the drift time from the ionization event to the MWPC at the end. This is done using the usual technique of a drift chamber. The two-dimensional gas detector, a multiwire chamber or a GEM detector, determines the other coordinates. The TPCs 3D localization makes it extremely useful in tracking charged particles in a high-track-density environment, and for identifying particles through their energy loss (dE/dx) due to ionization.

6.2 GEM-TPC

In conventional TPCs the end-caps consist out of multi-wire chambers. Avalanche amplification takes place around the anode wires, creating electrons that induce signals on the read-out plane under the wires. This type of detector provided good energy and spatial resolution for most of the experiments until now. The next generation of detectors, built for advanced linear colliders like the ILC, has to perform even better in both aspects. So, one has to try to reduce the present limitations. One of the major problems at this accuracy scale is the E×B distortion. During the last few mm of the drift region, the electric fields get superposed with the radial electric fields of the anode wires and thus the electrons encounter a region

Figure 6.1: The STAR projection chamber.

of non-parallel electric and magnetic fields. This causes deflections of their trajectory in the direction of the wires. In strong magnetic fields these effects result in a broadening of the electron cloud and a worsening of the resolution. The fact that induced signals are used, also leads to a broader cloud of arriving electrons and thus limits the granularity of the TPC.

The ions created at the wire (creating electrons can of course not be done without creating a similar amount of ions), drift away from the wire with an initially high drift velocity When leaving the region of enhanced electric fields, the ions slow down and add a slow component to the signal, a so-called ion tail. Ions can also build up macroscopic space-charges which change the electric fields and thus the drift properties of the next spill of electrons. Ion-gates can be used to reduce the ion feedback to values under 10^{-4}.(Amendolia *et al.*, 1985; Blum & L., 1993)

GEM-TPCs are able to overcome many of these shortcomings of traditional TPCs. The easier mechanics and especially the fact that no wires need to be tensed leads to increased robustness of the detector. Because GEM detectors are based on charge collection instead of induction, the signals are narrow, faster and do not have an ion-tail. With faster electronics the resolution can therefore be strongly improved. Also the single-point accuracy and multi-track resolution is strongly enhanced. The electric fields above the GEMs and in the holes are also parallel to the magnetic field which strongly suppresses the E×B distortions. (Sauli, 1999; Killenberg *et al.*, 2003)

GEMs also have a natural tendency to suppress ion feedback in these circumstances. This is a result of the combination of a low drift field (typical 150 V/cm) and a moderate/high transfer field (typically several kV/cm). Most of the ions formed in the multiplication process in the holes of the first GEM, will because of this be attracted to the upper GEM-electrode, strongly

reducing the number of ions released in the detector volume. Because of this, the distortions by ions of the electric field are also strongly suppressed. The fractional ion feedback, defined as the ratio between the number of charges released in the drift space (in our case collected on the drift electrode) and on the anode, can in an optimalisation process be reduced to 2.5 per mille. (Killenberg *et al.*, 2004; Sauli, 1999)

However, this value is still slightly too high. There will still be a space-charge accumulation of ions which will distort the electric field. To get completely rid of this disturbing effect, the fractional ion feedback should be lowered another order of magnitude. A standard working gain of 10^4 for minimum ionizing particles should be taken into account, a limit set by today's electronics. A fractional ion feedback of 10^{-4} would have as a result that the number of re-injected ions equals that one of the primary ions. This rough estimate points out that a working TPC requires even lower ion feedback values. The further reduction can for example be done with the conventional pulsed gating mechanisms. But this would cause major mechanical and electrical complications for the detector and would undo some of the big advantages. The mesh structure, consisting of wires with a few mm spacing, would introduce extra field distortions and thus E×B effects. We decided to look at a few alternative solutions.

6.3 Direct measurements

Basic ion feedback measurements were performed to better understand the influence of transfer fields and different GEM geometries. These direct measurements were made hoping to reduce ion feedback even further without having to use gating or other special techniques.

6.3.1 Different fields

The influence of the different transfer fields was investigated in a standard triple-GEM detector (and afterwards in detectors with slightly different geometries). The gas mixture was $Ar - CO_2$ 70-30 and we had some standard settings from which we always started when changing a parameter. In these typical conditions 350 V was put over each GEM, an induction field of 3kV/cm was used. Standard transfer fields were 3.25 kV/cm. The drift field was set at 100 V/cm, 200 V/cm and 1 kV/cm respectively, so that we would be in the region of the TPC (first two) and tracking conditions (last drift field setting). The results are shown in graph 6.2. The results of (Bondar *et al.*, 2003) were quickly confirmed and even extended. The first transfer field and the induction field should be set as high as possible to reduce the ion feedback while a low second transfer field also leads to a reduction. Asymmetry in GEM voltages gave a small decrease in the ion feedback, especially if we reduced the voltages on the first 2 GEMs and compensated this with the last GEM, pointing down that especially the top GEMs determine the ion feedback.

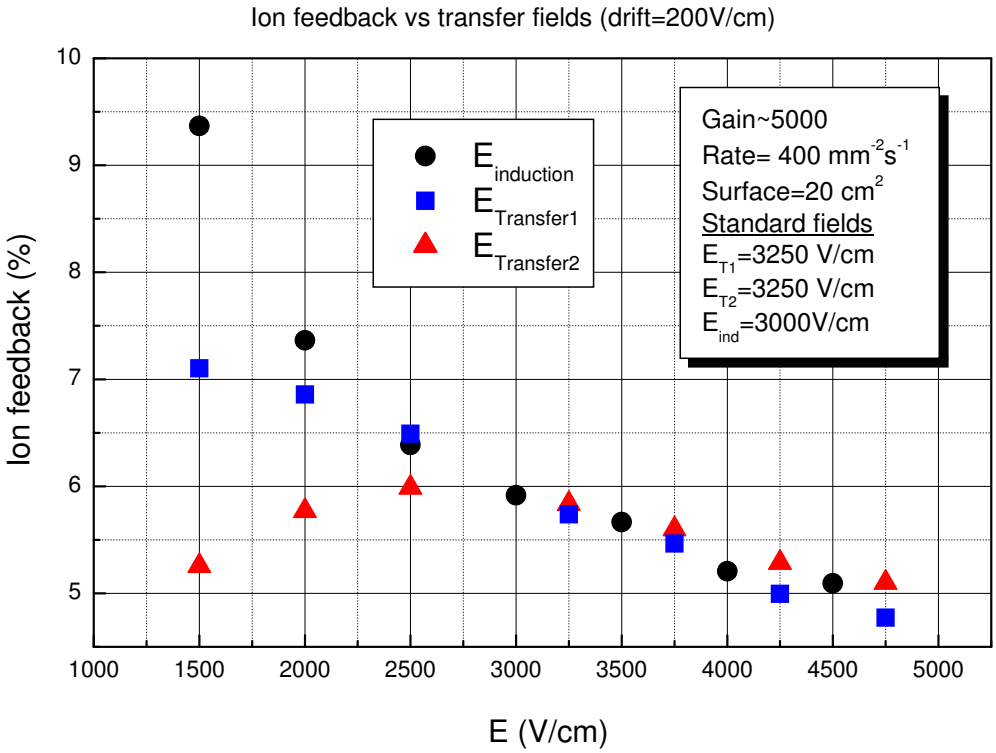

Figure 6.2: Influence of the different transfer fields on the ion feedback. (drift field =200 V/cm)

6.3.2 Different geometries

Influenced by (Bondar *et al.*, 2003), who noticed a considerable reduction, when placing a GEM with smaller holes in between two standard ones, we also tried to decrease the ion feedback further using different GEM geometries. The middle GEM was replaced by one with bigger as well as smaller holes. The regular settings described in the previous paragraph were also used this time. Contrary to Bondar *et al.* (2003) we did not notice any significant difference in the ion feedback (see fig 6.3). Probably the effect depends on more parameters than just bigger/smaller holes and the exact values of inner and outer radius and pitch should be taken into account. An alternative explanation for the results in (Bondar *et al.*, 2003) could be found in the optical opacity of their GEM-cascade, but this will be discussed in section 6.7. In this case those extra parameters would play a considerable role.

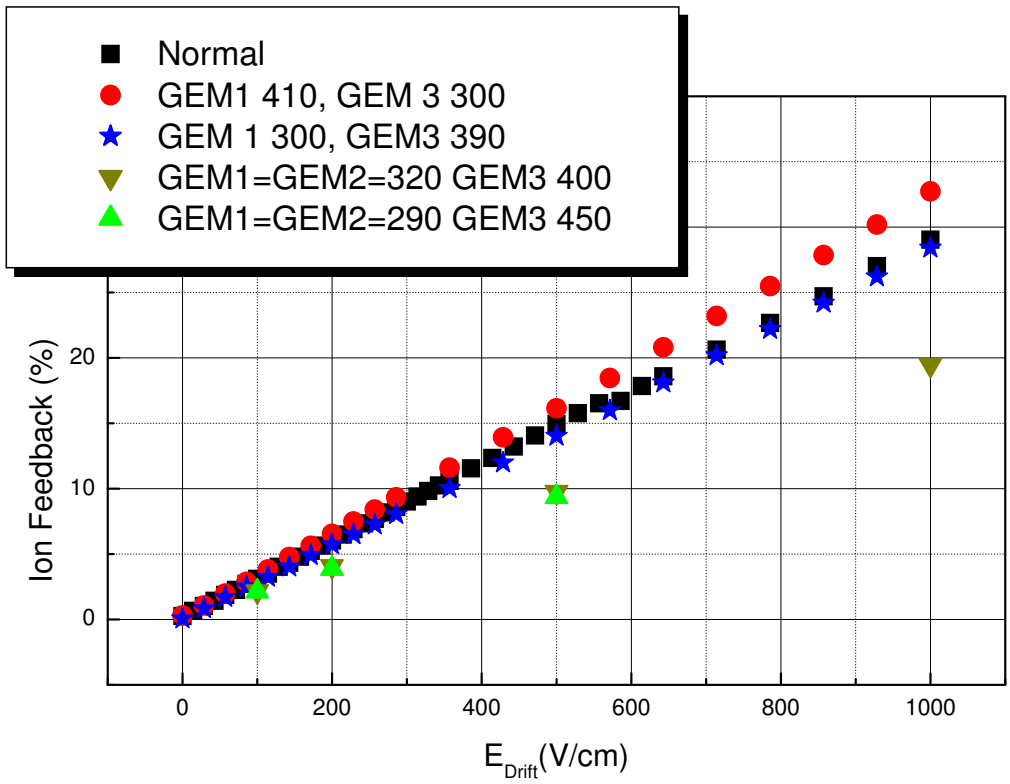

Figure 6.3: Influence of the GEM geometry on the ion feedback.

6.4 Charge transmission

Ion feedback has been extensively studied because of its major importance in TPCs and gaseous photomultipliers.(Buzulutskov *et al.*, 2000) With a single-GEM the ion feedback can be easily estimated: the fraction of ions released in the drift space equals more or less the ratio of the magnitude of drift to transfer fields. In cascaded structures, the number of ions is mostly determined by ions generated in the top GEM and a lot of ions end up at the top of the intermediate GEMs. Therefore the fractional ion feedback is further reduced. This value of ion feedback is actually determined by the charge propagation through GEMs. The exact values are quite difficult to determine, since they are the result of interplay between GEM geometry, applied fields and gas mixture. On the other hand, a simplified picture is not that hard to present.

Therefore we work with two basic configurations, as usually found in multiple-GEM structures. First we will look at propagation through a GEM from a low field (150 V/cm) to a high field (3 kV/cm) as usually appears as a first stage of our cascade. The following GEMs will have high fields (3 kV/cm) at both sides and therefore also this structure was looked

at. In fig. 6.4 one can find schematic drawings for the two cases. The numbers next to the arrows show approximately the relative sharing of electrons and ions ending up at one part of the structure. The values, deduced from Sauli *et al.* (2003), correspond to the operation of a standard GEM, with 70 μm holes at 140 μm pitch, in $Ar - CO_2$ 70-30, at 350 V. Due to the relatively low transfer fields (3 kV/cm) to prevent discharge propagation (section 4.4), the majority of the electrons (60%) end up at the bottom of the GEM. For example in the circumstances described above, the real gain actually reaches 50 whereas the effective gain (deduced from the collected electrons) reaches only $\propto$ 20. When the incoming field is also high, electrons are already lost at the top electrode of the GEM. Therefore the effective gain decreases even more and ends up around 16.

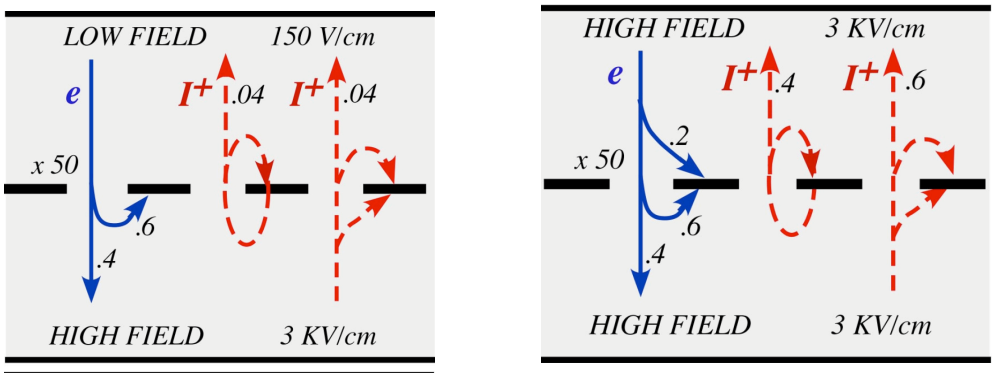

Figure 6.4: Schematic drawing of transfer properties of electrons and ions for two field settings: low-to-high and high-to-high. Sauli *et al.* (2006)

Now we can try to estimate the number of ion feedback for a very simple triple-GEM structure with a low drift field. Going from a low field to the high field, the electron is multiplied 50-fold and 60% of the electrons end up at the bottom of the GEM, while the other 40% are transferred to the next stage (GEM or read-out). This gives an effective gain of $50 \times 0.4 = 20$. At the same time the same number of ions are formed, but only 0.04% of them go back. So for the first GEM 2 ions flow back. The second and the third GEM have high fields all around the GEM, so we enter the second case. Now, 0.2% of the electrons are already lost before reaching the multiplication. Since the used GEM voltages are the same, the multiplication is still similar: a factor 50. Also the extraction properties stay the same and thus 0.4% is transferred on to the next stage. This yields an effective gain of $0.8 \times 50 \times 0.4 = 16$ in this case. The number of ions formed in the second multiplication process are now: $20 * 0.8 * 50 = 800$ of which 0.4% flows to the region between GEMs while the rest are collected on the GEM. This gives 320 ions who reach the first GEM. Of these ions 0.04% are transferred to the drift stage. So we finally end up with $\propto$ 13 ions. A similar calculation for the third GEM, taking into account the better ion transmission for the second GEM yields 123 ions coming from

that GEM flowing back to the drift space.

Combining the data from the two cases in fig. 6.4 an effective gain of $20 \times 16 \times 16 \approx 5000$ would be expected. Taking multiplication of ions into account, we would expect more or less 2 ions from GEM1, 13 from GEM2 and 123 from GEM3. In this example, the ion feedback is 2.76% (138/5000) which is in reasonable agreement with our measurements and also with Bachmann *et al.* (1999b). The main problem for this procedure is that one should know the single-GEM properties for all different combinations in order to do plausible estimates for different settings. But to get an idea of the order of magnitude this is certainly a valuable method.

6.5 Mesh gating

6.5.1 Introduction

To eliminate ion feedback even further, the standard method of gating could be used. In that case an intermediate drift space would be added, separated from the main drift volume by a wired mesh. This mesh electrode can be gated close, offsetting the voltage between these wires. This procedure is followed in conventional TPCs. The drift lines when the gate is open or closed, as shown in fig. 6.5. Drifting electrons are collected on the gating grid until gated open by a triggering event. A shielding grid at ground potential is used to terminate the drift region. Electrons drifting through an open gating grid (fig. 6.5b) pass through to the amplification region around the anode wires. Positive ions generated in the avalanche are detected on segmented cathode pads to provide precise measurements along the wire. The slow positive ions are blocked from entering the drift region by closing the gating grid after the electrons have drifted through. Good transmission would be assured by choosing a field of 300 V/cm in the region, double of that in the drift volume (typically 150 V/cm) or that was at least always believed. We verified this rule of thumb by measuring the electron transmission curves for 3 different meshes. A 6 mm gap would then be sufficient to delay the ions with 1 ms, as necessary for the International Linear Collider (ILC). In the current design the ILC has 0.95 ms bunch trains spills, spaced 0.2 s apart. So this delay is perfectly suited for ILC operation. Their injection in the drift field can then be inhibited pulse-closing the gate, after the delay, for a time equal to the spill length. We repeat at first the old transmission measurements for meshes of different thickness and in the next section we will then propose a new kind of gating exploiting GEM properties. The measurements were done in a simple parallel-plate detector to exclude the influence of the GEMs on the results.

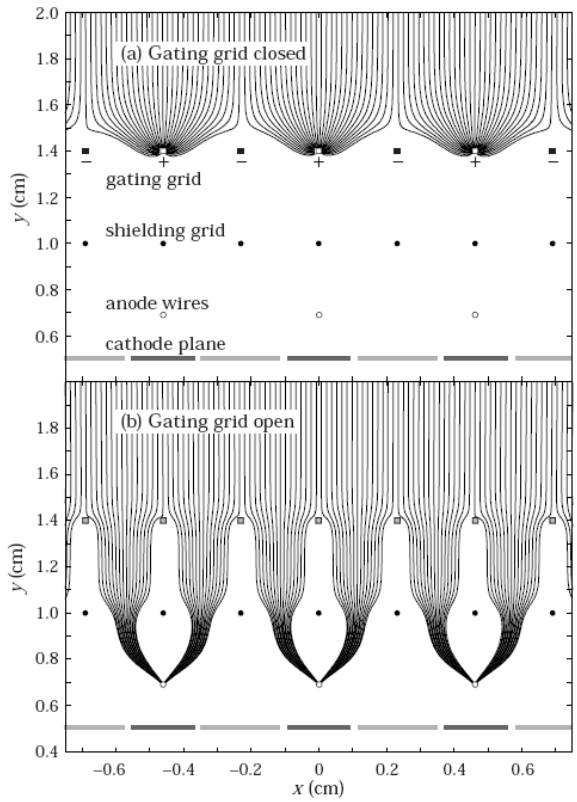

Figure 6.5: A gating grid: the field lines when the ions are blocked (a) and allowed to pass (b).(Eidelman *et al.*, 2004)

6.5.2 Parallel-plate measurements

For the mesh transparency measurements, we went back to basic parallel-plate set-up, although we changed the top plate with a mesh to eliminate some external influences. We tried to check the results of Breskin *et al.* (1979). Fig. 6.6 shows a schematic drawing of the set-up. The X-ray beam enters the detector by a Plexiglass window at the side. This allows us to direct the beam between drift electrode and mesh and thus only have conversions in this region to deal with. Because of the easy set-up the whole current on the drift electrode is due to the ions formed when X-rays create an electron-ion pair in the gas. The electrons get divided

between some who end up at the mesh and some reaching the read-out. The electron transmission can then easily be calculated as the ratio between the absolute value of the electron current on the read-out to that of the ion current on the drift. To be sure of having excluded all errors and offsets in our measurements, we added all the different currents with the right sign (+ for ions, - for electrons). This sum then had to be zero, since the total number of electrons created equals that of ions created since both of them are created simultaneously in the ionization process. In these measurements all fields where still sufficiently low in order not to have any multiplication process yet. Measurable currents were thus attained by increasing the beam intensity.

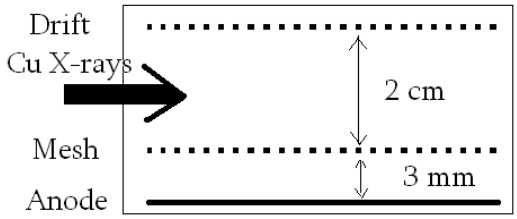

Figure 6.6: Parallel-plate set-up to measure electron transmission.

The measurements were done for three meshes of different density (fig. 6.7). The most dense one had an optical transparency of 45%, the middle one 65%, and the least dense mesh 89%. The results, displayed in graphs 6.8 are quite suprising since they show a lower transparancy than thought before. The rule of thumb which was always used was that the transfer field behind the mesh should be double of the drift field (before the mesh). But apperently that was without taking the mesh density into account. For a very thick mesh this could be the case. But fig. 6.8 shows that the transparancy we measured, was only around 20%, 55% and 70% for the three meshes with decreasing mesh density. For more or less full transparancy the field ratio had to be a factor 5 for the least dense mesh, slightly over 10 for the middle dense one and even higher for the densest mesh we used. The ratio's were proven to stay the same in different gas mixtures, so their gas independence is correct.

Placing the meshes in front of a GEM detector gave rise to field distortions. Then the transmission curves were not only dependent on the field ratio but even on their exact values. Also the distance from the mesh to the first GEM had a clear influence.

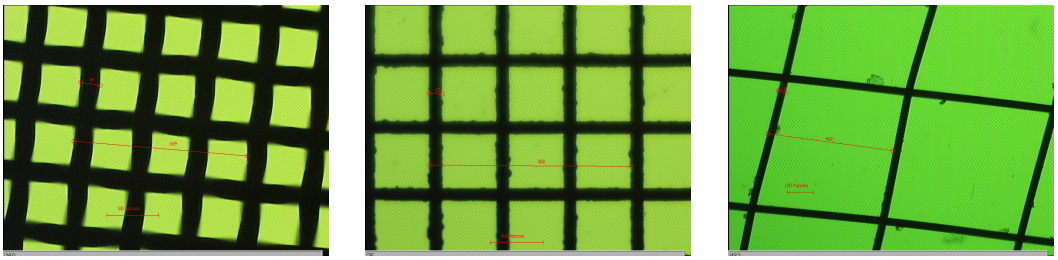

Figure 6.7: The microscopic pictures of the three meshes, from left to right with decreasing density

6.6 GEM gating

The main problem with this normal mesh gating procedure is that one looses part of the advantages that were acquired by using a GEM-endcap. A more elegant and attracting solution would be to use a GEM foil for the gating. Then one would use a low field (300 V/cm) for the first transfer field. Very few measurements have been done in this unusual situation. The only ones reported were done using pure methane and were used for the special case of electrons emitted by a photosensitive GEM electrode in pure methane. (Moermann *et al.*, 2004b) We have therefore measured electron transmission into moderate and low fields, compared to the standard settings, for a wider range of gases and geometry.

6.6.1 Method

Our measurements were all done with double-GEM detectors ($10 \times 10\,cm^2$ active field, as described in 3.3.1). The second and the third GEM were standard ones (70 μm holes and 140 μm pitch). We also used them in the standard settings for high gains. The first GEM was changed and we also changed the transfer field between low and moderate fields. The actual measurements were then done by varying the voltage on the first GEM and looking at the transmission. We used our usual soft X-ray generated beam with X-rays of 8.9 keV energy for these measurements.

To avoid normalization errors, the pulse measurements were done directly in contrast to the current methods used in previous work. In the geometry as shown in fig. 6.9, our spectra were a combination of two different contributions. This was the result of orienting the beam perpendicular to the detector. Due to this, we had conversions between every two components but because of the multiplication, only the conversions between the drift and the gating GEM and the conversions between gating GEM and first multiplying GEM were visible. In the transfer space between these two GEMs no multiplication occurred. The conversions in the other regions disappeared in the detector noise because of the small gain for conversions there.

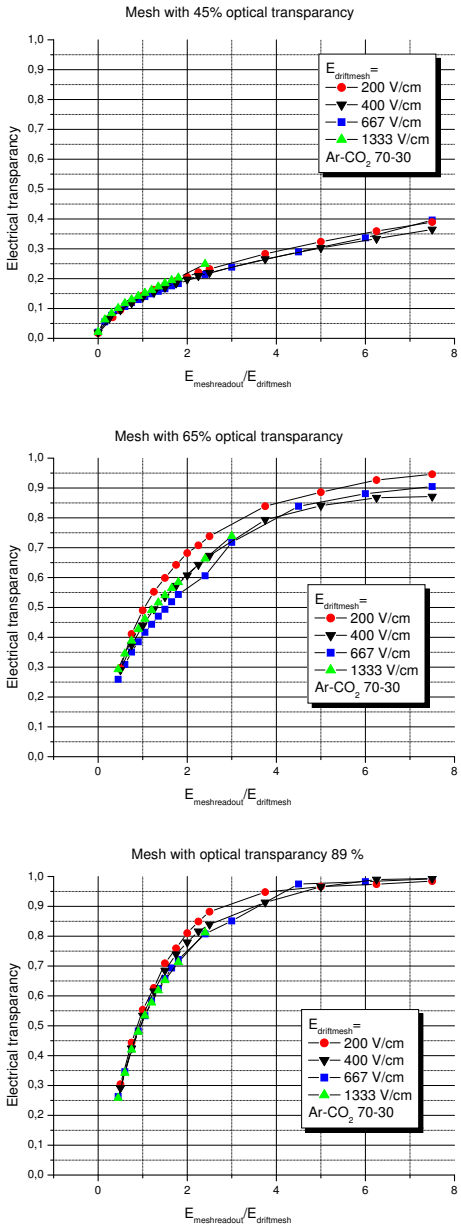

Figure 6.8: Electron transmission for meshes of three levels of density (45%,65% and 89%).

The first contribution was that due to conversions in the drift region, which is actually the signal that we want to measure. The second component was the double-GEM spectrum of the conversions between first and second GEM. This contribution can be easily resolved by inverting the drift field and subtracting it from the total spectrum. This spectrum also shows the multiplication by the last two GEMs, so that comparing the peaks in the pulse height gives an absolute estimate of the electron transmission through the first foil. (at least before multiplication sets in) We also checked the method with the current method, with the beam

entering from the side as described in the previous paragraph (6.5.2). This method gave similar behaviour, although for an unclear reason the exact values were shifted over about 10 %.

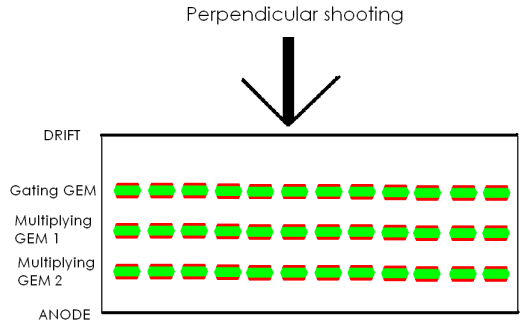

Figure 6.9: Set-up for pulse-height measurements of GEM gating. The beam is directed perpendicular to the set-up. The first GEM is the gating GEM, the others are multiplying GEMs.

6.6.2 Pulse height spectra

In fig. 6.10 one can find an example of one of our recorded spectra. One can see the total spectrum, the spectrum with inverted drift field and then finally also the subtracted spectrum. Very low GEM voltage was used so that we did not have any charge multiplication. The relative counting rates of the two spectra reflect the gap thicknesses (6.5 and 2 mm), taking into account the X-ray absorption of the first GEM foil which further reduces the event rate for conversions between the two GEMs. The ratio between the peak positions gives an idea of the electron transmission, in this example around 0.7.

Due to transmission losses the energy resolution degraded. In the standard GEM case the full width at half maximum (FWHM) for the 8.9 keV line is a little under 20% (see section 4.1), while in this case we notice an increase up to 30%. Probably this resolution is still sufficient for tracking. Increasing the voltage on the first GEM so that we use it in multiplication mode, improves the resolution (fig. 6.11) and the FWHM reaches 25%. But this value is still considerably worse than that from the standard spectrum, showing the effect of transmission losses between the first two GEMs because of the low field. (300 V/cm) The spectra shown here are those taken with GEMs with 100μm holes and standard pitch, since they give a clearer view. The FWHM-values have also been checked for standard GEMs and the values were similar.

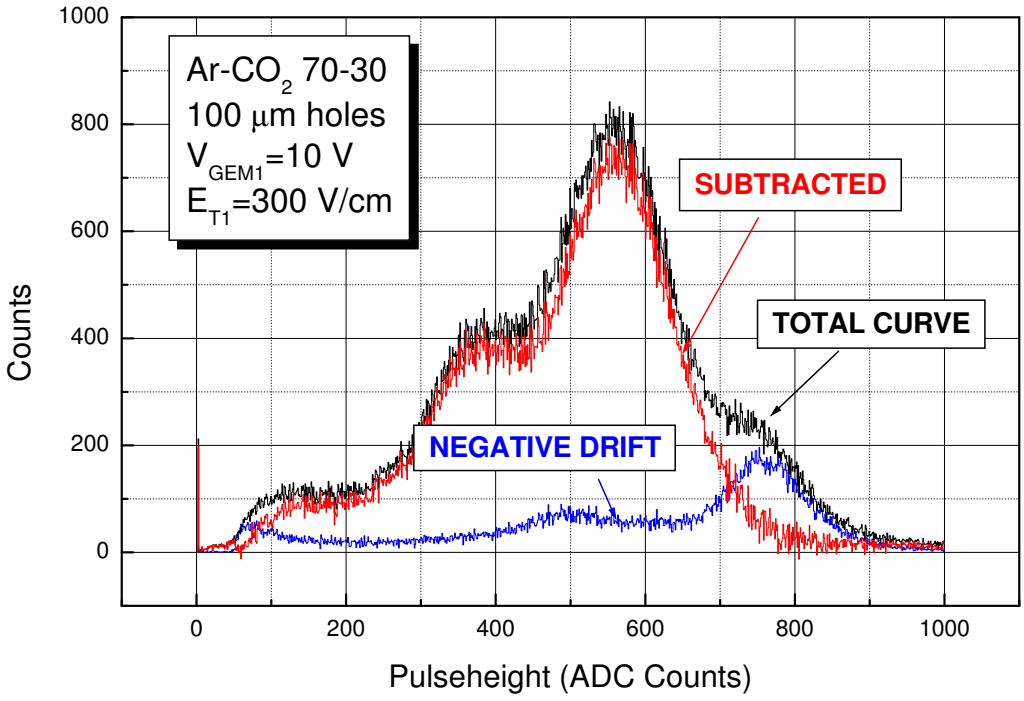

Figure 6.10: An example of a recorded spectrum with low transfer field and 10 V over the first GEM.

6.6.3 Results

For a standard GEM (70 μm holes, 140 μm pitch), the results are shown in fig. 6.12. The measurements were done for three settings of the transfer fields: 150, 300 and 3000 V/cm. The main observation is that the transmission is unexpectedly large at low GEM voltages. It attains 30% for V_{GEM} = 10 V, E_{DRIFT} = 150 V/cm and $E_{Transfer}$ =300 V/cm. At high GEM voltages, when amplification sets is, the signal is a superposition of transmission and multiplication and the two contributions can not be seperated anymore.

The electron transmission depends strongly on the gas mixture (fig. 6.13). It reaches 50% for equal fractions of argon and CO_2. As discussed in 6.6.4, this is likely due to a reduction in the electrons' transverse diffusion in the quencher-rich mixtures. This is confirmed by the fact that GEMs with larger holes (100 μm holes, 140 μm pitch) show larger electron transmission in the same mixture. The low voltage transmission now even rises up to 70% (fig. 6.14).

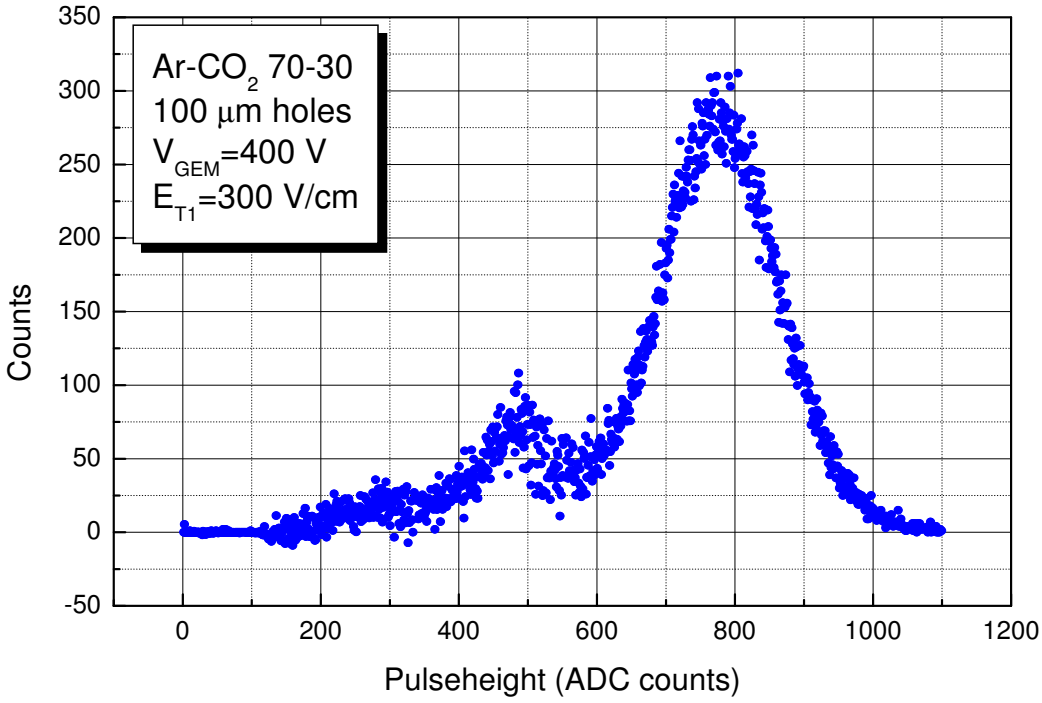

Figure 6.11: Pulse height spectrum with first GEM in multiplication mode (400 V) but low transfer field (300 V/cm).

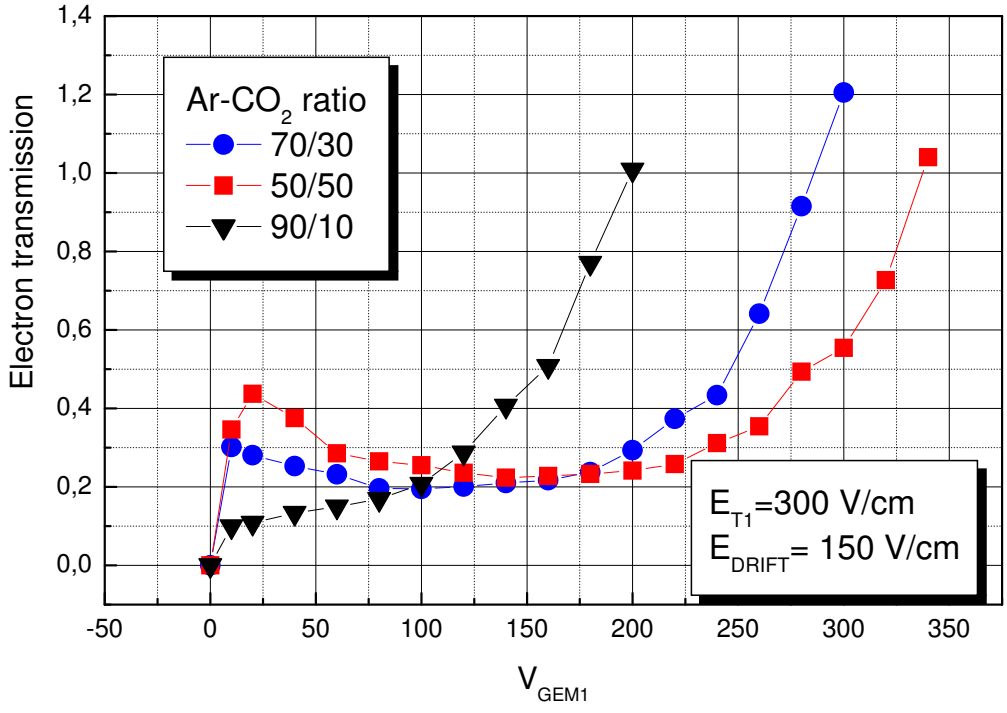

Figure 6.13: Electron transmission for a standard GEM with 150 V/cm drift field and 300 V/cm transfer field for $Ar - CO_2$ mixtures

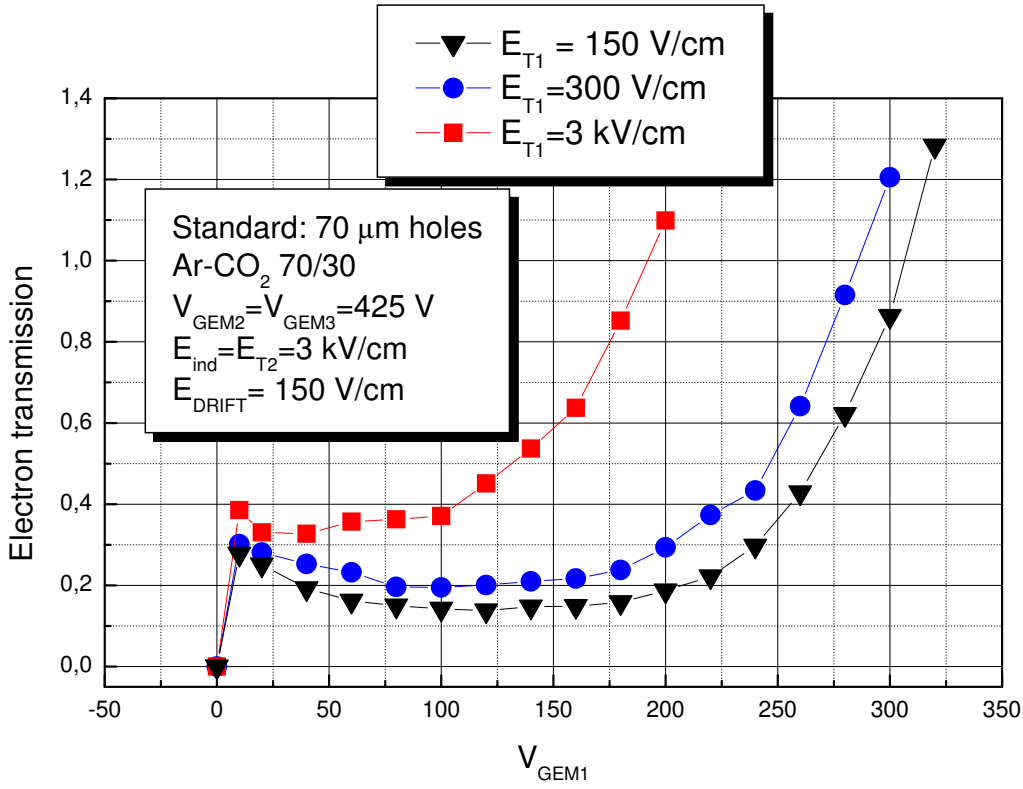

Figure 6.12: Electron transmission for a standard GEM with 150 V/cm drift field and different transfer fields.

Operating the GEM at a very low voltage seems a very attractive solution for the gating problem. At low voltages, certainly with GEMs with larger holes, the transmission is already quite good. As shown in 6.6.2 the worsening of the resolution is also limited, still permitting good accuracy. As such, a GEM in non-multiplying mode, could be used for ion gating with only around 10 volts of reverse pulse. GEMs in multiplying modes or wire meshes on the contrary require several hundreds of volts. The hope even existed that a reduced ion transmission of the GEM at these low voltages could lead to a DC-ion filter, but experiment showed this idea to be wrong. The ions turned out to be transmitted quite easily as well and the blocking effect became negligible.

The total structure could just stay a triple-GEM, since discharge and gain studies showed that an effective gain of around 10^4, needed for minimum ionizing particles, is still easily attainable by a double-GEM structure. If really necessary an extra GEM foil could be added, creating a quadruple-GEM of which the last three GEMs then would take care of the multiplication. One could also gate the first GEM in multiplication mode. But this would require gating of several hundreds of volts and will give rise to more electronic problems. Nevertheless it

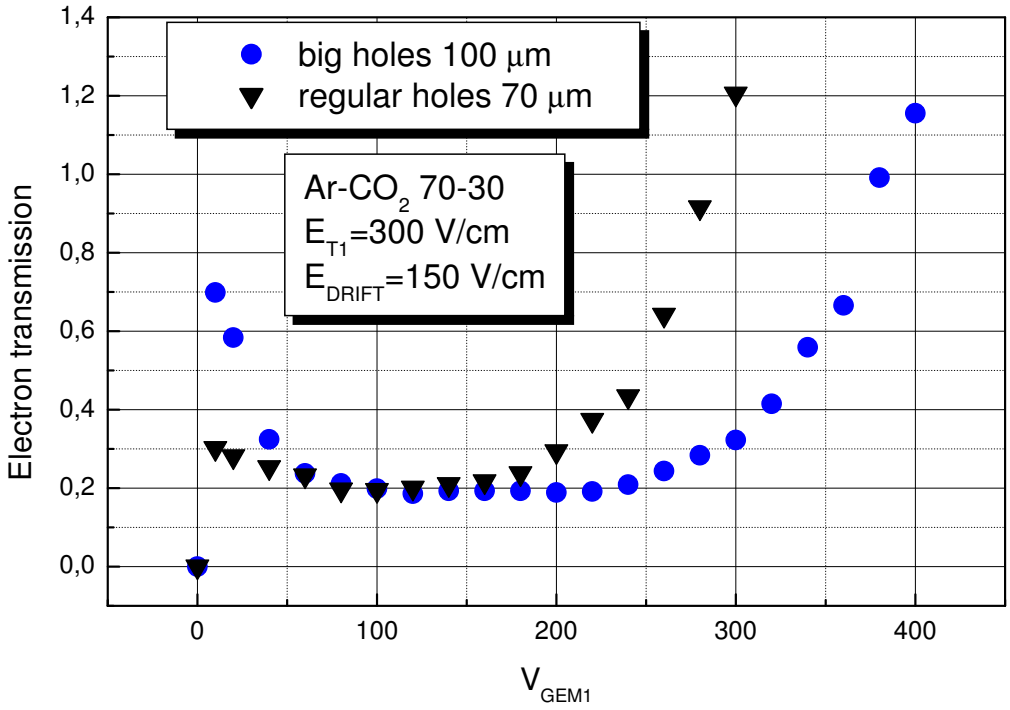

Figure 6.14: Electron transmission for different hole sizes, 150 V/cm drift and 300 V/cm transfer field.

stays a possibility. Because of the low transfer field, the effective gain of the whole detector will be slightly reduced in comparison with normal operation. For a voltage of 350 V, on the other hand, the gain still increases with a factor 6 compared to normal operation because multiplication occurs.

A fortunate coïncidence consists in the standard design of large GEM-foils. To reduce the capacitance of the foils and thus the energy of discharges occurring in the detector, these foils are built up of long fragments with independent powering. This has thus the same structure as a multiple transmission line. The fragments can be AC terminated with their characteristic impedance. This would suppress reflections and thus lower the noise pickup which is inevitable in such a gating structure.

A basic timing diagram is shown in graph 6.15. This triple-GEM structure has 6 mm spacing between the gating GEM and the double-GEM detector and the transfer field here is 300 V/cm. In se, reduction of the transfer field would also reduce the required space between the GEMs (150 V/cm would for example only require 3 mm), but the exact value of the low

GEM voltage also gets more crucial with these lower transfer fields. This can for example be noted in fig. 6.12. This can give more problems with the uniformity of the response over large detector area's. Of course the drift and diffusion properties also change with the gas mixture and therefore the structure needs to be optimised for the exact mixture used. The gap thickness and transfer fields can be adapted for this. Further research is needed to document these influences more profoundly.

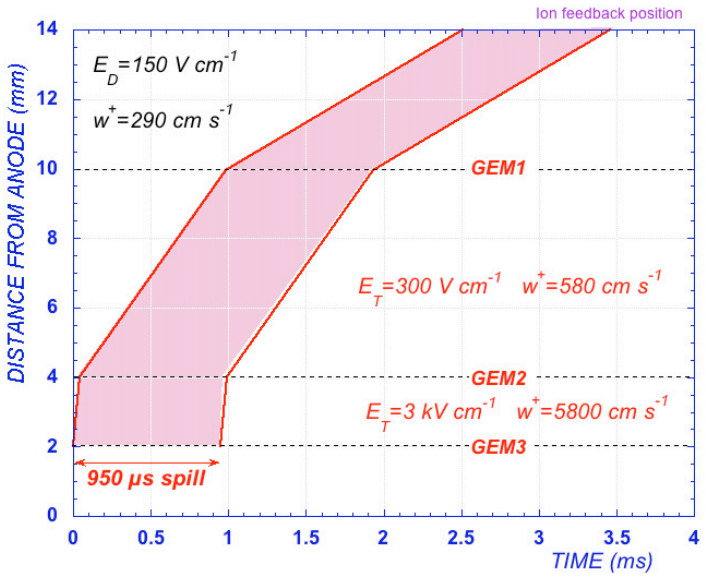

Figure 6.15: Timing diagram of the feedback ion flow in a triple-GEM structure, with the first foil, facing the drift volume, at larger distance and low transfer field (300 V/cm). Sauli *et al.* (2006)

6.6.4 Explanations

Electrons released by the ionization, move in the drift field and in the multiple-GEM section following the field lines. In absence of diffusion, the electrons would follow them exactly. The final distributions of electrons could then easily be deduced from a simple field line count and the transmission could be derived in the same way. Because of diffusion and more specifically transverse diffusion, this simple approach is not correct. The electrons are smeared out, especially during the multiplication phase in the narrow holes. Because of this electrons can end up on intermediate electrodes before reaching the anode. The number of transmitted electrons changed. This change is also influenced by the gas mixture and the GEM geometry. Increasing the fraction of the quencher gas (in our case CO_2) and the hole diameter leads to improved transmission of the electrons. Already shown before for standard conditions (Sauli *et al.* (2003)), this work now proves that these observations are also valid for low GEM

voltages and low transfer fields.

Using the program MAGBOLTZ (Biagi, 1999), the drift properties for different gas mixtures can be computed. For this research, drift properties of argon/carbon dioxide mixtures in the absence of a magnetic field have been calculated. Fig. 6.16 shows for example the transverse diffusion. Also the values for $Ar - CH_4$ 90-10 and for $Ar - CH_4 - CO_2$ 93-5-2 have been calculated but this time an applied magnetic field of 4 tesla was taken into account. Because of its favorable characteristics, like for example the non-flammability, this last mixture is one of the main candidates for the large TPCs. From the graph it can now be derived that in the low field region (hundreds of V/cm till 1 kV/cm) the transverse diffusion of this mixture is similar to that of $Ar - CO_2$ 70-30 without any magnetic fields. Therefore the transmission properties in the two mixtures will probably be quite similar. In Killenberg *et al.* (2004) an increase of the anode signal with a factor 2 was noticed in changing the magnetic field from 0 till 5 tesla. Killenberg *et al.* (2004) claim, on the basis of a Garfield simulation (Veenhof, 1998), that this improvement is due to a better extraction because of the changed field lines. The present research shines a new light on this result. The increase could be due to smaller losses due to reduced transverse diffusion. The reduction in ion feedback is due to a higher anode signal in this case. This should be further investigated since it could give new insights in the dependency of electron transmission on the gas properties.

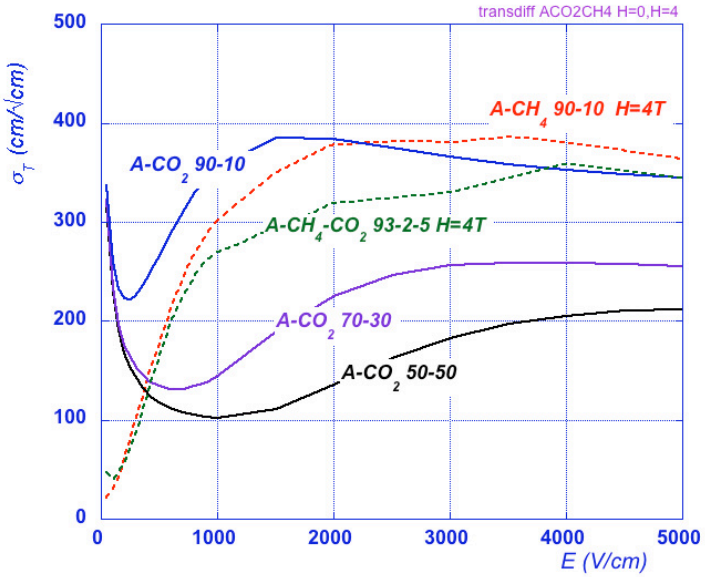

Figure 6.16: Computed transverse diffusion for 1 cm drift in different gas mixtures.Sauli *et al.* (2006)

The electrons produced after a spill have to traverse the region between the gating and first multiplying GEM. In this region there will be a pile-up of ions. But due to the narrowness of the gap, the distortions caused by this will stay limited. Operation at high rates showed

until now (Ketzer *et al.*, 2004) only a moderate deterioration of position accuracy and it could not even be confirmed whether this was due to the accumulation of ions in the gap or to the signal pile-ups and problems with the reconstruction software. It is thus quite likely that this proposed scheme gives no real additional problems.

6.7 DC ion filter

6.7.1 Introduction

Since diffusion properties for electrons and ions are quite different, a thorough investigation of them could lead to a so-called DC ion filter, which would block the ions flowing back more than the electrons going in the other direction. To illustrate this we show in graph 6.17 the calculated transverse diffusion for one cm drift space as a function of the drift field. For ions, up till very high fields, this diffusion is independent of the magnetic field and the type of ions. At the common values for the transfer fields between GEMs (several kV/cm), the transverse diffusion for electrons is almost an order of magnitude larger than that for ions. As a result, the electron cloud spreads out a lot more than the ion cloud.

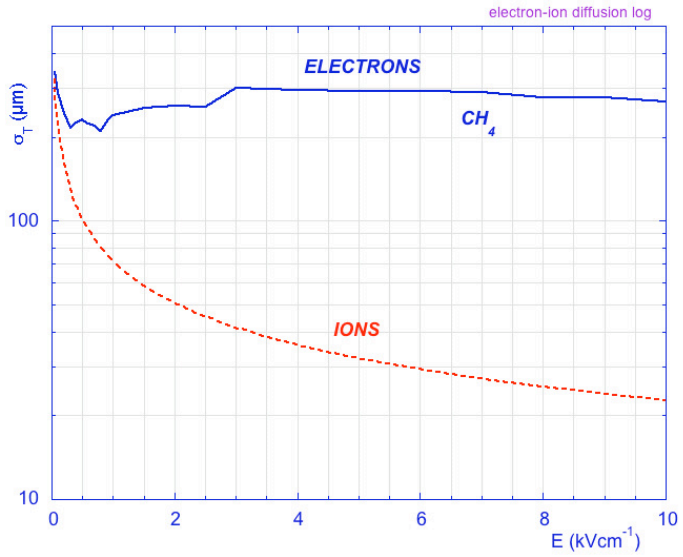

Figure 6.17: Electron transverse diffusion in pure CH_4 (full line), and ion diffusion (dashed line), as a function of electric field.Sauli *et al.* (2006)

This suggests that an adapted geometry of the multiple structure could further reduce the ion feedback. An increased optical opacity in the placing of the GEMs would lower the ion back-flow. Offsetting the position of the holes of the second GEM for example by half a pitch at a gap distance of the order of the magnitude of the pitch would have as a result that many

field lines out of the first series of holes would end up on the top electrode of the second GEM. Most of the ions would then be stopped, while a majority of the electrons, because of the increased transverse diffusion of the electrons, would still end up in the holes of the second GEM and get multiplied there. These two effects would then lead to a reduced fractional ion feedback. In presence of a magnetic field this filtering could be very effective. Amendolia *et al.* (1985) showed this in conventional TPCs. Perhaps the reduction of ion feedback can even be large enough to avoid the need of gating. Also for photosensitive GEM detectors, operated in pure methane or CF_4, this could reduce the ion feedback and photocathode degradation. (Moermann *et al.*, 2004a) In this case even the advantage occurs that electron transmission losses would only play a small role, because of the exponential charge distribution of single electron avalanches.

6.7.2 Method

Due to the requirement of the gap thickness and also the transverse positioning of the holes at half a pitch of each other, is hard to realise an experimental set-up with standard GEMs because of the limited proportions. It would be extremely difficult to create a moving mechanism for the GEM positioning at that scale. Therefore we decided to test and implement the scheme with the so-called thick GEMs of Chechik *et al.* (2004). The thick GEM-plates have an active volume of $2 \times 2\,cm^2$. The holes have a diameter of 300 μm in the insulator, around this there is a metal-free rim of 100 μm. The holes have a triangular pattern with pitch 800 μm.

For this research a gas-tight micrometer was installed in the frame, permitting to move the top GEM. This permitted us to change the positioning of the two GEMs from fully transparent to fully opaque. The only limitation was that we could only move the detector in one direction and therefore we could not reach the absolute minimum in transparency but only a local one. The absolute minimum would be placed in the middle of the square.

We used for these measurements a double-GEM detector to simplify the read-out of the data. Otherwise also the second transfer field and gap could play a role. These two GEMs were placed at a distance of 2 mm. This value was the result of a compromise: still in the order of magnitude of the pitch, this value also permitted a decent resolution in the pulse-height spectrum. Our trial to place the two GEMs at only 0.5 mm distance, which would probably have permitted a stronger effect, showed that we lost most of our energy resolution then and therefore the distance was enlarged. A picture of the inside of the detector is shown in graph 6.18.

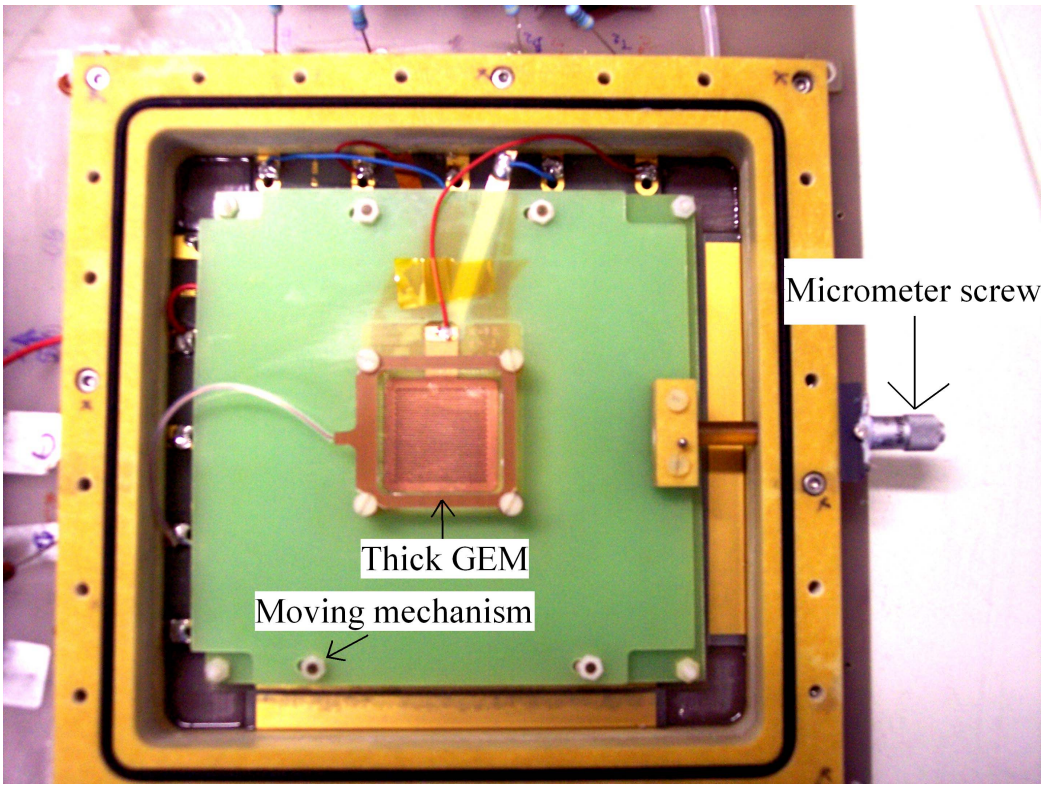

Figure 6.18: Our set-up with the thick GEM-foils that can move over a distance of 2.5 μ m.

To enhance the electron transverse diffusion and therefore undoing the opacity effect for the electrons, we operated the detector in a $Ar - CO_2$ 90-10 mixture. At a transfer field of about 3 kV/cm, the diffusion in this gas is quite close to the one attained in pure methane. (fig. 6.17) 1050 V was applied to each GEM, so that gains around 4000 were attained. With drift and transfer field chosen to be 150 V/cm and 3 kV/cm, conditions were similar to those in TPCs. The pulse height was measured on the anode and currents were measured both at the anode and the drift electrode. Irradiation was done using our standard soft X-ray generator with 8.9 keV X-rays. The beam area was around 1 cm^2.

6.7.3 Results

Fig. 6.19 shows the measured anode and drift currents under continuous irradiation. The electron current fluctuates in function of the relative GEM positioning, but its fluctuations are smaller than those for the ions. Therefore the fractional ion feedback also decreases considerably, from 10 to 6%. The sharp sides in the curve could show an insufficient opacity of the structure and indicates that diagonal movement in the triangular pattern could lead to

an even deeper minimum, since the opacity would be increased. Also increased pitch could lead to the same effect.

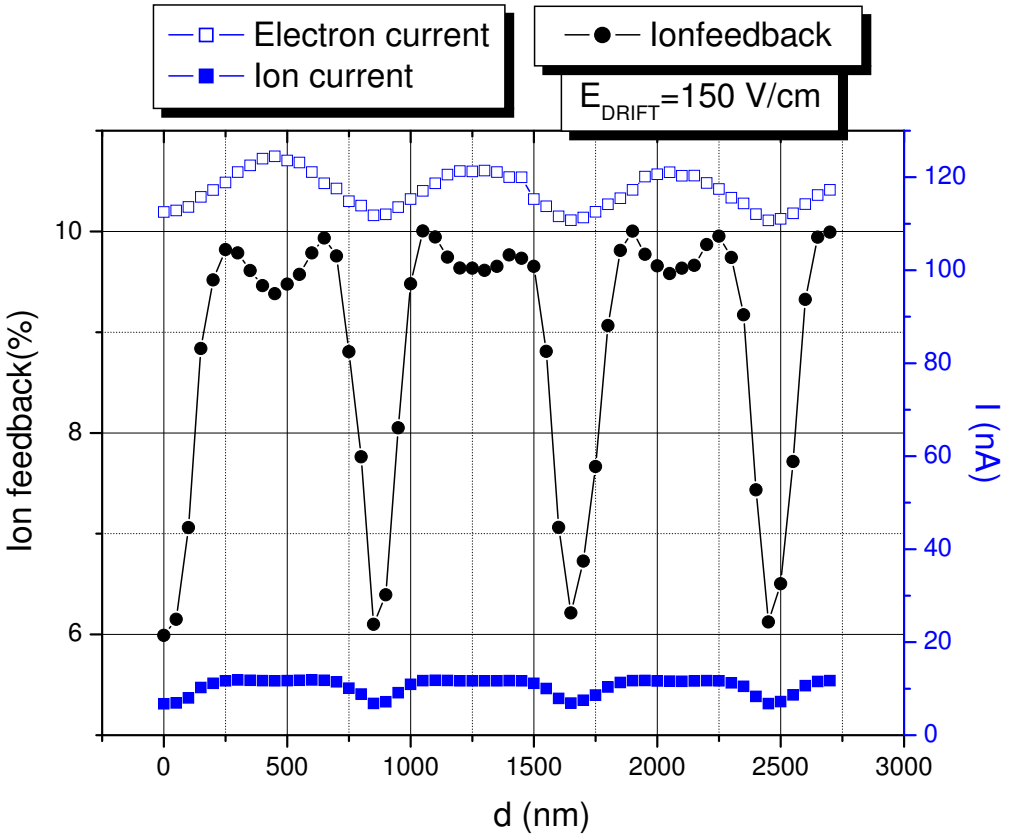

Figure 6.19: Modulation of the drift and anode currents, and of their ratio, as a function of the relative position of the holes'rows in two facing thick-GEM plates with low drift field (150 V/cm).

Using a stronger drift field (1 kV/cm) one obtains similar effects but the ion current and feedback now also follow a sinusoidal behavior (fig. 6.20). Because of the stronger field in the drift region, the transverse diffusion apparently plays a smaller role. Because of this the apparent hole size for the ions is smaller and therefore we do not have such a big transparent area. Increased speed of electrons and ions could also explain our observation that the magnitude of the relative change depended quite strongly on the used transfer field. An increased transfer field also leads to apparent larger holes for the ions. This indicates that probably drift and the transfer field cause the form of the curve, but that their ratio is important for this. A simulation study would be handy to come to an increased understanding of the observations, but such simulations, taking the transverse diffusion into account, are rather complex.

Pulse height spectra (fig. 6.21) in the valley and at the peak of the scan, indicate that the

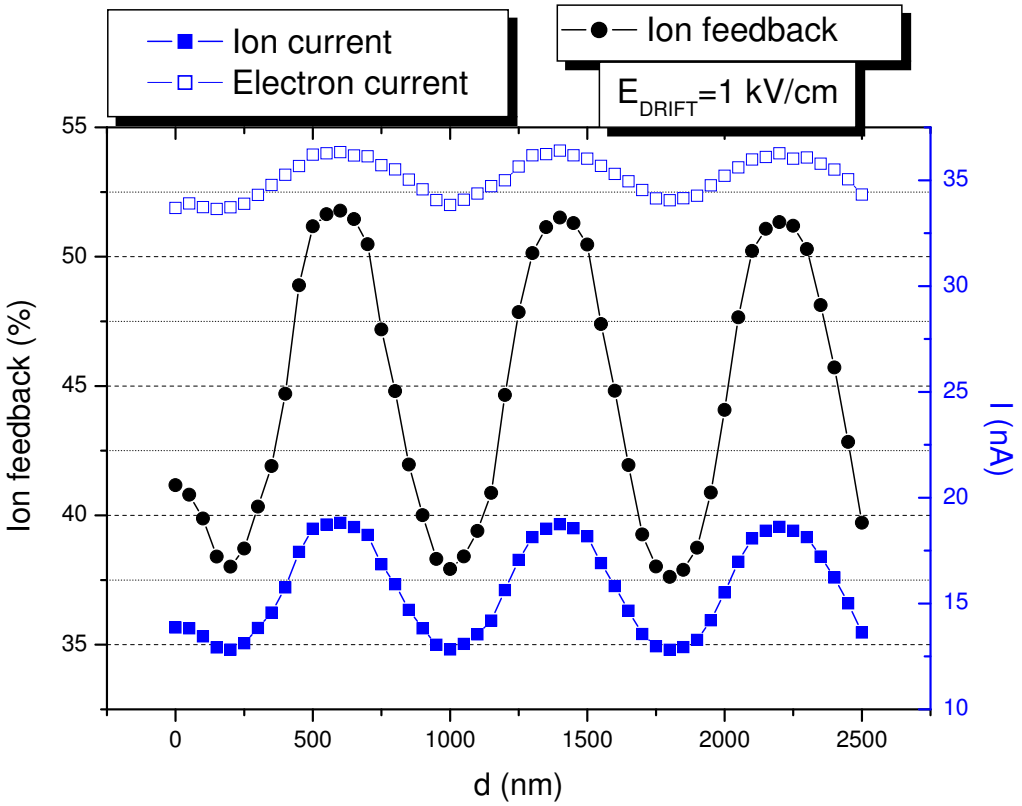

Figure 6.20: Modulation of the drift and anode currents, and of their ratio, as a function of the relative position of the holes' rows in two facing Thick-GEM plates with high drift field (1 kV/cm).

energy resolution does not deteriorate, but that the center of the curve just slightly shifts. The results described here showed the effects of a controlled misalignment of the hole patterns in GEMs. The effect is still rather small and therefore not really useful yet. A better study of GEM geometry and operating conditions to increase the opacity could improve the effect and really lead to the use of such a "DC ion filter". The best way would be to design a double-GEM pattern with adapted hole size and pitch so that maximum opacity could be reached when randomly placing these GEMs on top of each other. Now we can also give the other explanation for the reduced ion feedback of Bondar *et al.* (2003) when using a middle-GEM with other hole size. This configuration perhaps just leads to an increased opacity of their structure and because of this the ion feedback is further reduced.

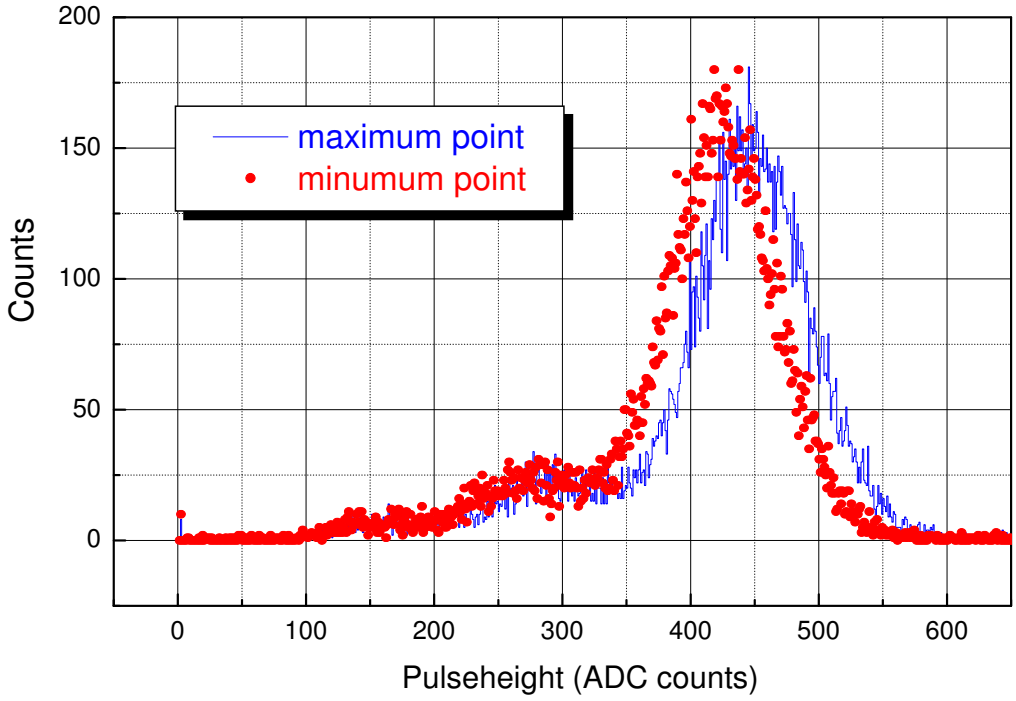

Figure 6.21: Anode pulse height spectra recorded on the minimum and maximum of the scan.

6.8 Conclusions

- The transmission of electrons through meshes is strongly dependent on the optical transparency of the mesh and turns out to be lower than expected before. By placing a mesh in front of a GEM structure, field distortions are clearly introduced.

- For large TPCs gating with an extra GEM foil with a low transfer field behind this foil, looks an attractive option. Even at very low voltages (10 V), the transmission reaches quite high values. An interesting option is to use a GEM with big holes (100 μm) since the transmission at 10 V reaches 70 % in this case. The limited voltage interval that has to be crossed, simplifies the electronics a lot.

- A DC ion filter looks feasible. Increased opacity leads to lower ion feedback because of the differences in transverse diffusion between electrons and ions. A decrease of 40 % was noted in standard conditions. Playing with the GEM geometry and the applied fields could possibly lead to a further decrease in the fractional ion feedback and real practical use.

Chapter 7

Conclusions and outlook

GEMs are still not used to their full capacity. In this work we tried to find solutions for many of the problems GEMs face nowadays. For example, one of the main restraints on the expansion of GEMs towards other applications than high-energy experiments is the limited CERN production capacity. Therefore we investigated GEMs from an outside manufacturer. The latest GEMs produced by this manufacturer gave promising results, showing similar behaviour to standard GEMs. But the production process did not follow a strict enough routine yet, since their hole geometry changed between individual GEMs while all CERN GEMs essentially have a biconical hole geometry and therefore show the same behavior. GEMs with larger holes (100 μm instead of 70 μm) were also investigated since they exhibit a smaller charging-up effect and they have an increased electron transparency. It turned out that they were not useful for detector purposes because of the increased discharge probability. Finally we tried to solve the limited size of the GEM foils (max. 30×30 cm^2) by eliminating the crucial step of aligning two macroscopic masks to a scale of a few microns. Therefore we investigated the behaviour of conical GEMs that only require a single mask. Although the discharge probability was worse than with standard GEMs, it was still sufficient for detector uses.

Another well-known limitation of most gaseous detectors was the gain losses that occur at high rates. Until now, nu such deterioration at high rates was measured for GEMs. In chapter 5 we crossed the $10^5\,Hzmm^{-2}$ that was usually measured and looked at even higher rates, up to $2\,10^6\,Hzmm^{-2}$. In these measurements two phenomena occurred. Firstly, an increase of the gain was measured at rates between $10^5\,Hzmm^{-2}$ and $10^6\,Hzmm^{-2}$. Systematic research pointed out that this was probably due to space-charge effects but finding the exact reason will still require a lot of extra research. Secondly, also a gain decrease was measured for the first time and this when we reached rates over $10^6\,Hzmm^{-2}$. In the future, formore demanding experiments, this could limit the use of GEMs.

Finally, in chapter 6, we investigated the ion feedback in GEM detectors and tried to find

new ways to suppress them. This could for example be useful for the ILC and for GEM photomultipliers. We first looked at the basic method of mesh gating used in TPCs for several years now. Our results indicated that the mesh transparency depends strongly on its density. Because mesh gating also introduces additional problems, like $\vec{E} \times \vec{B}$ distortions, another gating method was developed with a GEM replacing the mesh. The results show that GEMs already have decent transparency at 10 V. This reduces the necessary voltage shifts very much. With GEMs with larger holes (100 μm instead of 70 μm) we managed to reach a transparency of 70% at 10 V. One of the main problems might be that the exact voltage is quite a crucial parameter, since the peak in the transmission spectrum around 10 V is rather narrow. Misaligning two GEMs also leads to a reduction of the ion feedback, indicating that maybe a DC ion filter could be built. This technique, inspired on the different diffusion properties for ions and electrons, is influenced by the drift and transfer fields. Further research is certainly required in order to clarify the underlying mechanisms and to optimize the field settings and the detector geometry. Garfield simulations (Veenhof, 1998) can play an important role here.

Bibliography

M. C. Altunbas, M. Capéans, K. Dehmelt, J. Ehlers, I. Konorov, I. Gandi, S. Kappler, B. Ketzer, R. De Oliveira, S. Paul, S. Placci, L. Ropelewski, F. Sauli, S. F. & M. van Stenis (2002). Construction, test and commissioning of the triple-gem tracking detector for compass. *Nuclear Instruments and Methods A*, 490:177.

M. C. Altunbas, K. Dehmelt, S. Kappler, B. Ketzer, L. Ropelewski, F. Sauli & F. Simon (2003). Aging measurements with the gas electron multiplier (gem). *Nuclear Instruments and Methods A*, 515:249.

S. Amendolia, W. Blum, R. Benetta, G. Cherney, F. Fidecaro, J. P. Froberger, B. Hubbard, R. Jared, I. Lehraus, F. Liello, P. Marocchesi, R. Matthewson, J. May, J. Meyer, E. Milotti, F. Nanni, A. Peisert, M. Price, F. Ragusa, J. Richstein, R. Richter, F. Rolandi, W. Schlatter, J. Sedgbeer, R. Settles, U. Stierlin, M. Takashima, W. Tejessy, G. Tromba, W. Witzeling, S. Wu & W. Wua (1985). Influence of the magnetic field on the gating of a time projection chamber. *Nuclear Instruments and Methods A*, 234:47.

S. Bachmann, A. Bressan, M. Capeans, M. Deutel, S. Kappler & B. e. a. Ketzer (2002). Discharge studies and prevention in the gas electron multiplier (gem). *Nuclear Instruments and Methods A*, 479:295.

S. Bachmann, A. Bressan, B. Ketzer, M. Deutel, L. Ropelewski, F. Sauli, A. Bondar, A. Buzulutskov, L. Shekhtman, A. Sokolov, A. Tatarinov, A. Vasil'ev, S. Kappler & E. Shulte (2001). Performance of gem detectors in high intensity particle beams. *Nuclear Instruments and Methods A*, 470:548.

S. Bachmann, A. Bressan, L. Ropelewski, F. Sauli & D. Moermann (1999a). Operating principles of detectors based on gems. *Proceeding International Workshop on Micro-pattern Gas detectors, Orsay (June 28-30).*

S. Bachmann, A. Bressan, L. Ropelewski, F. Sauli, A. Sharma & D. Moermann (1999b). Charge amplification and transfer processes in the gas electron multiplier. *Nuclear Instruments and Methods A*, 438:376.

J. Benlloch, A. Bressan, C. B¨ttner, C. Capéans, G. M., M. Hoch, J. Labbé, A. Placci, L. Ropelewski, F. Sauli, A. Sharma & R. Veenhof (1998a). Development of the gas electron multiplier (gem). *IEEE Transactions on Nuclear Science*, NS-45:234.

J. Benlloch, A. Bressan, M. Capeáns, M. Gruwé, M. Hoch, J. Labbé, A. Placci, L. Ropelewski, & F. Sauli (1998b). Further developments and beam tests of the gas electron multiplier (gem). *Nuclear Instruments and Methods A*, 419:410.

S. Biagi (1999). Monte carlo simulation of electron drift and diffusion in counting gases under the influence of electric and magnetic fields. *Nuclear Instruments and Methods A*, 421:234.

D. Binnie (1985). Drift and diffusion of electrons in argon/co_2-mixtures. *Nuclear Instruments and Methods A*, 234:54.

W. Blum & R. L. (1993). *Particle detection with Drift Chambers*. Springer-Verlag, Berlin.

A. Bondar, A. Buzulutskov, L. Shekhtman & A. Vasiljev (2003). Study of ion feedback in multi-gem structures. *Nuclear Instruments and Methods A*, 496:325.

W. Bonivento, A. Cardini, G. Bencivenni, F. Murtas & P. D. (2002). A complete simulation of a triple-gem detector. *IEEE Transactions on Nuclear Science*, 49(4):1638.

R. Bouclier, B. Boimska, M. Capéans, W. Dominik, M. Hoch, G. Million, L. Ropelewski, F. Sauli & A. Sharma (1997). Update on discharge studies in msgcs. *CERN-CMS-NOTE-1997-020*.

O. Bouianov, M. Bouianov, R. Orava & V. Tikhonov (2001). Foil geometry effects on gem characteristics. *Nuclear Instruments and Methods A*, 458:698.

A. Breskin, G. Charpak, S. Majewski, G. M. G. Petersen & F. Sauli (1979). The multistep avalanche chamber: A new family of fast, high-rate particle detectors. *Nuclear Instruments and Methods A*, 161:19.

A. Bressan, J. Labbé, P. Pagano, L. Ropelewski & F. Sauli (1999). Beam tests of the gas electron multiplier. *Nuclear Instruments and Methods A*, 425:262.

A. Bressan, H. M., P. Ragano, L. Ropelewski, F. Sauli, S. Biagi, A. Buzulutskov, M. Gruwé, G. De Lentdecker, D. Moermann & A. Sharma (1998). High rate behavior and discharge limits in micro-pattern gas detectors. *Nuclear Instruments and Methods A*, 424:321.

J. C. Buettner, M. Capeáns, W. Dominik, M. Hoch, J. Labbé, G. Manzin, G. Million, L. Ropelewski, F. Sauli, & A. Sharma (1998). Progress with the gas electron multiplier. *Nuclear Instruments and Methods A*, 409:79.

A. Buzulutskov, A. Breskin, R. Chechik, G. Garty, F. Sauli & L. Shekhtman (2000). Further studies of the gem photomultiplier. *Nuclear Instruments and Methods A*, 442:68.

A. Buzulutskov, L. Shekhtman, A. Bressan, A. D. Mauro, L. Ropelewski, F. Sauli & S. Biagi (1999). Gem operation in pure noble gases and the avalanche confinement. *Nuclear Instruments and Methods A*, 433:471.

G. Charpak, R. Bouclier, T. Bressani, J. Favier & C. Zupančič (1968). The use of multiwire proportional counters to select and localize charged particles. *Nuclear Methods and Instruments*, 62:2362.

R. Chechik, A. Breskin, C. Shalem & D. Moermann (2004). Thick gem-like hole multipliers: properties and possible applications. *Nuclear Instruments and Methods A*, 535:303.

B. Coursey (2001). Http://physics.nist.gov/Divisions/Div846/Glossary/glossary.html.

S. Eidelman, K. Hayes, K. Olive, M. Aguilar-Benitez, C. Amsler, D. Asner, K. Babu, R. Barnett, J. Beringer, P. Burchat, C. Carone, C. Caso, G. Conforto, O. Dahl, G. D'Ambrosio, M. Doser, J. Feng, T. Gherghetta, L. Gibbons, M. Goodman, C. Grab, D. Groom, A. Gurtu, K. Hagiwara, J. Hernández-Rey, K. Hikasa, K. Honscheid, H. Jawahery, C. Kolda, K. Y., M. Mangano, A. Manohar, J. March-Russell, A. Masoni, R. Miquel, K. Mönig, H. Murayama, K. Nakamura, S. Navas, L. Pape, C. Patrignani, A. Piepke, G. Raffelt, M. Roos, M. Tanabashi, J. Terning, N. Törnqvist, T. Trippe, P. Vogel, C. Wohl, R. Workman, W.-M. Yao, P. Zyla, B. Armstrong, P. Gee, G. Harper, K. Lugovsky, S. Lugovsky, V. Lugovsky, A. Rom, M. Artuso, E. Barberio, M. Battaglia, H. Bichsel, O. Biebel, P. Bloch, R. Cahn, D. Casper, A. Cattai, R. Chivukula, G. Cowan, T. Damour, K. Desler, M. Dobbs, M. Drees, A. Edwards, D. Edwards, V. Elvira, J. Erler, V. Ezhela, W. Fetscher, B. Fields, B. Foster, D. Froidevaux, M. Fukugita, T. Gaisser, L. Garren, H.-J. Gerber, G. Gerbier, F. Gilman, H. Haber, C. Hagmann, J. Hewett, I. Hinchliffe, C. Hogan, G. Höhler, P. Igo-Kemenes, J. Jackson, K. Johnson, D. Karlen, B. Kayser, D. Kirkby, S. Klein, K. Kleinknecht, I. Knowles, P. Kreitz, Y. Kuyanov, O. Lahav, P. Langacker, A. Liddle, L. Littenberg, D. Manley, A. Martin, M. Narain, P. Nason, Y. Nir, J. Peacock, H. Quinn, S. Raby, B. Ratcliff, E. Razuvaev, B. Renk, G. Rolandi, M. Ronan, L. Rosenberg, C. Sachrajda, Y. Sakai, A. Sanda, S. Sarkar, M. Schmitt, O. Schneider, D. Scott, W. Seligman, M. Shaevitz, T. Sjöstrand, G. Smoot, S. Spanier, H. Spieler, N. Spooner, M. Srednicki, A. Stahl, T. Stanev, M. Suzuki, N. Tkachenko, G. Trilling, G. Valencia, K. van Bibber, M. Vincter, D. Ward, B. Webber, M. Whalley, L. Wolfenstein, J. Womersley, C. Woody, O. Zenin & R.-Y. Zhu (2004). Review of Particle Physics. *Physics Letters B*, 592:1+. URL `http://pdg.lbl.gov`.

M. Hoch (1998). *Development of Fast Tracking Detectors: Micro Strip Gas Chamber and GEM Gas Electron Multiplier*. Phd thesis, Technische Universität Wien.

M. Hoch (2004). Trends and new developments in gaseous detectors. *Nuclear Instruments and Methods A*, 535:1.

S. Kappler (2000). *Application of Multi-GEM Detectors in X-Ray Imaging.* Diploma thesis, IEKP, Karlsruhe University.

S. Kappler (2004). *Development of a GEM-based TPC Readout for Future Collider Experiments.* Phd thesis, IEKP, Karlsruhe University.

B. Ketzer, Q. Weitzel, S. Paul, F. Sauli & L. Ropelewski (2004). Performance of triple gem tracking detectors in the compass experiment. *Nuclear Instruments and Methods A*, 535:314.

M. Killenberg, S. Lotze, H. Mnich, A. Muennich, S. Roth, F. Sefklow, M. Tonutti, M. Weber & P. Wienemann (2004). Charge transfer and charge broadening of gem structures in high magnetic fields. *Nuclear Instruments and Methods A*, 530:251.

M. Killenberg, S. Lotze, J. Mnich, S. Roth, R. Schulte, B. Sobloher, W. Struczinski & M. Tonutti (2003). Modelling and measurement of charge transfer in multiple gem structures. *Nuclear Instruments and Methods A*, 498:369.

W. Leo (1992). *Techniques for Nuclear and Particle Physics Experiments.* Springer-Verlag.

T. Meinschad (2005). *GEM: A Novel Gaseous Particle Detector.* Phd thesis, Technische Universität Wien.

D. Moermann, A. Breskin, R. Chechik & D. Bloch (2004a). Evaluation and reduction of ion back-flow in multi-gem detectors. *Nuclear Instruments and Methods A*, 516:315.

D. Moermann, A. Breskin, R. Chechik & C. Shalem (2004b). Operation principles and properties of the multi-gem gaseous photomultiplier with reflective photocathode. *Nuclear Instruments and Methods A*, 530:258.

D. R. Nygren (1975). The time projection chamber: A new 4 pi detector for charged particles. *PEP-0144, Proceedings of PEP Summer Study, Berkeley*, p. 58.

A. Oed (1988). Position-sensitive detector with microstrip anode for electron multiplication with gases. *Nuclear Instruments and Methods A*, 263:351.

C. Richter (2000). *Development of Micro Pattern Gas Detectors for High Rate Experiments.* Phd thesis, University of Heidelberg.

F. Sauli (1977). Principles of operation of multiwire proportional and drift chambers. *CERN Yellow Report*, 77-09.

F. Sauli (1997). Gem: A new concept for electron amplification in gas detectors. *Nuclear Instruments and Methods A*, 386:531.

F. Sauli (1999). Gem readout of the time projection chamber. *CERN-EP-TA1 Internal Report, July 29.*

F. Sauli (2003a). Development and applications of the gas electron multiplier. *Nuclear Instruments and Methods A*, 505:195.

F. Sauli (2003b). Fundamental understanding of aging processes: review of the workshop results. *Nuclear Instruments and Methods A*, 515:358.

F. Sauli (2004). From bubble chambers to electronic systems: 25 years of evolution in particle detectors at cern (1979 to 2004). *Physics Reports*, 403-404:471.

F. Sauli, S. Kappler & L. Ropelewski (2003). Electron collection and ion feedback in gem-based detectors. *IEEE Transactions on Nulcear Science*, 50(3):803.

F. Sauli & A. Peisert (1984). Drift and diffusion of electrons in gases: A compilation. *CERN Yellow Report*, 84-08.

F. Sauli, L. Ropelewski & P. Everaerts (2006). Ion feedback suppression in time projection chambers. *Nuclear Instruments and Methods A*, 560:269.

F. Sauli & A. Sharma (1999). Micro-pattern gaseous detectors. *Annual Review of Nuclear and Particle Science*, 49:341.

M. A. Stanley (2000). *Sprites and their Parent Discharges.* Phd thesis, New Mexico Institute of Mining and Technology.

V. Tikhonov & R. Veenhof (2002). Gem simulation methods development. *Nuclear Instruments and Methods A*, 478:452.

R. Veenhof (1998). Garfield, recent developments. *Nuclear Instruments and Methods A*, 419:726.

Rate capability and ion feedback in GEM-detectors

Pieter Everaerts

Supervisors: Prof. Dr. L. Van Hoorebeke, Dr. L. Ropelewski, Dr. F. Sauli

Abstract—**The high-rate behaviour of the Gas Electron Multiplier (GEM) is investigated. Also an attempt is made to reduce the ion feedback of the detector without canceling its other major advantages like the improved resolution.**

Keywords—**Gas Electron Multiplier (GEM), high-rate, ion feedback**

I. Introduction

INTRODUCED by Sauli in 1996, the gas electron multiplier (fig. 1) consists of a two-side copper-clad Kapton foil, perforated with a high density of holes (typically around 100 per square mm).[1] Etched by a photolithographic process, these holes have a pitch of usually 140 μm and diameters of about 70 μm ('standard geometry'). Application of a potential difference between upper and lower electrodes creates a high electric field inside the holes. Almost all the field lines in the drift region are squeezed into the the holes in the GEM plates. In the holes the electrons following these field lines are multiplied because of the very high field. (fig. 2)

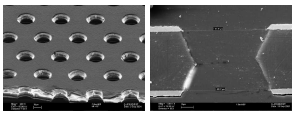

Fig. 1. Structure of a GEM plate (left) and of a GEM hole (right)

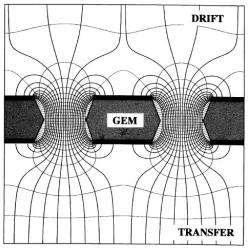

Fig. 2. The electric field lines are squeezed into the GEM hole.

The Gas Electron Multiplier is part of a new generation of gaseous detectors, the micropattern detectors, which are quickly replacing the Multi-Wire Proportional Chambers (MWPC) in the field of High-Energy Physics, because of the better accuracy and higher rate capability. The main advantages and characteristics of the GEM can be summarized as:

- Operation in most gas fillings, including pure noble gases
- Proportional gains above 105
- Energy resolution 18% FWHM at 5.9 keV
- Space localization accuracy 60μm rms or better
- Rate capability above 10^5 counts/mm^{2}sec
- Active areas up to 1000 cm^2
- Flexible detector shape and readout patterns
- Robust, Low cost

E-mail: Pieter.Everaerts@UGent.be .

II. High rate behavior

Until now rate capability above 10^5 counts/mm^{2}s was proven by [2]. We now investigated the rate capability above this frontier (fig. 3) and made 2 major observations. First, between 10^5 Hz/mm^{2}s and 10^6 Hz/mm^2, we noticed an increase of the gain. This increase turned out to be dependent on the field and voltage settings. Also the gas in the detector played a significant role. All these hints put together, our best guess for this phenomenon is a space-charge effect. The effect seems to start occurring at a certain charge/current threshold. The magnitude of the effect also depends on the circumstances. For example, at higher gains, the relative effect diminishes. A second observation was a decline starting above 10^6 Hz/mm^2, pointing in the direction of a high-rate limitation of the detector.

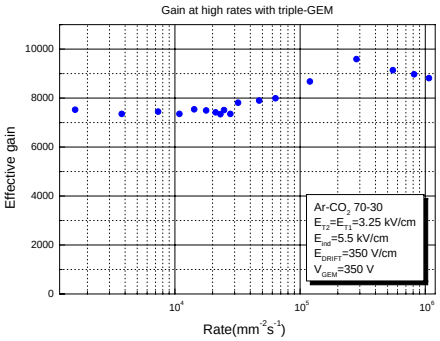

Fig. 3. Evolution of gain at high rates.

III. Ion feedback

One of the current major research areas in gaseous detector operation is the ion feedback suppression. For future colliders like the ILC, the working conditions will be more and more severe. Therefore, the available detectors have to be improved. For large volumes, Time Projection Chambers still look like the main option. A time projection chamber (TPC) consists of a gas-filled cylindrical chamber with two-dimensional gas detectors (nowadays often MWPC's) as endplates. Along its length, the chamber is divided into two halves by means of a central high voltage electrode disc, which establishes an electric field between the center and the endplates. The z-coordinate of the track is then determined by the drift time of the electrons from the track to the read-out. MWPCs are not capable of fulfilling the more stringent requirements. GEMs seem to be a good option because they have a natural tendency of suppressing ion feedback. However, with lowest values for ion feedback observed around 2 promille [3], still an order of magnitude needs to be gained. New alternative solutions are necessary.

A. Gating

For gating an intermediate drift space is added, separated from the main drift volume by a wired mesh. The voltage on this mesh

can be changed, gating the mesh open or close. Electrons drifting through an open gating grid pass through to the amplification region around the anode wires. Positive ions generated in the avalanche are detected on segmented cathode pads to provide precise measurements along the wire. The slow positive ions can now be blocked from entering the drift region by closing the gating grid after the electrons have drifted through. In this case the electron transmission through the mesh is important. We checked this for three meshes of different density (45, 65 and 89% optical transparancy). The old rule of thumb, taking the transfer field twice the drift field for obtaining a good tranmission, turned out to be only valid for very little dense, very transparant meshes. In the case of the densest mesh we only had a tranmission of 20% in this case.

One problem with gating is that some of the advantages of a GEM-TPC are canceled. For example, $\vec{E} \times \vec{B}$ distortions are introduced again because of the wires. This can also be noticed in an easy set-up with a wired mesh close to the first GEM. Therefore we looked for another solution which we found in GEM gating. GEMs turn out to have a very good transmission at low voltages. GEMs with larger holes (100 μm holes, 140 μm pitch) turned out to have a transmission of 70% at 10 V over the GEM. (fig. 4) Inverting the GEM voltage immediately blocks the ions drifting back. Therefore the voltage variation is much smaller (10 V instead of several hundred V's) and we do not introduce additional field distortions. This method does seem very favorable.

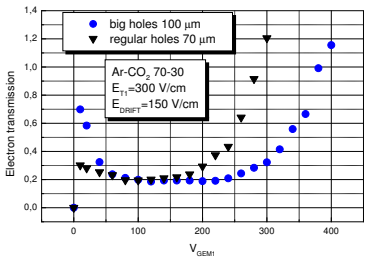

Fig. 4. Electron transmission for different hole sizes, 150 V/cm drift and 300 V/cm transfer field.

B. DC ion filter

Since diffusion properties for electrons and ions are quite different, a thorough investigation of them could lead to a so-called DC ion filter, which would block the ions flowing back more than the electrons going in the other direction. At the common values for transfer fields between GEMs (several kV/cm), the transverse diffusion for electrons is almost an order of magnitude larger than that for ions. As a result, the electron cloud spreads out a lot more than the ion cloud. This suggests that an adapted geometry of the multiple structure could further reduce the ion feedback. An increased optical opacity in the placing of the GEMs would lower the ion back-flow. Offsetting the position of the holes of the second GEM for example by half a pitch at a gap distance in the order of magnitude of the pitch would have as a result that many field lines out of the first series of holes would end up on the top electrode of the second GEM. Most of the ions would then be stopped, while a majority of the electrons, because of the increased transverse diffusion of the electrons, would still end up in the holes of the second GEM and get multiplied there. In the presence of an magnetic field this filtering could be very effective.

Due to the requirement of the gap thickness and also the transverse positioning of the holes at half a pitch of each other, it is hard to realise an experimental set-up with standard GEMs because of the limited proportions. A moving mechanism -like the one we preferred- would be even harder to build. Therefore we decided to test and implement the scheme with the so-called thick GEMs of [4]. The thick GEM-plates have a hole diameter of 300 μm in the insulator, around this there is a metal-free rim of 100 μm. The holes have a triangular pattern with pitch 800 μm.

Fig. 5 shows the measured anode and drift currents under continuous irradiation. The electron currents fluctuate in function of the relative position between GEMs, but their fluctuations are smaller than those for the ions. Therefore the fractional ion feedback also decreases considerably, from 10 to 6%. The sharp sides in the curve could show an insufficient opacity of the structure and indicates that diagonal movement in the triangular pattern could lead to an even deeper minimum, since the opacity would be increased. Also increased pitch could lead to the same effect.

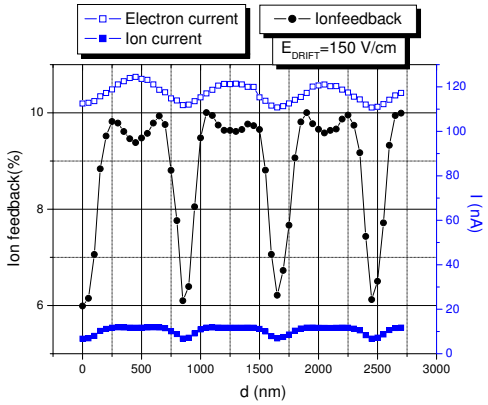

Fig. 5. Modulation of the drift and anode currents, and of their ratio, as a function of the relative position of the holes'rows in two facing thick-GEM plates with low drift field (150 V/cm).

IV. Conclusions

This abstract gives an idea of the observed frontiers of rate capability for GEM-detectors. It also introduces two main concepts useful in the fight against back-flowing ions in Time Projection Chambers and reviews some of the old measurements done in these fields.

Acknowledgments

I would like to thank my CERN supervisors, Dr. F. Sauli and Dr. L. Ropelewski, Miranda Van Stenis who assisted me when technical difficulties occurred and my supervisor at Ghent University, Prof. Dr. L. Van Hoorebeke.

References

[1] F. Sauli, *GEM: A new concept for electron amplification in gas detectors*, Nuclear instruments and Methods A, vol. 386, p.531, 1997.

[2] A. Bressan and J. Labbé and P. Pagano and L. Ropelewski and F. Sauli, Beam tests of the Gas Electron Multiplier, *Nuclear Instruments and Methods A, vol 425, p. 262, 1999.*

[3] M. Killenberg and S. Lotze and H. Mnich and A. Muennich and S. Roth and F. Sefklow and M. Tonutti and M. Weber and P. Wienemann, Charge transfer and charge broadening of GEM structures in high magnetic fields., *Nuclear Instruments and Methods A, vol 530, p. 251, 2004.*

[4] R. Chechik and A. Breskin and C. Shalem and D. Moermann, Thick GEM-like hole multipliers: properties and possible applications, Nuclear Instruments and Methods A, vol 535, p. 303, 2004.